Modulating Molecular Chaperones To Treat Demyelinating Neuropathies

By

Xinyue Zhang

Submitted to the graduate degree program in Department of Pharmacology and Toxicology and the Graduate Faculty of the University of Kansas in partial fulfillment of the requirements for the degree of Doctor of Philosophy.

Chair: Dr. Rick Dobrowsky

Dr. Erik Lundquist

Dr. Honglian Shi

Dr. Douglas Wright

Dr. Liqin Zhao

Date Defended: May 18, 2018

The dissertation committee for Xinyue Zhang certifies that this is the approved version of the following dissertation:

Modulating Molecular Chaperones To Treat Demyelinating Neuropathies

Chair: Dr. Rick Dobrowsky

`

Date Approved: May 18, 2018

Abstract

Peripheral neuropathies can be classified into two categories, demyelinating or axonal neuropathy. Demyelinating neuropathies are characterized by damaged myelin but intact axons. Recent evidence suggests that the leucine zipper transcription factor c-jun is at the center of driving demyelination. c-Jun is required for Schwann cells (SCs) to dedifferentiate after injury, and up-regulation of c-jun has been reported in human neuropathies. It remains to be tested whether c-jun would be a valid target for treating demyelinating neuropathies. Previously, our published work has shown that modulating the expression of heat shock protein 70 (Hsp70) using a novel small molecule drug called KU-32 attenuated the expression of c-jun and the extent of demyelination in SC-dorsal root ganglia (DRG) co-cultures in an Hsp70 dependent manner.

To extend these data, this work examined the *in vivo* effects of modulating molecular chaperones using the next generation novologue KU-596 in two mouse models of demyelinating neuropathies. MPZ-Raf mice are a conditional transgenic mouse line that exhibits a demyelinating neuropathy due to the SC-specific induction of mitogen-activated protein kinase (MAPK) and c-jun induction after tamoxifen (TMX) injections in adult mice. Five days of TMX treatment induced a severe motor deficits starting from day 8 and treating the MPZ-Raf mice with 20 mg/kg of KU-596 every other day reduced c-jun levels in the sciatic nerves. The decrease in c-jun correlated with an improvement in the myelination status of the nerves and motor function. In line with previous findings, the effects of KU-596 were Hsp70-dependent, as MPZ-RAF × Hsp70 knockout (KO) mice did not show improvement following drug treatment. This study provides proof of principal that modulating molecular chaperones would be beneficial in treating demyelinating neuropathies. However, as this model is less relevant to an actual disease,

we complemented our study using a model of human X-linked Charcot-Marie-Tooth disease (CMT1X).

CMT1X is caused by the mutation of gap junction beta 1 gene *(GJB1)* that encodes the gap junction protein connexin 32 (Cx32). Recent evidence suggests an elevated c-jun expression is associated with the disease. Since c-jun could promote demyelination, targeting c-jun using KU-596 could provide a potential therapeutic strategy to treat CMT1X. The pathology of Cx32 deficient (Cx32def) mice occurs in two stages where young mice develop a pre-demyelinating axonopathy, which progresses to a more severe demyelinating neuropathy in older mice. We show that in young mice that exhibit a pre-demyelinating axonopathy, one-month of KU-596 treatment decreased c-jun expression and improved motor nerve conduction velocity (MNCV) and compound muscle action potential (CMAP). In older Cx32def mice that developed a demyelinating neuropathy, 3 months of KU-596 treatment decreased c-jun expression and improved grip strength, MNCV and CMAP. Hsp70 is required for drug efficacy as neither young nor old Cx32def × Hsp70 KO mice showed improvement following KU-596 treatment. Collectively, our data indicates that modulating molecular chaperones is beneficial in managing demyelinating neuropathies.

Acknowledgements

First and foremost, I would like to thank my mentor, Dr. Rick T. Dobrowsky, who is the best mentor one could ever find. I'm grateful to be his student. His passion towards science has always been inspirational to me and motivated me to move forward. His constant guidance, patience, and encouragement helped me through the ups and downs of my graduate study, without which no work within this dissertation would be possible. He also offered a lot of opportunities to move my career forward and valuable suggestions on career choices, which help guide my future career path. I would like to thank my committee members, Dr. Erik Lundquist, Dr. Honglian Shi, Dr. Doug Wright and Dr. Liqin Zhao for their valuable suggestions and help on my projects. I would also like to thank professors and core facilities that have helped me with my projects and enlightened me with knowledge from areas that I may never explore myself. Dr. Brian S. Blagg provided the compound KU-596, without which my research would not be possible. Dr. Stephen Fowler and Dr. Marco Bortolato's lab helped me analyzed my actometer data. The MAI lab helped me greatly with my imaging data and provided a lot of joyful talks. I would like to thank the department for giving me the opportunity to obtain a graduate training in this wonderful program.

Life is beautiful when you have friends along the way. I am grateful I made a lot of them during my graduate study. Past and current members of the Dobrowsky lab have not only helped me with lab work but also have been a good source of friendship. I would like to thank Dr. Pan Pan who taught me how to run my first gel. I would like to thank Dr. Vicky Ma who taught me how to isolate RNA. Thanks to Dr. Chanel Li whom I

followed like a duckling in the first year and taught me most of the lab skills. I would like to thank Mason McMullen, Alicia Smith, and Dr. Sean Emery who have taught me skills and offered advice within and beyond the lab. I would like to thank Dr. Zhenyuan You, who I spent the most time with in the lab, has offered constant help and encouragement. I would like to thank Yssa Rodriguez who is always supportive and brings joy to the lab. I would like to thank everyone in the department for making my graduate study a precious memory. I would like to thank Dr. Wenqi Cui and Xuan Gu, who have been good roommates and trusted friends, for taking care of me and Marble. I would like to thank Dr. Lan Lan, Dr. Lu Wang, Dr. Wenqi Cui, Ning Liu, Yuxiao Guo, Ding Dan, Yuyu Wang and Xiaomeng Su for not only adding diversity to my "mouse life", but also for their help, support and delightful adventures.

I would also like to thank my family for their unconditional love and support. My grandma is the one that encouraged me to pursuit what I want, be persistent and never be held back for being a woman. I would not have accomplished anything without them.

Lastly, I would like to thank funding sources that made my graduate research possible. This work is supported by grant from National Institutes of Health National Institute of Diabetes and Digestive and Kidney Diseases [Grant DK095911] (to R.T.D.).

Table of Contents

ABSTRACT ..... **III**

ACKNOWLEDGEMENTS ..... **V**

LIST OF FIGURES ..... **IX**

LIST OF TABLES ..... **X**

LIST OF ABBREVIATIONS ..... **XI**

CHAPTER 1. INTRODUCTION **1**

1.1. Overview of Peripheral Myelination 1
1.1.1. Positive regulators of myelination 2
1.1.2. Negative regulators of myelination 4
1.1.3. CMT1X 9
1.2. Heat shock proteins (Hsps) 14
1.2.1. Small heat shock proteins (sHsps) 15
1.2.2. Hsp70 16
1.2.3. Hsp70 cochaperones 18
1.2.4. Hsp90 20
1.3. Targeting Hsps to Treat Peripheral Neuropathies 23
1.3.1. Targeting Hsp90 to Modulate Hsp70 Expression and Treat Peripheral Neuropathies 24
1.3.2. Modulating Hsp70 to Attenuate Protein Aggregates in CMT1A 27
1.3.3. Modulating Chaperones to Treat Diabetic Peripheral Neuropathy 29
1.3.4. Modulating Hsp70 to Treat Demyelinating Neuropathies 32

CHAPTER 2. TARGETING HEAT SHOCK PROTEIN 70 TO AMELIORATE C-JUN EXPRESSION AND IMPROVE DEMYELINATING NEUROPATHY **35**

2.1. Introduction 37
2.2. Materials and Methods 39
2.3. Results 45
2.3.1. KU-596 decreased TMX-induced c-Jun expression 45
2.3.2. KU-596 improves demyelination in MPZ-Raf mice 48
2.3.3. KU-596 improves motor function in MPZ-Raf mice 51
2.3.4. KU-596 improves a pre-existing motor deficit in MPZ-Raf mice 54
2.3.5. Hsp70 is required for drug efficacy 57
2.4. Discussion 59

CHAPTER 3. MODULATING MOLECULAR CHAPERONES IMPROVES DEMYELINATING NEUROPATHY IN A MOUSE MODEL OF CHARCOT-MARIE-TOOTH 1X **63**

3.1. Introduction 65
3.2. Materials and Methods 68
3.2.1. Materials 68
3.2.3. Immunoblot Analysis 70
3.2.4. Immunofluorescence Analysis 71
3.2.5. Behavioral Tests 71
3.2.6. Electrophysiological measurements 72
3.2.7. Luciferase activity assay 72
3.3. Results 73
3.3.1. KU-596 treatment decreased c-Jun expression in young Cx32 def mice 73

3.3.2. KU-596 TREATMENT INCREASED THE MOTOR FUNCTION IN YOUNG CX32DEF MICE .. 75
3.3.3. KU-596 TREATMENT DECREASED C-JUN EXPRESSION IN OLD CX32DEF MICE. 77
3.3.4. KU-596 TREATMENT INCREASED THE MOTOR FUNCTION IN OLD CX32DEF MICE. 79
3.3.5. KU-596 REQUIRES HSP70 FOR EFFICACY. 82
3.3.6. KU-596 MAY IMPROVE THE NEUROPATHY BY DECREASING MACROPHAGE RECRUITMENT 85
3.4. DISCUSSION 88
CHAPTER 4. OUTLOOKS 95
APPENDIX 100
REFERENCE 101

List of Figures

Figure 1.1.1.1: Schematic illustraion of SC lineage and regulators of SC myelination. 3
Figure 1.1.3.1 Cx32 gap junction channel and reported mutations. 11
Figure 1.2.1: Schematic illustration of HSR. 15
Figure 1.2.4.1: The structure and conformational cycle of Hsp90. 21
Figure 1.3.1.1: Structures of novologues. 26
Figure 2.3.1.1: KU-596 decreases c-jun expression in TMX treated MPZ-RAF mice. 47
Figure 2.3.2.1: KU-596 improves myelin integrity. 49
Figure 2.3.2.2: KU-596 decreased abnormally myelinated fibers. 50
Figure 2.3.3.1: KU-596 improves motor function of TMX treated MPZ-RAF mice. 52
Figure 2.3.4.1: KU-596 improves a pre-existing motor deficit. 56
Figure 2.3.5.1: KU-596 improves the motor deficit in an Hsp70 dependent manner. 58
Figure 3.3.1.1: KU-596 decreases c-jun expression in young Cx32def mice. 74
Figure 3.3.2.1: KU-596 improves motor function in young Cx32def mice. 76
Figure 3.3.3.1: KU-596 decreases c-jun expression in old Cx32def mice. 78
Figure 3.3.4.1: KU-596 improves motor function of old Cx32def mice. 81
Figure 3.3.5.1: KU-596 improves the motor deficit in an Hsp70 dependent manner. 84
Figure 3.3.6.1: KU-596 decreases CCL2 luciferase activity. 87
Figure 3.4.1: Proposed mechanism of action of KU-596. 94

List of Tables

Table 1.2.2.1: The human Hsp70 family. 16
Table 3.2.1.1: Primers for genotyping 69

List of Abbreviations

17-AAG	17-allylamino-17-demethoxygeldanamycin
ACD	α-crystallin domain
AD	Alzheimer's disease
AHA1	ATPase homologue1
AIDP	acute inflammatory demyelinating neuropathy
ALCAR	acetyl-L-carnitine
ANOVA	analysis of variance
APP	amyloid precursor protein
AUC	area under the curve
BAG1	Bcl-2 associated athanogene 1
CAP	Captisol
CCL2	C-C motif chemokine
CHIP	Carboxy terminus of heat shock cognate protein 70 (Hsc70) interacting protein
CMAP	Compound muscle action potential
CMT	Charcot-Marie-Tooth disease
CMT1X	X-linked Charcot-Marie-Tooth disease
CMT2E	Charcot-Marie-Tooth disease Type 2E
CMT1A	Charcot-Marie-Tooth disease Type 1A
CNS	central nervous system
CO	Corn oil
CSF-1	colony stimulating factor-1

CTD	C-terminal domain
CTE	C-terminal extension
Cx32	connexin 32
Cx32def	connexin 32 deficient
DAPI	4',6-diamidino-2-phenylindole
db-cAMP	dibutryl cAMP
DC	detergent compatible
DMSO	dimethyl sulfoxide
DPN	Diabetic Peripheral Neuropathy
DRG	dorsal root ganglia
Fbw7	F-box WD repeat domain-containing protein 7
FPA	force-plate actometer
GAP	growth-associated protein
GBS	Guillain-Barre syndrome
GDNF	glial-derived neurotrophic factor
GJB1	Gap junction beta 1
Grp78	glucose-regulated protein 78
HD	Huntington's disease
HOP	Hsc70/Hsp90-organinzing protein
HPD	His, Pro and Asp domain
Hsc70	heat shock cognate 70
HSE	heat shock elements
HSF1	heat shock factor 1

Hsp	heat shock protein
Hsp27	heat shock protein 27
Hsp40	heat shock protein 40
Hsp70	heat shock protein 70
Hsp70 KO	Hsp70.1/Hsp70.3 knockout
Hsp90	heat shock protein 90
HSR	heat shock response
JNK	Jun-NH_2-terminal kinase
KO	knockout
MAG	myelin-associated glycoprotein
MAPK	Mitogen-activated protein kinase
MBP	myelin basic protein
MD	middle domain
MEEVD	Met-Glu-Glu-Val-Asp
MFN2	mitofusin2
MNCV	Motor nerve conduction velocity
NCAM	neuronal cellular adhesion molecule
NCV	nerve conduction velocity
NEF	nucleotide exchange factor
NGS	normal goat serum
NICD	Notch intracellular domain
NTD	N-terminal domain
OCT	Optimum cutting temperature

Oct-6	octamer binding transcription factor 6
P0, MPZ	myelin protein zero
PBS	phosphate-buffered saline
PBST	PBS with 0.1% Tween-20
PD	Parkinson's disease
pMAPK	phosphorylatied Mitogen-activated protein kinase
PMP22	peripheral myelin protein 22
PNS	peripheral nervous system
PPIase	Peptidyl-prolyl cis-trans isomerase
RBPJ	recombination signal-binding protein Jκ
RLU	relative luminescence unit
ROS	reactive oxygen species
SBD	substrate binding domain
SC	Schwann cell
SCP	Schwann cell precursor
SEAP	secreted alkaline phosphatase
SEM	standard error of the mean
sHsp	small heat shock protein
TMX	Tamoxifen
TPR	tetratricopeptide repeat
UPS	ubiquitin-proteasome system
WLD^s	the slow Wallerian degeneration protein
WT	wild type

Chapter 1. Introduction

1.1. Overview of Peripheral Myelination

Myelin insulates the axons and enables the fast conduction of electrical signals along the length of the nerve fiber. Schwann cells (SCs) supply the myelin for the peripheral nervous system (PNS) and were first described by Theodor Schwann as the ensheathing structure around peripheral axons. SCs originate from neural crest cells, which segregate from the neural folds during neurulation and migrate either laterally and ventrally to form various neurons (Jessen & Mirsky 2005). SCs mature over three transitional periods (Figure 1.1.1.1) with Schwann cell precursors (SCPs) first differentiating from neural crest cells around embryonic day 12-13 (E12-13). Surprisingly, SCPs are not required for nerves to reach their targets (Grim et al 1992, Morris et al 1999) but are required for nerve fasciculation (Birchmeier 2009). SCPs provide trophic support for sensory and motor neurons and give rise to endoneurial fibroblasts, melanoblasts, and parasympathetic neurons in addition to SCs (Dyachuk et al 2014, Espinosa-Medina et al 2014, Jessen & Mirsky 2005, Joseph et al 2004, Kaucka & Adameyko 2014, Nitzan et al 2013).

At E15-16, SCPs transition into immature SCs. A series of lineage-specific markers distinguishes SCPs from immature SCs. For example, SCPs express the low affinity p75 neurotrophin receptor and growth-associated protein (GAP)-43, while immature SCs mainly express S100 and neuronal cellular adhesion molecules (NCAMs) (Kubu et al 2002, White et al 2001). Immature SCs then differentiate into either myelinating or non-myelinating SCs depending on the axons they ensheath. In particular, axons with a

diameter larger than 1μm are typically myelinated (Corfas et al 2004, Sherman & Brophy 2005). Radial sorting enables immature SCs to form 1:1 relationships with axons and initiates a pro-myelinating stage, during which promyelinating proteins such as myelin-associated glycoprotein (MAG), protein zero (P0), and octamer binding transcription factor (Oct-6) are expressed (Ogata et al 2006). The myelination process initiates at birth and is characterized by the downregulation of Oct-6 and increased expression of Krox-20, a key transcription factor that functions as a positive regulator of myelination (Jaegle & Meijer 1998).

Myelinated SCs maintain a striking plasticity that enables them to switch off myelination, re-enter the cell cycle, and re-adopt a phenotype that is similar to immature SCs. Dedifferentiation of SCs often occurs in injured nerves, when they lose contact with the axons. Demyelinated axons are also a common feature in human neuropathies, such as Charcot-Marie-Tooth disease (CMT) and Refsun disease, even in the absence of direct nerve injury (Scherer & Wrabetz 2008). Dedifferentiated SCs can re-differentiate and remyelinate the axons under appropriate conditions. Since SC differentiation and dedifferentiation are tightly regulated by the interplay between different intracellular signals, elucidating the underpinning molecular events is the key to help understand SC biology and devise treatments for demyelinating neuropathies.

1.1.1. Positive regulators of myelination

Several transcription factors, including Krox-20, Oct-6, Brn-2, Sox-10 and NF-κB have been identified to be pro-myelinating. Krox-20 is a zinc finger transcription factor and is necessary for driving SC myelination as well as the formation and maintenance of the myelin sheath (Decker et al 2006). Specifically, Krox-20 activates myelin genes,

suppresses the expression of negative regulators of myelination (see below), helps SCs exit the cell cycle and blocks proliferation. Consistent with its important role in myelination, Krox-20 null mice fail to express genes necessary for myelin differentiation even after the SCs reach the promyelinating stage (Parkinson et al 2003). Enforced Krox-20 expression is sufficient to induce expression of myelin gene P0 and periaxin in dedifferentiated SCs (Nagarajan et al 2001).

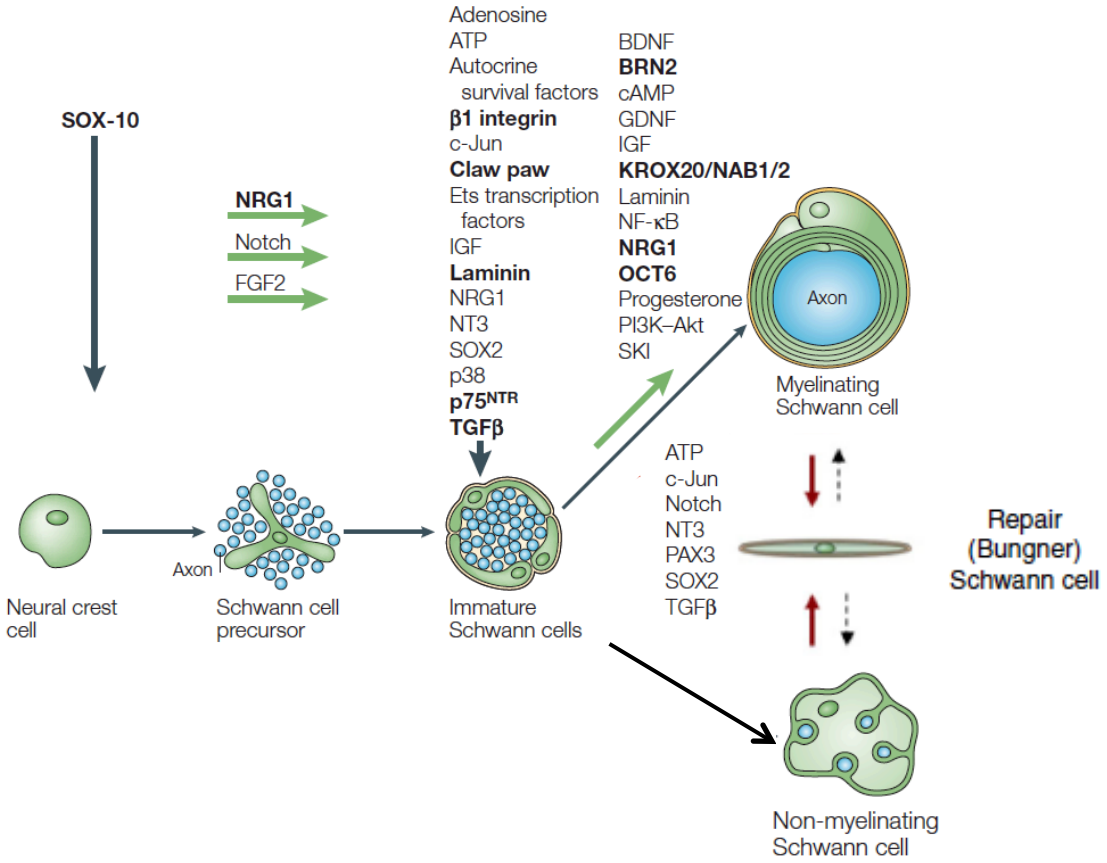

Figure 1.1.1.1: Schematic illustraion of SC lineage and regulators of SC myelination.
SC maturation is a three-phase process, including migration of neural crest cells, differentiation into immature SCs, and maturation into myelinating or non-myelinating SCs. Large fibers are ensheathed with myelinating SCs, and small caliber fibers form Remak bundles with non-myelinating SCs. Red arrows indicate SC dedifferentiation upon injury or in pathological settings. Factors regulating each transition process are listed above. Factors in bold are evidenced with observations in mutant animals. *Adapted from (Jessen & Mirsky 2005)*.

1.1.2. Negative regulators of myelination

Negative regulators, such as c-jun, Notch, Sox-2, and Id2, inhibit myelination and can dedifferentiate SCs back into the immature phenotype in injured nerves. Since this transformation of SCs creates an environment that is preferable for axonal survival and regeneration, negative regulators are crucial for nerve recovery after injury. Mechanistically, Parkinson *et al.* suggested that c-jun and Notch may directly antagonize the myelin-promoting transcription factor, Krox-20 (Parkinson et al 2008). Therefore, negative and positive regulators maintain a dynamic balance between myelination and demyelination in peripheral nerves by functionally complementing each other. However, this balance may be disturbed and abnormal induction of negative signaling may cause pathological demyelination in a variety of human pathologies, including CMT. Hence, a clear elucidation of the molecular and cellular functions of the negative regulators in SCs will be particularly instructive for developing effective therapies for treating some myelin-related diseases.

1.1.2.1. c-Jun

c-Jun, together with JunB and JunD, belongs to the mammalian Jun protein family and is a major component of the AP-1 transcription factor complex (Mechta-Grigoriou et al 2001). Although most of the activities of c-jun depend on its N-terminal phosphorylation by Jun-NH_2-terminal kinase (JNK), c-jun-mediated myelin gene regulation appears to be independent of this pathway. In support of this, expression of a mutant c-jun that is resistant to JNK phosphorylation retained its inhibitory effects on myelin gene expression compared to wild-type c-jun (Parkinson et al 2008). c-Jun is highly expressed in immature SCs and is down regulated as SCs begin to myelinate and

Krox-20 expression increases. Overexpression of Krox-20 suppressed basal c-jun levels in cultured SCs *in vitro* (Parkinson et al 2004) and consistent with this observation, c-jun levels remained high in the postnatal nerves of Krox-20 null mice but were suppressed in wild type nerves (Mirsky et al 2008). Wild-type (WT) and mutant c-jun (resistant to JNK phosphorylation) also antagonized the expression of Krox-20 induced by another pro-myelinating molecule, dibutryl cAMP (db-cAMP) (Parkinson et al 2008).

The above data support that Krox-20 can block c-jun expression but c-jun also has a cross-inhibitory relationship with Krox-20. c-Jun inhibits myelin genes during development and in c-jun-null SCs, Krox-20-induced myelin gene expression was shown to be elevated. However, inhibition of c-jun pathway alone was not sufficient to induce differentiation in myelinated nerves (Parkinson et al 2008). Modest overexpression of c-jun during development delays myelination, and higher expression of c-jun inhibits myelination (Fazal et al 2017).

During nerve injury, loss of axonal contact causes myelinated SCs to arrest myelination and revert to a phenotype similar to the immature stage. This process is characterized by cessation of myelin gene expression and reactivation of genes characteristic of immature SCs, such as downregulation of Krox-20 levels and upregulation of c-jun levels. To characterize the role of c-jun in this process, researchers generated mice containing a SC specific, conditional knockout of c-jun. In these mice, there was a significant delay in injury-induced myelin sheath degradation and loss of myelin mRNA and protein expression. Particularly, while Krox-20 expression disappeared in WT mice 24h after the removal of axon contact, it remained detectable 2d after loss of axon contact in the c-jun null mice. Contrarily, c-jun expression is highly

upregulated following nerve cut in WT mice but remained low in the mutant mice with the conditional deletion. These results indicate that c-jun is necessary for SCs to re-adopt the immature phenotype (Parkinson et al 2008).

The essential role of c-jun during regeneration after injury is also well illustrated using the slow Wallerian degeneration protein (*WLD*^{s}) mice (Coleman & Freeman 2010). In *WLD*^{s} mice, SCs remain differentiated, were unable to induce c-jun expression and the transected myelinated nerves degenerated much slower than wild-type nerve (Jessen & Mirsky 2008). However, this impaired nerve regeneration in *WLD*^{s} mice was rescued by forcing c-jun expression (Arthur-Farraj et al 2012). Further investigation by Fontana and colleagues suggested that two genes that are directly targeted by c-jun, glial-derived neurotrophic factor (GDNF) and artemin, might mediate c-jun-dependent nerve regeneration, since exogenous delivery of GDNF and artemin to selectively deleted c-jun in SCs mice partially rescued axonal regeneration (Fontana et al 2012a). Therefore, it seems clear that c-jun negatively regulates myelination, and more importantly, c-jun drives the dedifferentiation program and guides axon regeneration after injury.

1.1.2.2. Notch

Notch is a Type I transmembrane receptor and functions as another important negative regulator of SC myelination. The Notch receptor family includes four members (Notch 1-4) that can be activated by five endogenously expressed ligands: Jagged-1, -2 and Delta-1, -3, -4. All four Notch receptors share a similar structure: an extracellular domain consisting of 36 epidermal growth-like repeats and an intracellular domain containing various sequences that are crucial for functions such as receptor transactivation and nuclear localization (Aparicio et al 2013, Deregowski et al 2006,

Jurynczyk & Selmaj 2010, Oberg et al 2001). Notch receptors form heterodimers on the plasma membrane and can be activated by two successive cleavages following ligand binding. Notch is first cleaved by a disintegrin and metalloproteinase (ADAM) at site 2, creating a membrane tethered intermediate, which is then further cleaved by γ-secretase, releasing the Notch intracellular domain (NICD). The NICD then translocates to the nucleus, where it associates with the DNA binding protein (recombination signal-binding protein Jκ (RBPJ) in mammals) and other transcriptional coactivators to bind and activate target genes (Kopan & Ilagan 2009). Notch signaling promotes SC development and aberrant Notch signaling could transform rat SCs (Li et al 2004).

In the context of negatively regulating myelination, Notch appears to be independent of RBPJ, since the NICD suppressed cAMP-induced expression of myelin proteins and Krox-20 in the absence of RBPJ (Woodhoo et al 2009). Interestingly, Notch appears to be able to induce myelin loss even in uncut nerves *in vitro* and *in vivo*. In these studies, adenovirus overexpressing Notch (Ad-NICD) induced myelin damage in myelinated neuron-SCs co-cultures; the same result was obtained when injecting Ad-NICD into intact nerves (Woodhoo et al 2009). Notch also functions in nerve repair. The addition of recombinant Jagged-1 (ligand for Notch 1) promoted nerve regeneration and recovery after nerve injury (Boerboom et al 2017, Wang et al 2015). This indicates that a tight control of Notch signaling is essential for maintaining myelin integrity.

Similar to c-jun, the NICD can be suppressed by Krox-20 expression *in vivo* and *in vitro*. For example, Krox-20 inhibits expression of the NICD in myelinating SCs. Conversely, NICD levels remain high in Krox-$20^{-/-}$ animals (Woodhoo et al 2009). All of

these findings indicate that Notch signaling is a potentially powerful negative regulator of myelination, yet it may play a minor role in comparison with c-jun.

1.1.2.3. Mitogen-activated protein kinases (MAPKs)

Apart from the observation of c-jun and Notch described above, demyelination also requires the engagement of intracellular signaling pathways. The Ras/Raf/ERK pathway was demonstrated both *in vitro* (Harrisingh et al 2004) and *in vivo* (Napoli et al 2012b) to negatively regulate myelination. Raf activation blocks SC differentiation and induces dedifferentiation even in uninjured nerves (Harrisingh et al 2004). Using specially engineered mice with a tamoxifeninducible, Raf-kinase/estrogen receptor fusion protein (RafTR) expressed specifically in myelinating SCs, tamoxifen-induced Raf activation downregulated myelin protein expression and induced demyelination in sciatic nerves. c-Jun and Notch ligand expression were strongly upregulated by Raf activation, placing both c-jun and Notch downstream of ERK signaling (Napoli et al 2012b). Conversely, another group demonstrated that Rac-MKK7-JNK pathway, but not the Raf-ERK pathway, functions as a negative regulator of myelination. They found that inhibition of Rac could suppress c-jun induction in injured nerves, but inhibition of ERK could not. Microarray analysis also showed that the expression of regeneration-associated genes is dependent on Rac but not ERK (Shin et al 2013). It is possible that Rac and Raf function as distinct pathways and the latter does not act through c-jun to regulate myelination.

p38 MAPK has been shown to play a dual role in myelination. Both *in vivo* and *in vitro* inhibition of p38 MAPK blocks SC demyelination, while activation of p38 MAPK by MKK6, a direct and specific upstream activator of p38 MAPK, is sufficient to drive SC demyelination and dedifferentiation following injury. In addition, activation of p38

MAPK suppresses the expression of Krox-20 and induces c-jun expression (Parkinson et al 2004). Therefore, it is possible that c-jun and p38 MAPK function in the same pathway regulating the adoption of an immature SC phenotype after injury (Yang et al 2012). However, using pharmacological inhibitors of p38, other groups reported that p38 MAPK pathway is pro-myelinating. Inhibition of p38 blocked vitamin C induced Krox-20 expression, decreased myelin gene expression, blocked myelination, and these effects could be partially reversed by overexpressing Krox-20 (Haines et al 2008, Hossain et al 2012, Salzer 2008). This seemingly paradoxical role could be the result of differential conditions that trigger the action of p38 MAPK. Though many of the pathways function as upstream regulators of c-jun and Notch, relatively little is known about how the integration of transcriptional mechanisms and signaling pathways affect myelination. However, recent work helps illustrate the role c-jun plays in SC dedifferentiation and neuropathy in the context of a mixed neuropathy called X-linked CMT (CMT1X) (Klein et al 2014).

1.1.3. CMT1X

CMT1X is the second most common type of CMT disease, accounting for nearly 20% of CMT1 cases (Braathen 2012). It is caused by mutations in the gap junction beta 1 gene (*GJB1*) (Gal et al 1985), which encodes the gap junction protein connexin 32 (Cx32). As CMT1X is an X-linked dominant disorder, males are typically more severely affected and manifest an earlier onset of neuromuscular weakness. Milder symptoms and later onset in females have been hypothesized to be associated with X-inactivation (Murphy et al 2012b, Siskind et al 2011). Similar with CMT Type 1A (CMT1A), patients of CMT1X present classic symptoms of muscle weakness and atrophy starting from the

distal leg muscles and slowly progressing to the upper limbs (Shy et al 2007). Foot drop, steppage gait, and pes cavus are common in CMT1X patients. In addition, males tend to have split hand syndrome where the intrinsic muscles of the hand become atrophied (Brennan et al 2015). Based on electrophysiological findings, males usually have intermediate (25-45m/s) motor nerve conduction velocity (MNCV) whereas the MNCV is usually >35m/s in females (Saporta et al 2011). Consistently, compound muscle action potentials (CMAP) are reduced in patients (Birouk et al 1998), indicative of axonal loss in addition to demyelination.

The gap junction protein Cx32 is a four transmembrane spanning protein that localizes to the Schmidt-Lantermann incisures and non-compact myelin (Scherer et al 1995). Six Cx32 monomers form a hemi-channel, and two hemi-channels form a gap junction channel. Depending on the cell specific expression of various connexin family members, hemi-channels can be homotypic, composed of identical hemichannels, or heterotypic (Abrams & Freidin 2015). In the PNS, Cx32 forms homotypic channels (Figure 1.1.3.1, right), whereas in the central nervous system (CNS), Cx32 may form heterotypic channels with other members from the connexin family (Kleopa & Sargiannidou 2015). Cx32 gap junctions form a radial pathway that allow molecules less than 1 kDa to pass through the SC cytoplasm with a thousand-fold shorter distance (Balice-Gordon et al 1998, Scherer et al 1995).

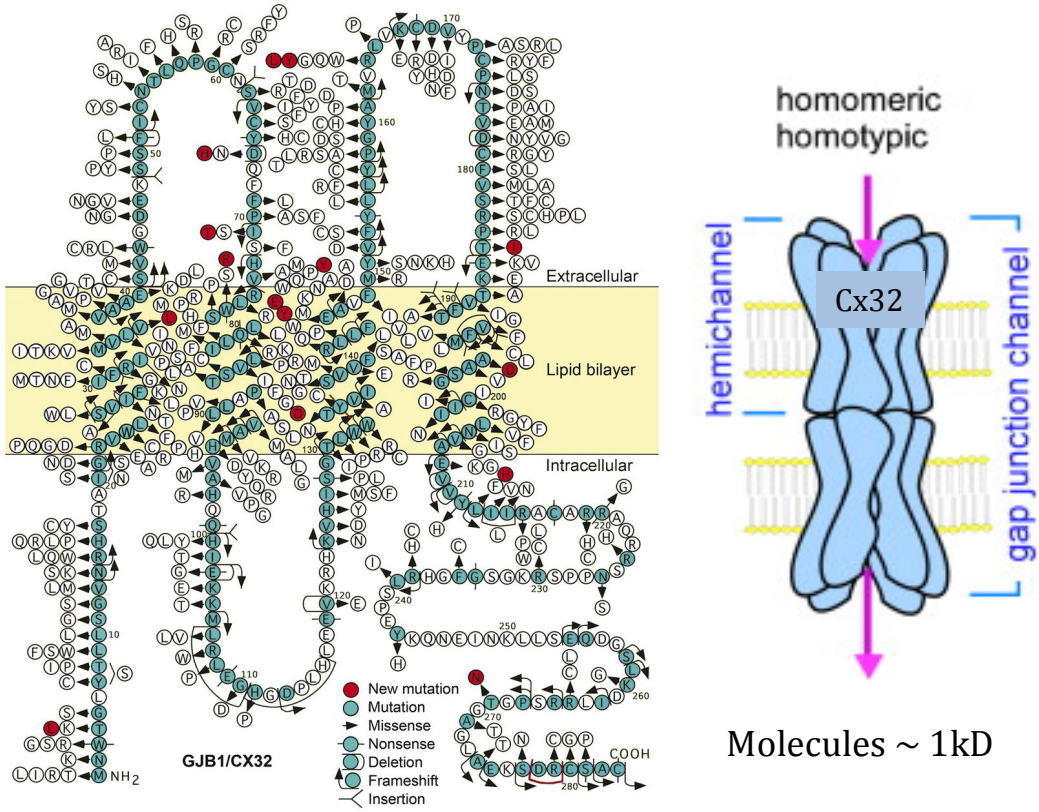

Figure 1.1.3.1 Cx32 gap junction channel and reported mutations.

Illustrations of Cx32 gap junction channel (right) and all 420 Cx32 mutations reported (left). *Adapted from (Kleopa & Sargiannidou 2015, Panosyan et al 2017).*

The loss of function of Cx32 accounts for the peripheral symptoms in CMT1X. Over 400 mutations (Figure 1.1.3.1, left) of the *GJB1* gene have been reported to be associated with CMT1X (Kleopa et al 2012, Panosyan et al 2017). Although most mutations are solely linked to peripheral neuropathic symptoms, the T55I and R75W mutants cause symptoms only in the CNS, (Kleopa et al 2002). Patients with CNS symptoms exhibit pathological changes in visual, acoustic and motor pathways (Bahr et al 1999). It is suspected that a toxic gain of function underlies the symptoms in the CNS (Abrams & Freidin 2015). Moreover, mutations such as R142Q and R164W cause both PNS and CNS symptoms. From *in vitro* studies, the possibility of a mutation causing

CNS manifestations depends on the ability of the mutants to form a gap junction channel (Abrams et al 2017).

Cx32 deficient (Cx32def) mice are used as a mouse model of human CMT1X. Besides an association with liver injury, initial discovery of Cx32def mice revealed that these mice exhibit a progressive neuropathology. The Willecke group did not observe any neurological changes when Cx32def mice were observed at three month of age (Nelles et al 1996). However, later findings showed that axonal pathology precedes demyelination in this model where axonal damage started to occur at 2 months of age (Vavlitou et al 2010). This early predemyelinating axonopathy was associated with an increase in SC c-jun expression and a decrease in the phosphorylation state of axonal neurofilaments, a marker of axon damage (Klein et al 2014)**.** Morphologically, this biochemical damage is reflected by an increase in smaller diameter axons without overall axon dropout, suggesting a decrease in the diameter of existing axons (Vavlitou et al 2010). Functionally, a decrease in neurofilament phosphorylation and axon diameter is associated with decreased nerve conduction velocity (NCV) (Hoffman et al 1987). During the predemyelinating neuropathy, c-jun expression correlates with an increase in GDNF (Klein et al 2014) since c-jun transcriptionally induces GDNF (Arthur-Farraj et al 2012). The precise mechanism of such axonal damage independent of demyelination is so far unknown. However, one possible candidate would be Ca^{2+} since its concentration changes during neural activity and regulates gap junction channel opening. (Anselmi et al 2008, De Vuyst et al 2006, Lev-Ram & Ellisman 1995).

The second stage of CMT1X is a progressive demyelinating neuropathy that begins evolving around 6 months of age in the Cx32def mice. This stage of the

neuropathy is associated with a robust increase in c-jun expression (Klein et al 2014) and is driven by a SC-dependent secondary inflammation that stimulates macrophage-mediated demyelination (Groh et al 2010, Groh et al 2015). Two key proteins contribute to this secondary inflammation. C-C motif chemokine (CCL2) is derived from SCs, is induced transcriptionally by c-jun (Wolter et al 2008) and attracts macrophages to infiltrate the endoneurium (Kohl et al 2010). Colony stimulating factor-1 (CSF-1) is secreted by endoneurial fibroblasts (Groh et al 2016, Groh et al 2015) and activates the macrophages to promote neurodegeneration. Importantly, macrophages directly contribute to myelin degeneration in CMT1X (Martini & Willison 2016) and their role is not secondary to myelin breakdown as seen in Wallerian degeneration (Martini et al 2013).

Though it is unclear how a loss-of-function of Cx32 contributes to the neuropathic phenotype, it is the causal lesion (Scherer & Kleopa 2012) and somatic or embryonic gene therapy would be the gold standard treatment. However, these approaches are difficult to achieve practically or ethically. Alternatively, intrathecal gene delivery of Cx32 in Cx32def mice can markedly improve the motor neuropathy (Kagiava et al 2016), but the clinical path for this approach also has many hurdles. Clearly, a more translationally friendly approach is needed to serve the immediate needs of this neglected patient population. To fill this **significant gap,** we have explored an innovative small molecule approach that is based on modulating molecular chaperones to decrease c-jun expression and neuroinflammation in CMT1X and other peripheral neuropathies.

1.2. Heat shock proteins (Hsps)

Heat shock proteins (Hsps) are a group of highly conserved proteins that function as molecular chaperones to prevent inappropriate interaction within and between peptides, enhance *de novo* protein folding, as well as promoting the refolding of misfolded proteins (Hartl & Hayer-Hartl 2002). Hsps can be classified into six main families based on their molecular weight, i.e. small Hsps (sHsps), Hsp40, Hsp60, Hsp70, Hsp90, and Hsp100 (Saibil 2013). Certain stress conditions, such as temperature elevation, trigger a program known as the heat shock response (HSR) (Figure 1.2.1). Upon activation, heat shock factor 1 (HSF1) dissociates from Hsp90 and undergoes phosphorylation and trimerization. The released HSF1 then enters the nucleus and binds to heat shock elements (HSE) within the promoter region of heat shock genes, leading to the transcription of Hsps, such as Hsp70 (Calabrese et al 2003). The HSR and induction of Hsps serves as a crucial cellular protective mechanism and acts as a first line of defense against numerous conditions that promote proteotoxic stress.

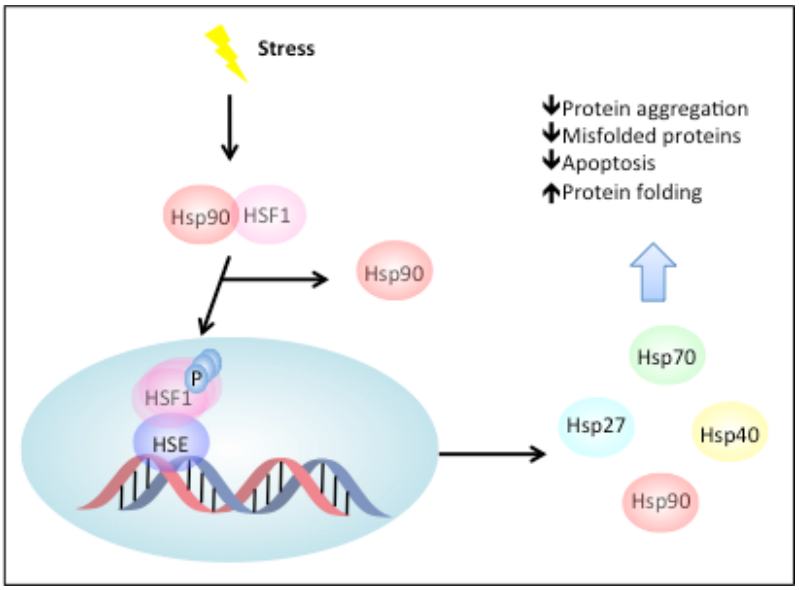

Figure 1.2.1: Schematic illustration of HSR.
Various cellular stresses dissociate HSF1 from the Hsp90-HSF1 complex. Released HSF1 goes through phosphorylation and trimerization before entering the nucleus. HSF1 binding with HSE leads to transcription of Hsps and subsequent changes in the protein quality control system.

1.2.1. Small heat shock proteins (sHsps)

sHsps range from 12-43kDa and they share a common structure containing a conserved α-crystallin domain (ACD) of 80-100 amino acids, a N-terminal domain (NTD) and a C-terminal extension (CTE) (Franck et al 2004, Kappe et al 2003, Kriehuber et al 2010). sHsps can be classified based on their distribution. Class I is widely distributed whereas Class II is restricted to specific tissues. Hsp27 is a stress-inducible Class I sHsp that is ubiquitously expressed, with highest expression in heart, striated and smooth muscles (Taylor & Benjamin, 2005). Besides chaperone activity, Hsp27 is also involved in stabilizing the cytoskeleton, autophagy and exhibits anti-apoptotic and anti-oxidant properties (Asthana et al 2014, Mehlen et al 1996, Perng et al 2009, Taylor & Benjamin 2005). Mutations of the gene encoding Hsp27 lead to neuropathies such as distal motor neuropathy and CMT2 (Muchowski & Wacker 2005). Hsp27 has also been found associated with diabetic peripheral neuropathy (DPN) and results from the

EURODIAB Prospective Complications Study have shown an association between serum Hsp27 levels and the presence of a distal symmetrical polyneuropathy (Gruden et al 2008).

1.2.2. Hsp70

The Hsp70s are a family of ubiquitously expressed Hsps that are involved in a number of processes, including the folding of nascent peptides, refolding of misfolded peptides and protein trafficking (Lackie et al 2017). There are 13 gene products (Table 1.2.2.1) in the human Hsp70 family and they are encoded by a multigene family, including 17 genes and 30 pseudogenes (Radons 2016). Widely studied forms include the cytosolic heat shock cognate 70 (Hsc70), stress-induced cytosolic Hsp72 (Hsp70 in mice), glucose-regulated protein 78 (Grp78) located in the endoplasmic reticulum (ER) and mitochondrial Grp75 (Fink 1999).

Table 1.2.2.1: The human Hsp70 family.

Protein	Alternative names	Gene	Cellular localization	Stress-inducible
Hsp70-1a	Hsp70, Hsp72, Hsp70-1	HSPA1A	Cytosol, nucleus, cell membrane	√
Hsp70-1b	Hsp70, Hsp72, Hsp70-2	HSPA1B	Cytosol, nucleus	√
Hsp70-1t	Hsp70-hom, Hsp70-1L	HSPA1L	Cytosol, nucleus	×
Hsp70-2	Hsp70.2	HSPA2	Cytosol, nucleus, cell membrane	×
Hsp70-5	Bip, Grp78	HSPA5	ER	×

Hsp70-6	Hsp70B'	HSPA6	Cytosol	√
Hsp70-7	Hsp70B	HSPA7	Blood microparticles	√
Hsp70-8	Hsc70, Hsc71, Hsp71, Hsp73	HSPA8	Cytosol, nucleus, cell membrane	×
Hsp70-9	Grp75, HspA9B, MOT, MOT2, PBP74, mot-2, mtHsp70, mortalin	HSPA9	Mitochondria, nucleus	×
Hsp70-12A	FLJ13874, KIAA0417	HSPA12A	Intracellular	×
Hsp70-12B	RP23-32L15.1, 2700081N06Rik	HSPA12B	Endothelial cells, intracellular, blood plasma	×
Hsp70-13	Stch	HSPA13	ER, microsomes	×
Hsp70-14	Hsp70L1	HSPA14	Cytosol, membrane	√

Modified from (Radons 2016)

All Hsp70s share a conserved structure, an N-terminal ATPase domain and a C-terminal substrate binding domain (Tavaria et al 1996), joined together by a short, flexible linker (Jiang et al 2005). The 40kDa N-terminus regulates client association and the 25kDa C-terminal recognizes the hydrophobic residues of substrate proteins (Bukau et al 2006, Rudiger et al 1997). Hsp70 is found in most cellular compartments, and together with its co-chaperone Hsp40, facilitates the stabilization and folding of numerous substrates (Bukau & Horwich 1998). Although Hsp70 is mostly found as a monomer (Bertelsen et al 2009), recent evidence suggests that it can form an antiparallel dimer and aid client protein transfer from Hsp70 to Hsp90. Hsp40 stabilizes the Hsp70

dimer and the transfer of client proteins to Hsp90. In addition, post-translational modifications, such as phosphorylation and acetylation stabilize the dimerization of Hsp70 (Morgner et al 2015).

As Hsps play a role in refolding and degradation of denatured proteins, it is not surprising that Hsp70s levels are elevated in protein aggregation diseases, such as Alzheimer's disease (AD) (Hamos et al 1991, Perez et al 1991). Substantial evidence suggests that an elevated level of Hsp70 could ameliorate the Aβ burden of AD. Overexpression of Hsp70 protects primary neurons against intracellular $A\beta_{42}$-induced toxicity (Magrane et al 2004). Intranasal administration of Hsp70 ameliorated spatial memory deficits and cognitive abnormalities in AD mouse models (Bobkova et al 2014). GRP78, the ER isoform of Hsp70, binds to immature but not mature amyloid precursor protein (APP) and decreases the secretion of $A\beta_{40}$ and $A\beta_{42}$ (Yang et al 1998). Moreover, upregulation of GRP78 by acetyl-L-carnitine (ALCAR), an endogenous mitochondrial membrane compound that helps maintain mitochondrial function, reduced Aβ induced protein oxidation, lipid peroxidation and neuronal loss (Abdul et al 2006). Thus, modulating the expression of Hsp70 paralogs may provide an avenue to treat AD, as well as other neurodegenerative diseases as discussed below.

1.2.3. Hsp70 cochaperones

1.2.3.1. Hsp40

The Hsp40 family, often referred to as the J protein family, function as co-chaperones of Hsp70. Structurally, they share the same conserved J domain that contains about 70 amino acids. Hsp40s can be classified into three classes based on their structure.

Class I proteins have an N-terminal J domain, a Gly Phe-rich region, a zinc finger motif and a C-terminal extension. Class II proteins lack the zinc finger motif and Class III contains all proteins with other structures (Kampinga & Craig 2010). As an Hsp70 cochaperone, Hsp40 first binds to the client protein and prevents its degradation and then delivers it to Hsp70 for further processing. In addition, Hsp40 can simulate Hsp70 ATPase activity. The His, Pro and Asp domain (HPD) is crucial for stimulation of Hsp70 ATPase activity and aiding Hsp70 function. The exact mechanism is unknown but it is proposed that the J domain provides a surface for Hsp70 to interact with the substrate (Greene et al 1998, Jiang et al 2007). ATP hydrolysis can be stimulated by both Hsp40 and the client and causes a conformational change of Hsp70 to stabilize client protein interaction. Hsp40 then leaves and nucleotide exchange factor (NEF) binds to ADP-bound Hsp70 and dissociates ADP. ATP then binds to Hsp70 and the client protein is released following ATP hydrolysis. If the desired conformation of the client protein is not achieved, the above process is repeated (Kampinga & Craig 2010). Various members of the Hsp40 family have been identified to be involved in the progression of Parkinson's Disease (PD) (Hasegawa et al 2017) and upregulation of Hsp40 or Hsp40/Hsp70 may provide a therapeutic strategy to these protein-folding diseases.

1.2.3.2. Heat shock cognate protein 70 (Hsc70) interacting protein (CHIP)

Carboxy terminus of heat shock cognate protein 70 (Hsc70) interacting protein (CHIP) is an E3 ligase that mediates the proteasomal clearance of Hsp70 substrates by directly binding to the C-terminus of Hsp70 (Dickey et al 2007c). CHIP contains three tetratricopeptide repeat (TPR) motifs within its N-terminus, a middle domain and a C-terminal U-box domain (Ballinger et al 1999, Zhang et al 2005). As an important member

of the ubiquitin-proteasome system (UPS), CHIP has dual functions; it is both a co-chaperone of Hsp70 and an E3 ligase. CHIP associates with Hsp70 through the TPR domain, and facilitates the transfer of polyubiquitin chains to substrates (Jiang et al 2001). CHIP also mediates the crosstalk between Hsps and the UPS through Bcl-2 associated athanogene 1 (BAG1), a protein that binds to the 26S proteasome and assists in the degradation of specific Hsp substrates (Lüders et al 2000). Several lines of evidence suggest that CHIP and its associated chaperone complex play a key role in regulating Aβ and tau levels. Kumar *et al.* observed that CHIP could promote the association of ubiquitin with βAPP and forced CHIP and Hsp70/90 expression reduced steady state cellular Aβ levels and accelerated its degradation (Kumar et al 2007). CHIP can also interact with Hsp70/90 directly and promote the ubiquitination of tau (Petrucelli et al 2004).

1.2.4. Hsp90

Hsp90 is another important member of the Hsp family (Smith et al 1998), which helps stabilize misfolded proteins and regulates a variety of signaling proteins, including steroid hormone receptors, tyrosine receptors, nitric oxide synthase and calcineurin (Young & Hartl 2002). Humans have two HSP90 genes that encode constitutively expressed HSP90β and stress inducible HSP90α (Shen et al 1997, Zhang et al 1999).

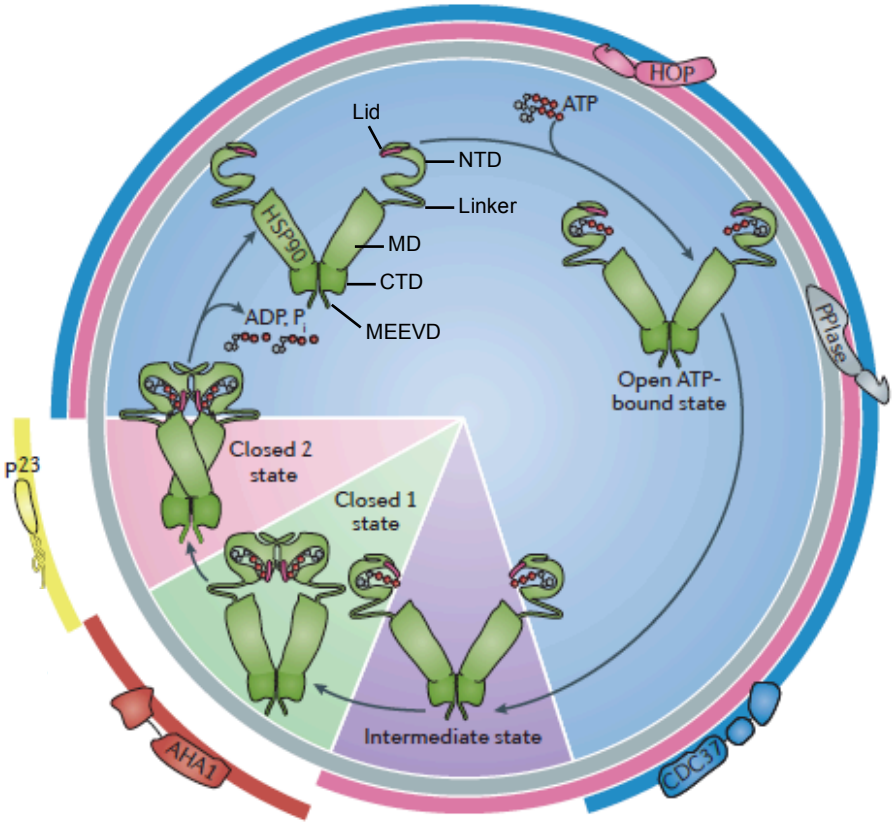

Figure 1.2.4.1: The structure and conformational cycle of Hsp90.
Hsp90 contains an NTD, a flexible linker, MD and CTD. The MEEVD within the CTD is important for interaction with co-chaperones. Upon ATP binding, Hsp90 homodimer transits from an open state to an intermediate state where the lid is closed. Closed 1 state refers to the interaction of NTDs of the monomers and then twisting of the monomers (closed state 2). ATP is then hydrolyzed, releasing ADP and Pi, and Hsp90 returns to the open state. Co-chaperones, HOP, PPIase, AHA-1, CDC37 and p23 assist at different stages. *Adapted from (Schopf et al 2017).*

Hsp90 contains three conserved domains, an NTD, which contains the ATPase activity a middle domain (MD) responsible for binding with clients, and a C-terminal domain (CTD), which is important for dimerization (Harris et al 2004, Prodromou et al 1997). The Met-Glu-Glu-Val-Asp (MEEVD) motif within the C-terminal tail interacts with the TPR domains of co-chaperones (Buchner 1999). Binding with ATP induces a conformational change of Hsp90, to transit the protein from the V- shape open state to an intermediate state, where the lid is closed, followed by a closed 1 state where the NTDs

of the monomers interact. ATP hydrolysis takes place after the monomers twist in the closed 2 state. ADP and Pi are then released and Hsp90 returns to the open state (Cunningham et al 2008, Meyer et al 2003) (Figure 1.2.4.1).

Co-chaperones interact with Hsp90 at different stages. Hsc70/Hsp90-organinzing protein (HOP) binds to Hsp90 and stabilizes the open state (Li et al 2011). HOP is also responsible for the transfer of clients between Hsp70 and Hsp90 (Wegele et al 2006). CDC37 binds to Hsp90 at the open state and is important for the recruitment of client kinases specifically (Li et al 2011, Taipale et al 2012, Taipale et al 2014). Peptidyl-prolyl cis-trans isomerases (PPIases) bind to Hsp90 at all stages whereas activator of Hsp90 ATPase homologue1 (AHA1) binds at closed 1 state and p23 at closed 2 state to facilitate ATP hydrolysis (Li et al 2011).

The expression and activity of Hsp90 can be regulated through multiple mechanisms. Stress dissociates Hsp90 from the Hsp90/HSF1 complex where HSF1 is released and leading to a subsequent increase in Hsp90 transcription and expression (Shi et al 1998). Not surprisingly, PTMs regulate the activity of Hsp90. Phosphorylation slows down the conformational cycle of Hsp90 and affects its interaction with clients and co-chaperones (Mollapour & Neckers 2012, Soroka et al 2012). Acetylation of Hsp90 inhibits its ability to bind co-chaperones (Kovacs et al 2005) while S-nitrosylation impairs the ATPase activity of Hsp90 (Martinez-Ruiz et al 2005). SUMOylation of one Hsp90 protomer is crucial for the recruitment of AHA-1 but not other co-chaperones (Mayer & Le Breton 2015, Mollapour et al 2014).

Hsp90 client proteins have been reported to be involved in a number of diseases, including cancer (Vartholomaiou et al 2016), neurodegenerative diseases (Dickey et al

2007a, Geller et al 2013, Geller et al 2012) and infectious diseases (Geller et al 2012, Roy et al 2012). The stabilization of certain client proteins by Hsp90 generally contributes to the progression of the disease, such as AD and cancer. Thus, inhibiting Hsp90 could serve as a therapeutic strategy in numerous diseases and we have focused on the role of modulating Hsp90 in treating peripheral neuropathies.

1.3. Targeting Hsps to Treat Peripheral Neuropathies

Peripheral neuropathies are generally classified as axonal or demyelinating and manifest from diverse etiologic backgrounds, e.g., genetic, metabolic, autoimmune, drug or trauma-induced. Axonal and demyelinating peripheral neuropathies form the most common group of neurologic disorders and their medical management continues to present a significant medical liability as they affect well over 20 million people in the US alone (Hoke 2012). Peripheral neuropathies are often associated with painful paresthesias that include tingling, prickling or burning sensations, as well as numbness and muscle weakness if motor fibers are involved (Edwards et al 2008). On the molecular side, loss of axonal contact during nerve injury causes myelinated SCs to arrest myelination and dedifferentiate into a phenotype similar to an immature premyelinating SC (Parkinson et al 2008). The dedifferentiated SCs express molecules distinct to this phenotype, such as L1, GDNF, and N-cadherin, in addition to the reactivation of the transcription factor c-jun (Jessen & Mirsky 2008). Demyelinated axons are a common feature in human neuropathies, such as CMT1A and CMT1X (Hutton et al 2011), Refsun disease (Scherer & Wrabetz 2008), chronic inflammatory demyelinating polyneuropathy (Hur et al 2011) and diabetic peripheral neuropathy (Behse et al 1977).

1.3.1. Targeting Hsp90 to Modulate Hsp70 Expression and Treat Peripheral Neuropathies

Since pharmacologically modulating the HSR can serve as a powerful approach to ameliorate neurodegenerative diseases, modulating molecular chaperones may prove beneficial in managing certain neuropathies (Pratt et al 2015). Multiple lines of evidence suggest that modulating Hsp70 is beneficial in a variety of diseases associated with abnormal protein aggregates, such as AD (Magrane et al 2004) and PD (Aridon et al 2011). Unfortunately, small molecule approaches to directly activate or inhibit Hsp70 are not sufficiently evolved for clinical applications (Assimon et al 2013). On the other hand, Hsp70 expression can be indirectly modulated by exploiting Hsp90 as a drug target. However, effective pharmacologic control of Hsp90 to attain a specific therapeutic efficacy requires dissociating cytotoxicity, due to inhibiting the folding of client proteins, from cytoprotection induced by activation of the HSR.

Numerous small molecules have been designed that function as N-terminal Hsp90 inhibitors (Garg et al 2016). N-terminal Hsp90 inhibitors act by blocking the ATPase activity of Hsp90. Inhibiting ATP hydrolysis blocks protein folding and promotes client protein degradation. Since many Hsp90 client proteins are oncoproteins, incomplete folding promotes their degradation and N-terminal Hsp90 inhibitors are being evaluated as chemotherapeutics (Miyata et al 2013). Unfortunately, drug concentrations that induce client protein degradation and cytotoxicity also release HSF1 and induce a HSR. This upregulates the expression of chaperones, such as Hsp70 and Hsp90, which

can facilitate oncoprotein refolding and antagonize the goal of promoting tumor cytotoxicity (Peterson & Blagg 2009).

While increasing Hsp70 may be a problem for chemotherapy, this aspect of targeting Hsp90 may be useful to improve neurodegenerative diseases associated with protein aggregation. In this respect, N-terminal Hsp90 inhibitors can decrease tau aggregation in AD (Dickey et al 2007a, Luo et al 2007b), huntingtin protein in motor neurons (Waza et al 2005) and peripheral myelin protein 22 (PMP22) aggregates in SCs of CMT1A mice (Chittoor-Vinod et al 2015). However, this efficacy does not avoid the issue related to dissociating client protein degradation from induction of the HSR. Now the converse caveat exists, promoting client protein degradation will antagonize the neuroprotective phenotype. Therefore, an effective Hsp90 modulator for treating neurodegeneration requires a drug with a sufficient therapeutic window that can upregulate Hsp70 but induce minimal client protein degradation to antagonize the protective HSR. Though current N-terminal chemotherapeutics have been unable to adequately divest these competing actions, the chemical biology of targeting the C-terminus of Hsp90 has identified such compounds (Anyika et al 2016, Kusuma et al 2012b).

The antibiotic novobiocin weakly binds the Hsp90 C-terminal domain (Marcu et al 2000) and systematic modification of the coumarin ring of novobiocin identified compounds such as KU-32 and KU-174 (Figure 1.3.1.1A and B). KU-174 is an effective cytotoxic compound that contains a biaryl ring system that is necessary to induce degradation of client proteins such as Akt, but without promoting the expression of Hsp70 (Samadi et al 2011). The noviose sugar is critical for these novobiocin derivatives

to interact with the C-terminal domain of Hsp90 (Ghosh et al 2015) but differences in the side chains dictate distinct biologic outcomes. In KU-174, its cytotoxicity is related to the presence of the bulky biaryl side chain that binds to the co-chaperone Aha 1. Aha 1 increases the N-terminal ATPase activity of Hsp90 and disrupting this interaction blocks protein folding and facilitates client protein degradation (Ghosh et al 2015). In contrast, KU-32 contains an ethyl acetamide substitution and induces Hsp70 at concentrations ~500 fold lower than those that promote client protein degradation (Urban et al 2010). The neuroprotective phenotype promoted by KU-32 is highly dependent on the length of the side chain; increasing the length of the alky chain inverts the biologic response leading to inhibition Hsp90-dependent refolding activity, disrupting the interaction between Hsp90 and Aha1 and producing a linear increase in anti-proliferative activity (Ghosh et al 2016).

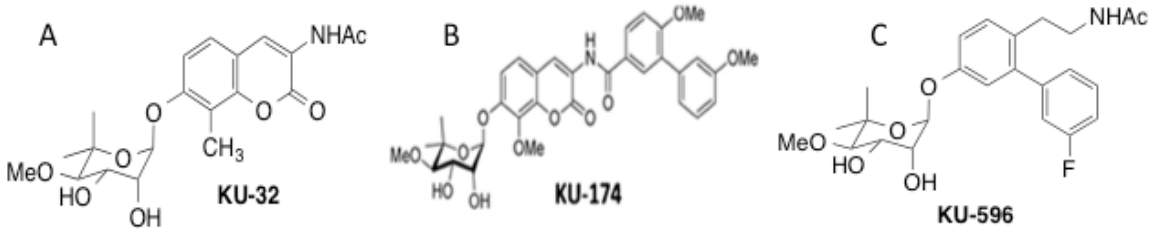

Figure 1.3.1.1: Structures of novologues.
Structures of KU-32 (A), KU-174 (B) and KU-596 (C).

Efforts to further optimize KU-32 led to substitution of a fluorinated biphenyl ring for the coumarin moiety and the identification of KU-596 (Figure 1.3.1.1C) as a new class of C-terminal analogs called novologues (Kusuma et al 2012b) Like KU-32, KU-596 does not bind to Hsp70 and does not induce client protein degradation at concentrations necessary for neuroprotective efficacy. Thus, targeting the C-terminal of Hsp90 provides a sufficient therapeutic window that divests cytotoxicity from

cytoprotection and may facilitate the development of potentially effective neurotherapeutics to treat peripheral neuropathies.

1.3.2. Modulating Hsp70 to Attenuate Protein Aggregates in CMT1A

Historically, targeting Hsp70 to treat neurodegenerative diseases has largely focused on disease etiologies associated with protein aggregation (Pratt et al 2015, Pratt et al 2014). For example, decreasing PMP22 aggregates in CMT1A (Okamoto et al 2013, Rangaraju et al 2008a) or neurofilaments in CMT type 2E (CMT2E) (Gentil et al 2013, Tradewell et al 2009). CMT disease is the most prevalent inherited neuropathy, and is caused by mutations in over 50 genes involved in myelin formation and maintenance. About 90% of diagnosed CMT patients have a mutation in one of four genes, *PMP22, MPZ, GJB1* and *MFN2* (Latour et al 2006, Murphy et al 2012a, Saporta et al 2011). Depending on the neurophysiological manifestations, CMT can be divided into demyelinating (CMT1 and CMT4) and axonal CMT (CMT2) (Brennan et al 2015). Among all subtypes, the autosomal dominant CMT1A accounts for 60%-70% of all CMT patients (Saporta et al 2011). CMT1A is caused by duplication of a 1.5Mb region on the short arm of chromosome 17 that encodes a major component of the peripheral myelin, PMP22 (Lupski et al 1991, Lupski & Garcia 1992). As a demyelinating form of CMT, MNCV of CMT1A patients is often less than 38m/s while compound muscle action potential (CMAP) is rarely affected. Sensory action potentials are reduced or absent (Tazir et al 2014, Vallat et al 2004). Classical CMT symptoms include distal weakness, atrophy, and loss of sensation and foot deformities. Despite intensive research, there is currently no cure and treatment relies only on physical therapy, orthopedic surgeries, supportive braces and pain management (Brennan et al 2015). Though CMT1A is not

lethal, the quality of life of CMT1A patients is impacted in all dimensions. Many studies showed that patients with CMT have significantly lower health-related quality of life scores (El-Abassi et al 2014), which correlates with pain and muscle weakness (Abresch et al 2002, Abresch et al 2001, Burns et al 2010, Calvert et al 2013, Carter et al 1995, Padua et al 2010, Redmond et al 2008). Thus, a quest for potential target for pharmacological intervention is of importance.

PMP22 is an indispensable component of the myelin. PMP22-deficient mice showed delayed onset of myelination, severe demyelination, and functional impairment similar to hereditary neuropathy with liability to pressure palsies (Chance et al 1993, Perea et al 2001). Overexpressed PMP22 will overload the trafficking system and proteasome degradation pathway and form aggregates in a late Golgi compartment (Goldberg 2003, Niemann et al 1999), resulting in demyelination as seen in CMT1A. Molecular chaperones, ubiquitin-proteasomal and lysosomal pathways are found consistently elevated in the affected nerves, but overtime, they fail to prevent the accumulation of PMP22 aggregates (Chittoor et al 2013, Fortun et al 2003, Ryan et al 2002). Following this thought, one approach in trying to find a potential treatment for CMT1A focuses on clearing up the protein aggregates of PMP22 with the help of molecular chaperones.

Geldanamycin, an N-terminal Hsp90 inhibitor, or simply heat shock treatment upregulated the expression levels of Hsps, especially Hsp70, and reduced aggresome formation (Fortun et al 2007, Rangaraju et al 2008b). Another Hsp90 inhibitor, EC137 showed similar effects in SC-DRG co-cultures prepared from CMT1A mouse model (Rangaraju et al 2008b). Furthermore, the same lab reported that the Hsp90 inhibitor

BIIB021 helps attenuate the proteasome dysfunction in cells from a CMT1A patient in an Hsp70 dependent manner (Chittoor-Vinod et al 2015). Taken together, inducing Hsp70 seems a promising therapeutic strategy for CMT1A.

Though targeting Hsp70 to treat neurodegenerative diseases has been limited to etiologies associated with protein aggregation, over the last seven years, we have unambiguously demonstrated that novologue therapy decreases inflammation, increases the density of unmyelinated sensory fibers and reverses electrophysiologic, bioenergetic and psychosensory deficits of diabetic peripheral neuropathy (DPN) in an Hsp70-dependent manner (Ma et al 2014, Ma et al 2015, Urban et al 2010, Urban et al 2012, Zhang et al 2012). Since the etiology of DPN is not linked to protein aggregation, this work has presented a new paradigm that modulating Hsp70 is inherently neuroprotective and may ameliorate DPN by increasing neuronal tolerance to diabetic stress (Calcutt 2010). The ability of Hsp70 to treat neuropathies with differing etiologies is linked to its role in refolding and/or removing damaged or disease-modifying proteins in a cell distinct manner. This lack of mechanistic selectivity for neuroprotection by Hsp70 is not a drawback but represents a flexible paradigm for translational development. Thus, an effective therapeutic approach for treating complex, chronic neurodegenerative diseases may not require targeting a single pathway or protein that contributes to disease onset or progression (Dobrowsky 2016), but benefit from increasing the activity of inherently neuroprotective pathways associated with Hsp70.

1.3.3. Modulating Chaperones to Treat Diabetic Peripheral Neuropathy

According to the Center for Disease Control and Prevention, 30.3 million (about 9.4% US population) people had diabetes in 2017. Diabetes is associated with the onset

of a variety of complications including autonomic neuropathy, retinopathy, nephropathy, and DPN (Balakumar et al 2009). DPN is the most prevalent complication of diabetes and often manifests as a distal, symmetric, sensorimotor neuropathy that exhibits a stocking-glove distribution since symptoms start in the feet or hands and progress proximally. DPN arises due to the degeneration of small, unmyelinated or thinly myelinated sensory fibers that mediate pain/temperature sensation (C and Aδ fibers) and larger myelinated fibers that are involved primarily in tactile sensation (Aβ fibers) (Zochodne 2007). Diabetes-induced changes in unmyelinated C-fibers lead to the development of small fiber neuropathy that often produces localized painful (positive) symptoms while degeneration of thinly myelinated Aδ fibers produces a more diffuse pain. Progressive neurodegeneration often resolves the neuropathic pain, but decreased response thresholds (Lennertz et al 2011) and loss of epidermal innervation of C-fibers in the feet (Beiswenger et al 2008) can contribute to insensate neuropathic symptoms such as thermal hypoalgesia. Similarly, degeneration of Aβ fibers leads to a loss of vibration and tactile sensation (Christianson et al 2007) with eventual segmental demyelination in long-term DPN (Zochodne 2007). Patients with insensate DPN are at high risk to develop foot ulcerations and DPN is the number one cause of non-traumatic lower-limb amputations (Callaghan et al 2012, Gordois et al 2003, Margolis et al 2011). Current FDA approved treatments for DPN target mainly painful neuropathy (Griebeler et al 2014) but no FDA approved pharmacologic options are available for patients with insensate neuropathy (Calcutt et al 2009).

In individuals with Type 1 diabetes, data from the Diabetes Control and Complications Trial provided substantial support for the hypothesis that DPN develops

because of increased blood glucose levels (DCCT Research Group 1988, DCCT Research Group et al 1993). However, this relationship is not as central to the pathogenesis of DPN in individuals with Type 2 diabetes since insulin deficiency/resistance and dyslipidemia may be critical contributors (Kim & Feldman 2012, Wiggin et al 2008). Moreover, hyperglycemia and dyslipidemia provoke downstream alterations in numerous pathways that have been well characterized to contribute to DPN. This includes enhanced activity of the polyol pathway, protein kinase C and poly(ADP-ribose) polymerase, an increase in inflammatory pathways, protein modification by advanced glycation end products and N-acetylglucosamine, increased oxidative and nitrosative stress, decreased neuronal mitochondrial bioenergetics and a reduction in neurotrophic factor support (Feldman et al 2017, Pop-Busui et al 2016).

Although targeting any one of these pathways in animal models of DPN can improve neuropathic endpoints, this success has not resulted in any translational advancements in treating human DPN. One difficulty in treating DPN is that the contribution of these various metabolic insults to the onset of the neuropathy does not necessarily occur in a temporally and/or biochemically uniform fashion. In the absence of identifying a convergent node critical to disease progression, it is likely that multiple pathways lead to the progressive distal axonopathy and poor regenerative potential that characterize diabetic neuropathy. Alternatively, an effective therapeutic approach for treating complex, chronic neurodegenerative diseases may benefit from increasing the activity of inherently neuroprotective pathways associated with molecular chaperone signaling. For example, overexpression of Hsp70 can reduce reactive oxygen species (ROS) under hypoxia (Guo et al 2007) and improve mitochondrial function in neurons

after ischemia (Xu et al 2010). Similarly, we have shown C-terminal Hsp90 modulators can improve DPN in an Hsp70-dependent manner.

KU-32 was the first C-terminal Hsp90 modulator shown to reverse a sensory hypoalgesia and loss of intra-epidermal nerve fibers in diabetic mice, a morphologic marker of small fiber damage in DPN (Urban et al 2010, Urban et al 2012). Using Hsp70 knockout (KO) mice, this study also linked Hsp70 to drug efficacy. Although the absence of Hsp70 did not interfere with the development of DPN in Hsp70 KO mice, it did abrogate the ability of KU-32 to improve the sensory hypoalgesia. Mechanistically, KU-32 improved mitochondrial bioenergetic deficits in models of type 1 and type 2 diabetes in an Hsp70 dependent manner (Ma et al 2014). In addition, Hsp70 induction correlated with decrease in inflammatory markers and improvement in painful neuropathy (Ortmann & Chattopadhyay 2014, Yoon et al 2015).

KU-596 is a next generation novologue that showed greater Hsp70 induction and a 14-fold greater efficacy in preventing glucose induced toxicity of sensory neurons (Kusuma et al 2012b). RNA-sequencing results from diabetic mice receiving weekly doses of KU-596 showed that it reversed a diabetes-induced increase in inflammatory in a largely Hsp70-dependent manner (Ma et al 2015). Taken together, this indicates that Hsp70 inducers may provide a promising approach in the treatment of DPN and other neuropathies.

1.3.4. Modulating Hsp70 to Treat Demyelinating Neuropathies

The goal of this work was to assess whether KU-596 could improve a demyelinating neuropathy whose etiology was unassociated with protein aggregation, but linked to changes in c-jun expression and inflammation. To this end, we employed two

mouse models of demyelinating neuropathy to test the effects of *in vivo* treatment with KU-596 *on biochemical, physiological and morphological measures of neuropathy.* The first mouse model we used is the MPZ-Raf mice and is described in Chapter 2. These mice express a tamoxifen inducible, estrogen receptor fused with Raf kinase, downstream of the SC-specific promoter, P0. After a series of tamoxifen injections, MPZ-Raf mice displayed a demyelinating neuropathy induced specifically by SC c-jun. This mouse line was crossed with Hsp70KO mice to study the role of Hsp70 in drug action. Studies conducted with these models provided proof-of principle that KU-596 may be effective in treating demyelinating neuropathies. Though powerful, this transgenic mouse model has certain drawbacks. For example, the motor deficits occurred within the first 10 days, which makes it extremely difficult to optimize the experimental design to maximize the effects of KU-596. More importantly, this model does not mimic any complexities in axonal/demyelinating neuropathies, not to mention it does not recapitulate any real human diseases. To circumvent these issues, we complemented our study with Cx32def mice, a mouse model of CMT1X.

As described in Section 1.1.3 and Chapter 3, recent evidence suggests that elevated c-jun expression is associated with the progression of the disease (Klein et al 2014). The mechanistic goal of these studies was to test whether KU-596 could ameliorate the neurodegeneration and examine if regulating c-jun expression was involved in the mechanism of drug action and determine if Hsp70 was also critical for drug efficacy in the context of the genetic deletion of Cx32. Our translational goal is to identify if KU-596 may provide an avenue for the therapeutic management of CMT1X since this

compound is poised to enter Phase 2 clinical trials for treating various peripheral neuropathies.

Chapter 2. Targeting Heat Shock Protein 70 to Ameliorate c-Jun Expression and Improve Demyelinating Neuropathy

Reprinted (adapted) with permission from Zhang, Z., Li, C., Fowler, S. C., Zheng, Z., Blagg, B.S.J., and Dobrowsky, R.T. (2018) Targeting Heat Shock Protein 70 to Ameliorate c-Jun Expression and Improve Demyelinating Neuropathy. *ACS Chem Neurosci.* **9**, 381-390.

Abstract

Increased expression of the c-jun transcription factor occurs in a variety of human neuropathies and is critical in promoting Schwann cell (SC) dedifferentiation and loss of the myelinated phenotype. Using cell culture models, we previously identified KU-32 as a novobiocin-based C-terminal heat shock protein 90 (Hsp90) inhibitor that decreased c-jun expression and the extent of demyelination. Additional chemical optimization has yielded KU-596 as a neuroprotective novologue whose mechanistic efficacy to improve a metabolic neuropathy requires the expression of Hsp70. The current study examined whether KU-596 therapy could decrease c-jun expression and improve motor function in an inducible transgenic model of a SC-specific demyelinating neuropathy (MPZ-Raf mice). Treating MPZ-Raf mice with tamoxifen activates the MAPK kinase pathway, increases c-jun expression and produces a profound demyelinating neuropathy characterized by a loss of motor function and paraparesis. KU-596 therapy did not interfere with MAPK activation but reduced c-jun expression, significantly improved motor performance and ameliorated the extent of peripheral nerve demyelination in both prevention and intervention studies. Hsp70 was necessary for the drug's neuroprotective

efficacy since MPZ-Raf × Hsp70 knockout mice did not respond to KU-596 therapy. Collectively, our data indicate that modulating Hsp70 may provide a novel therapeutic approach to attenuate SC c-jun expression and ameliorate the onset of certain demyelinating neuropathies in humans.

2.1. Introduction

Peripheral neuropathies are generally classified as axonal or demyelinating and manifest from diverse etiologic backgrounds, e.g., genetic, metabolic, autoimmune, drug or trauma-induced. Demyelinating neuropathies are typically characterized by damaged myelin but intact axons. At the molecular level, recent evidence suggests that the c-jun transcription factor is a critical node in regulating demyelination (Parkinson et al 2008). Interestingly, upregulation of c-jun is reported in human axonal and demyelinating neuropathies including Charcot-Marie-Tooth disease (CMT) Type 1A (CMT1A), X-linked CMT (CMT1X) and chronic inflammatory demyelinating polyneuropathy (Hur et al 2011, Hutton et al 2011). However, it remains unclear if targeting c-jun may provide a viable approach to ameliorate certain neuropathies.

c-Jun is highly expressed in immature Schwann cells (SC) and is downregulated as SC begin to myelinate (Mirsky et al 2008). Although c-jun is minimally expressed in healthy nerves, it is rapidly upregulated in pathological or injured nerves. During nerve injury, loss of axonal contact causes myelinated SC to arrest myelination and dedifferentiate into an immature phenotype (Parkinson et al 2008). c-Jun is required for SC dedifferentiation since its SC-specific deletion results in a marked delay in the rate of myelin sheath degradation (Parkinson et al 2008). However, despite the role of c-jun-N-terminal kinase (JNK) in regulating the transcriptional activity of c-jun by phosphorylation, c-jun-mediated demyelination appears to be independent of this pathway (Parkinson et al 2008, Raivich & Behrens 2006). Thus, pharmacological approaches that antagonize c-jun expression may yield a novel strategy to treat certain human neuropathies. To this end, we have found that modulating molecular chaperones

can antagonize the expression of c-jun and subsequent demyelination in SC-DRG (dorsal root ganglia) co-cultures (Li et al 2012b).

Molecular chaperones, such as heat shock proteins 70 (Hsp70) and Hsp90, function in the folding of nascent polypeptides, refolding of misfolded proteins and the clearing of damaged proteins or protein aggregates (Pratt et al 2015, Pratt et al 2014). Hsp90 contains N- and C-terminal nucleotide-binding domains that are joined by a middle domain, which binds co-chaperones, client proteins and the transcription factor, heat shock factor 1 (HSF1) (Ciglia et al 2014). The C-terminal domain is essential for forming a functional Hsp90 homodimer and the N-terminal ATPase is required for the protein's chaperone activity (Ciglia et al 2014, Hall et al 2014). Through its intrinsic ATPase activity and interaction with co-chaperones, isomerases and immunophilins, Hsp90 directs the folding of "client" proteins into their biologically active conformations (Assimon et al 2013, Dekker et al 2015, Peterson & Blagg 2009). Inhibiting this ATPase activity can increase client protein degradation and may be useful in treating certain malignancies. However, Hsp90 also serves another important biologic role since it is a direct regulator of the cellular heat shock response (HSR) by binding to HSF1 and suppressing its transactivating capacity (Vihervaara & Sistonen 2014). Upon exposure to proteotoxic stress or binding of small molecules, conformational changes in Hsp90 disrupt its interaction with HSF1 and lead to the transcriptional induction of cytoprotective proteins, such as Hsp70.

Modulating Hsp70 expression is emerging as an attractive target to improve neurodegenerative diseases associated with protein aggregation. In this respect, N-terminal Hsp90 inhibitors have been reported to decrease tau aggregation in Alzheimer's

disease (Dickey et al 2007a, Luo et al 2007b), huntingtin protein in motor neurons (Waza et al 2005) and PMP22 aggregates in CMT1A mice (Chittoor-Vinod et al 2015). However, many N-terminal inhibitors are unable to dissociate client protein degradation from induction of the HSR. This limitation can increase the degradation of Hsp90 client proteins necessary for normal cell homeostasis and antagonize the neuroprotective phenotype. Therefore, an effective Hsp90 modulator for treating neurodegeneration requires a drug with a sufficient therapeutic window that can upregulate Hsp70 but induce minimal client protein degradation to antagonize the protective HSR. To this end, we have identified a series of compounds called novologues that bind to the C-terminal domain of Hsp90 and induce Hsp70 at concentrations ~500 fold lower than those that promote client protein degradation (Kusuma et al 2012b, Urban et al 2010).

KU-596 (Figure 2.3.1.1A) is a highly bioavailable novologue that has shown efficacy in improving sensory deficits in models of diabetic peripheral neuropathy (Ma et al 2015). The current study assessed the ability of KU-596, to prevent c-jun-induced demyelination in two transgenic mouse models of a SC-specific demyelinating motor neuropathy (Napoli et al 2012a). These proof-of-concept data suggest that attenuating c-jun induction may provide a novel therapeutic strategy in treating certain demyelinating neuropathies.

2.2. Materials and Methods

Corn oil (CO), p-phenylenediamine and dimethyl sulfoxide (DMSO) were purchased from Sigma-Aldrich (St. Louis, MO). Tamoxifen (TMX) was purchased from Cayman Chemical (Ann Arbor, MI). KU-596, N-(2-(5-(((3R,4S,5R)-3,4-dihydroxy-5-methoxy-6,6-dimethyltetrahydro-2H-pyran-2-yl)oxy)-3′-fluoro-[1,1′-bi- phenyl]-2-yl)ethyl)-

acetamide was synthesized as previously described (Kusuma et al 2012b). Compound purity routinely exceeded 95%.

c-Jun antibody was purchased from Cell Signaling Technology (#9165**,** Danvers, MA). Biotinylated Hsp70 antibody was purchased from Enzo Life Sciences (#ADI-SPA-810B, Farmingdale, NY). β-actin antibody, GAPDH antibody, goat anti-mouse HRP conjugated secondary antibody and goat anti-rabbit HRP conjugated secondary antibody were purchased from Santa Cruz Biotechnology (Santa Cruz, CA). Goat anti-rabbit Alexa Fluor-647 conjugated secondary antibody, streptavidin-HRP and Diamond prolong antifade mounting solution with 4',6-diamidino-2-phenylindole (DAPI) were purchased from Thermo-Fisher Scientific Inc. (Grand Island, NY).

Tissue-Tek Optimum cutting temperature (OCT) was purchased from Electron Microscopy Sciences (Hatfield, PA). Captisol (CAP) was purchased from Cydex Pharmaceuticals Inc. (Lenexa, KS)

2.2.1. Animals

Hemizygous MPZ-Raf mice were obtained from Jackson Laboratory (Bar Harbor, ME) and bred to homozygosity. Hsp70.1/Hsp70.3 knockout (Hsp70 KO) were originally obtained from the Mutant Mouse Resource and Research Center (Davis, CA) and MPZ-Raf$^{+/+}$ × Hsp70 KO mice were generated by crossing the strains. The Raf transgene was confirmed using the following primers (forward:GCAGCCCACACTGAGGATA; reverse:TTGATCGAGTAATCCCCAGCAG,1.1kb). Hsp70 was detected using (forward:GTACACTTTAAACTCCCTCC; reverse:CTGCTTCTCTTGTCTTCG, 450bp) while the Hsp70 KO was verified using (forward: ATGGGATCGGCCATTGAACAAG and reverse:ACTCGTCAAGAAGGCGATAGAAGG, 850 bp). The reactions contained

1x PCR buffer, 0.5 mM dNTPs, 0.5 mM of each primer, 200–300ng genomic DNA and 0.2U Omni KlenTaq polymerase (DNA Polymerase Technology, St Louis, MO). PCR conditions were: (94^{o}C for 5 min; 35 cycles of 94^{o}C for 30s; 65^{o}C for 30s; 72^{o}C for 30s; 72^{o}C for 5 min). All animals were maintained on a 12h light/dark cycle and given ad libitum access to chow (NIH diet 7005) and water.

Demyelination was induced by intraperitoneal injection of 2 mg of TMX in CO on administration schedules that are indicated in the text. A stock solution of 4 mg/ml KU-596 in 0.1M Captisol in phosphate-buffered saline (PBS) was prepared and animals were dosed by oral gavage (0.2 ml) with the dose and administration schedules indicated in the text. Control animals received identical doses of CO and 0.1M Captisol only. All animals were randomly assigned to each treatment group and both male and female mice were used in all experiments. TMX treated mice showing extensive limb paralysis were monitored closely with veterinary supervision, given moistened food directly on the cage floor and euthanized if they were unable to access food and water or reached a body condition score of 1 (Ullman-Cullere & Foltz 1999). All procedures complied with protocols approved by the Institutional Animal Care and Use Committee and with National Institutes of Health standards and regulations for the care and use of laboratory rodents.

2.2.2. Immunoblot analysis

Sciatic nerves were homogenized and sonicated in lysis buffer containing 50mM Tris-HCl, pH 7.4, 150mM NaCl, 1mM EDTA, 1% NP-40, 1% deoxycholate, 0.1% SDS, 0.5 mM sodium orthovandate, 40mM NaF, 10mM β-glycerophosphate and 1X Complete Protease Inhibitors. Lysates were centrifuged at 10,000 x g for 10 min at 4^{o}C and protein

concentration was determined using the *DC* (detergent compatible) protein assay (Bio-Rad Laboratories, Inc.) with bovine serum albumin as the standard. 20μg of protein was separated by SDS/PAGE and transferred to nitrocellulose membrane for immunoblot analysis. The membranes were blocked for 1h with 5% non-fat milk in PBS with 0.1% Tween-20 (PBST) and incubated with primary antibodies overnight at 4^{o}C. Membranes were washed 3 times with PBST and incubated with HRP-conjugated goat anti-rabbit or goat anti-mouse secondary antibodies for 2h at room temperature. Following 3 washes with PBST, immunoreactivity was visualized using enhanced chemiluminescence detection kit (GE Healthcare Life Sciences). The films were scanned and the density of each blot was analyzed using Image J.

2.2.3. Immunofluorescence analysis

Sciatic nerves were harvested from MPZ-Raf mice and immersed in Zamboni's fixative overnight at 4°C. Nerves were washed with PBS and cryoprotected in 30% sucrose until the desired dehydration was achieved. Nerves were mounted in OCT and cut at 10 μm using a cryostat. Cryosections were collected onto charged slides and stored at -80^{o}C until use. Sections were re-hydrated with PBS (3x for 5 min) and permeabilized with 0.1% Triton X-100 in PBS for 20 min at room temperature. Tissues were incubated overnight at 4^{o}C with primary antibodies diluted in 10% normal goat serum in PBS. Sections were washed with PBS and incubated with goat anti-rabbit Alexa Fluor-647 conjugated secondary antibody for 2h at room temperature. Slides were mounted with Diamond prolong antifade with DAPI and imaged on an Olympus/3I Spinning Disk Confocal/TRIF Inverted Microscope. 5 random sections were captured using SlideBook 6.4 (Intelligent Imaging Innovations Inc.). The number of c-jun positive profiles per

section was quantified using CellProfiler. Individual nuclei with a diameter of 15-120 pixels were identified using Otsu's thresholding method. Identified nuclei with c-jun intensity greater than 0.03 were classified as positive.

2.2.4. Teased Nerve fibers

Teased nerves were prepared as previously described (Viader et al 2011). Sciatic nerves were harvested and fixed with 3% glutaraldehyde overnight at 4°C. Following 3 washes with 0.1M phosphate buffer, nerves were secondarily fixed with 1% osmium tetroxide and 1.5% potassium ferricyanide in 0.5M phosphate buffer for 1 hour. Nerves were washed with PBS and incubated with a series of glycerol solutions (33%, 66%, 100%) for 6h each. Nerves were stained with 0.6% Sudan Black in 70% ethanol for 30 min, washed with 70% ethanol and water and stored in glycerol. Nerves were teased in glycerol on glass slides, allowed to dry and examined under a light microscope.

2.2.5. Nerve Cross sections

Sciatic nerves were fixed in 2.5% glutaraldehyde in 0.1M HEPES, pH 7.4 for 24h at 4^{o}C. Nerves were then washed with 0.1M HEPES and secondarily fixed with 2% osmium tetroxide for 2h. After washing twice with distilled water, nerves were dehydrated with a series of 30%, 50%, 70% ethanol solutions for 10 min each. Nerves were then rinsed twice with 95% ethanol, 100% ethanol and propylene oxide for 15 min. The nerves were placed in a mixture of 50% propylene oxide and 50% resin for 2h, transferred into 100% resin and placed in a vacuum chamber overnight. Nerves were embedded in flat embedding molds (Ted Pella Inc.) with 100% resin and put in an oven overnight at 60^{o}C. 1 μm sections were obtained using a Leica Ultratome system (Leica Microsystems Inc.). Sections were collected onto glass slides and stained with 2% p-

phenylenediamine in 50% ethanol for 10s on a hot plate at 65°C. Slides were washed, a coverslip adhered and examined by light microscopy.

2.2.6. Behavioral Tests

Mice were placed on an accelerating rotorod (4-40 rpm) (Med Associate Inc, Fairfax, VT) for 5 trials each day with a cutoff of 300s per trial. The latency to fall was recorded and the median of the 5 trials was determined. Mice were trained for 5 days before the start of a study and were tested every other day.

As a second assessment of motor function, locomotor activity was quantified with high temporal (10 ms) and spatial (2 mm) resolution using a force-plate actometer (FPA) (Bioanalytical Systems Inc.) (Fowler et al 2009, McKerchar et al 2006). Mice were placed in the FPA chamber for a 10 min session as previously described (Fowler et al 2001). Data was analyzed using custom-written Free Pascal software and the distance traveled in the chamber was calculated. The FPA also measures ambulation rhythmicity (stride) and force of paw placement during the strides. The resulting force-time waveform reflects the rhythmicity of ambulation while the amplitude of the wave measures the force of paw placement during the series of strides. The force data is normalized to body weight (%bw) so that variations in amplitude are independent of this variable (Fowler et al 2009). Max power and integrated power output were calculated after Fourier transformation of the force-time waveform data using a Hanning data window and Matlab's Signal Processing Toolbox.

2.2.7. Statistical Tests

Data are presented as means ± standard error of the mean (SEM). After verifying equality of variance between groups, parametric data were assessed using a one-way

analysis of variance (ANOVA) and Tukey's post-hoc test. Non-parametric data were analyzed using a Kruskal–Wallis and Dunn's test. A p value < 0.05 was considered significant and for clarity, only this value is listed even if the significance was lower. All analyses were performed using Systat (v13.1), ProStat (v4.83) or R (v3.4.1) software.

2.3. Results

2.3.1. KU-596 decreased TMX-induced c-jun expression

To investigate the *in vivo* efficacy of KU-596 to attenuate c-jun-induced demyelination, we utilized MPZ-Raf mice. MPZ-Raf mice express a human Raf kinase gene fused to a modified estrogen receptor ligand binding domain downstream of the myelin protein zero (MPZ) promoter (Napoli et al 2012a). MPZ is expressed specifically in SCs and is an important structural component of peripheral nerve myelin. TMX administration activates the Raf kinase-fusion protein in myelinated SCs and drives downstream activation of the p42/p44 mitogen-activated protein kinase (MAPK) pathway, which induces the expression of c-jun. MAPK activation and c-jun induction promotes a rapid and robust motor neuropathy characterized by severe demyelination of peripheral nerves (Napoli et al 2012a).

Male and female MPZ-Raf mice were treated with 2 mg TMX dissolved in corn oil (CO) every other day for 14 days to induce MAPK activation. KU-596 (20 mg/kg) or vehicle (0.1M Captisol, CAP) was given orally on alternate days starting from day 0 (Figure 2.3.1.1B). The dose of KU-596 was chosen based on prior studies that 20 mg/kg of the drug could improve diabetic peripheral neuropathy. After 14 days, the mice were euthanized and immunoblot analysis of sciatic nerve lysates was performed. As expected, treating the MPZ-Raf mice with TMX induced the phosphorylation of MAPK (pMAPK)

and increased c-jun expression in sciatic nerve (Figure 2.3.1.1C and D). Although KU-596 treatment did not alter the activation of MAPK, it significantly reduced the level of c-jun (Figure 2.3.1.1D). Since KU-596 did not decrease pMAPK, the decline in c-jun expression is downstream of MAPK activation. Importantly, these results were confirmed using cross sections of sciatic nerves stained with antibodies against c-jun and myelin basic protein (MBP) (Figure 2.3.1.1E and F). TMX increased the number of c-jun positive nuclei and this was significantly attenuated by KU-596. Similarly, TMX also decreased MBP immunoreactivity, which was markedly improved by KU-596 treatment. No c-jun positive nuclei were noted in animals that received only CO and KU-596.

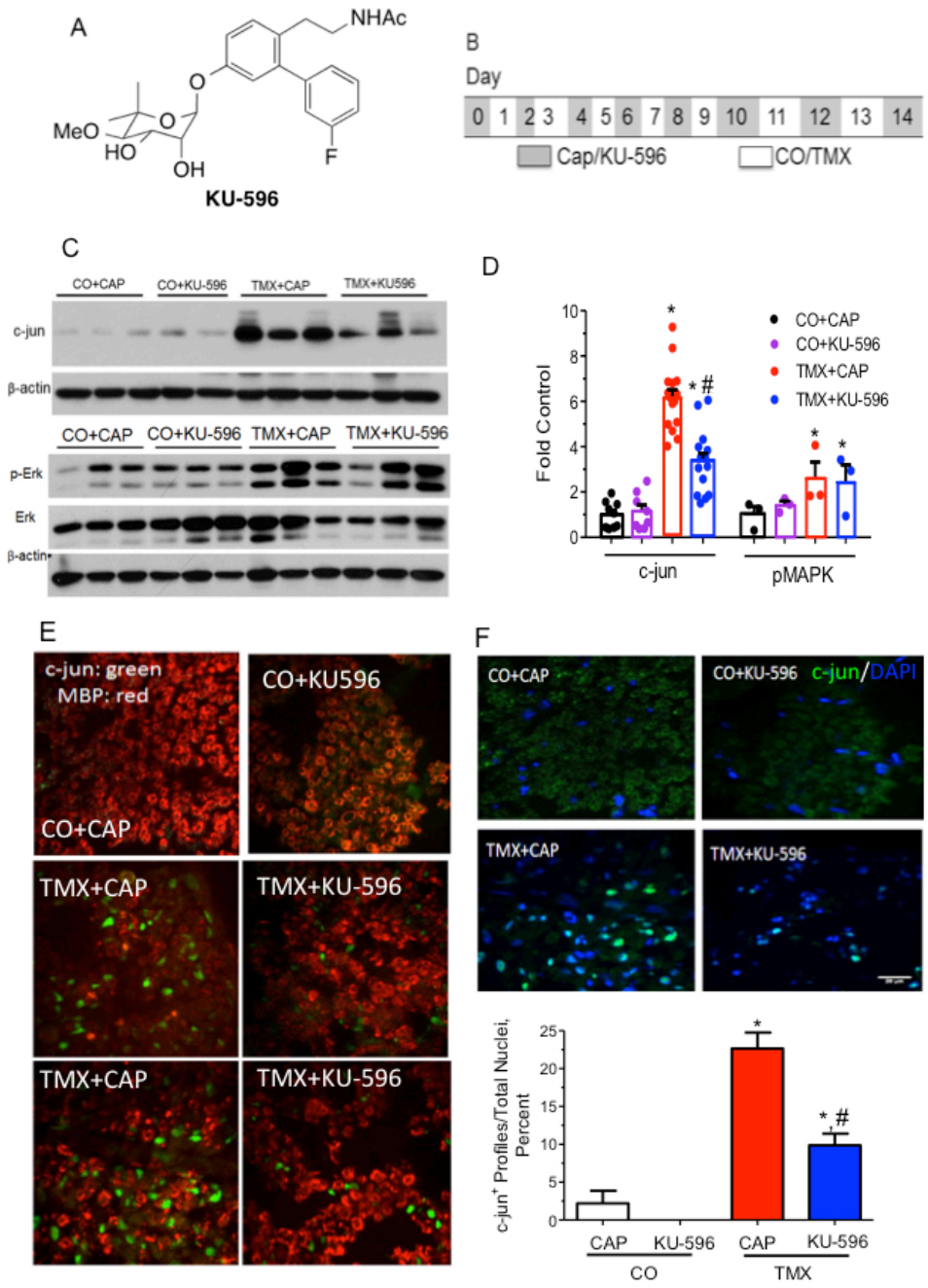

Figure 2.3.1.1: KU-596 decreases c-jun expression in TMX treated MPZ-RAF mice.
A) Structure of KU-596. B) Dosing regimen of MPZ-RAF mice. Mice were treated with Captisol (CAP) or KU-596 (20mg/kg) every other day for 14 days starting from Day 0. Beginning on day 1, mice received corn oil (CO) or 2 mg tamoxifen (TMX) every other day for 14 days. C) Mice were sacrificed on day 15, lysates of the sciatic nerves prepared and pMAPK, total MAPK, c-jun and β-actin levels determined by immunoblot analysis. D) Quantification of pMAPK (n=3 per group) and c-jun expression (CO+CAP, n=9; CO+KU-596, n=8; TMX+CAP, n=15; TMX+KU-596, n=15). *, $p<0.05$ compared with CO+CAP. #, $p<0.05$ compared with TMX+CAP. E) Immunostaining of sciatic nerve cross-sections of MPZ-RAF mice. Frozen sections were stained for c-jun (green) and MBP (red). F) Frozen sections were stained for c-jun (green) and nuclei were visualized with DAPI. The number of c-jun positive nuclei were counted and normalized to

the total number of nuclei in two sections obtained from 3 animals per group. *, $p<0.05$ compared with CO+CAP. #, $p<0.05$ compared with TMX+CAP. Scale bar=20μm.

2.3.2. KU-596 improves demyelination in MPZ-Raf mice

To determine the effect of KU-596 on myelination profiles, MPZ-RAF mice were treated with TMX and KU-596 using the dosing schedule shown in Figure 2.3.1.1B. Sciatic nerves were fixed with osmium tetroxide, teased in glycerol and examined under a light microscope. Whereas control mice (CO+CAP, CO+KU-596) showed normal myelination with well demarcated nodes of Ranvier, nerves from TMX+CAP treated mice showed large regions denuded of myelin (Figure 2.3.2.1A). Although KU-596 trended toward reducing the length of the demyelinated region, the effect was variable (Figure 2.3.2.1B). To further quantify the effect, a teased fiber was considered damaged if the distance between two myelinated sections was at least 10% greater than the average distance between internodes of CO+CAP treated animals (Figure 2.3.2.1B). By this criterion, the drug significantly decreased the percentage of damaged fibers (Figure 2.3.2.1C). In addition, cross sections of sciatic nerves indicated an increased number of abnormally myelinated fibers in the TMX+CAP group (Figure 2.3.2.2A). KU-596 treatment reduced by 25% the number of abnormally myelinated fibers defined as those with a myelin sheath, exhibiting myelin splitting, having myelin debris, onion bulbs, myelin ovoids or presence of regeneration clusters (Figure 2.3.2.2B). Despite the rapid onset and robust level of demyelination induced by TMX, these data suggest that KU-596 can ameliorate but not prevent the degeneration.

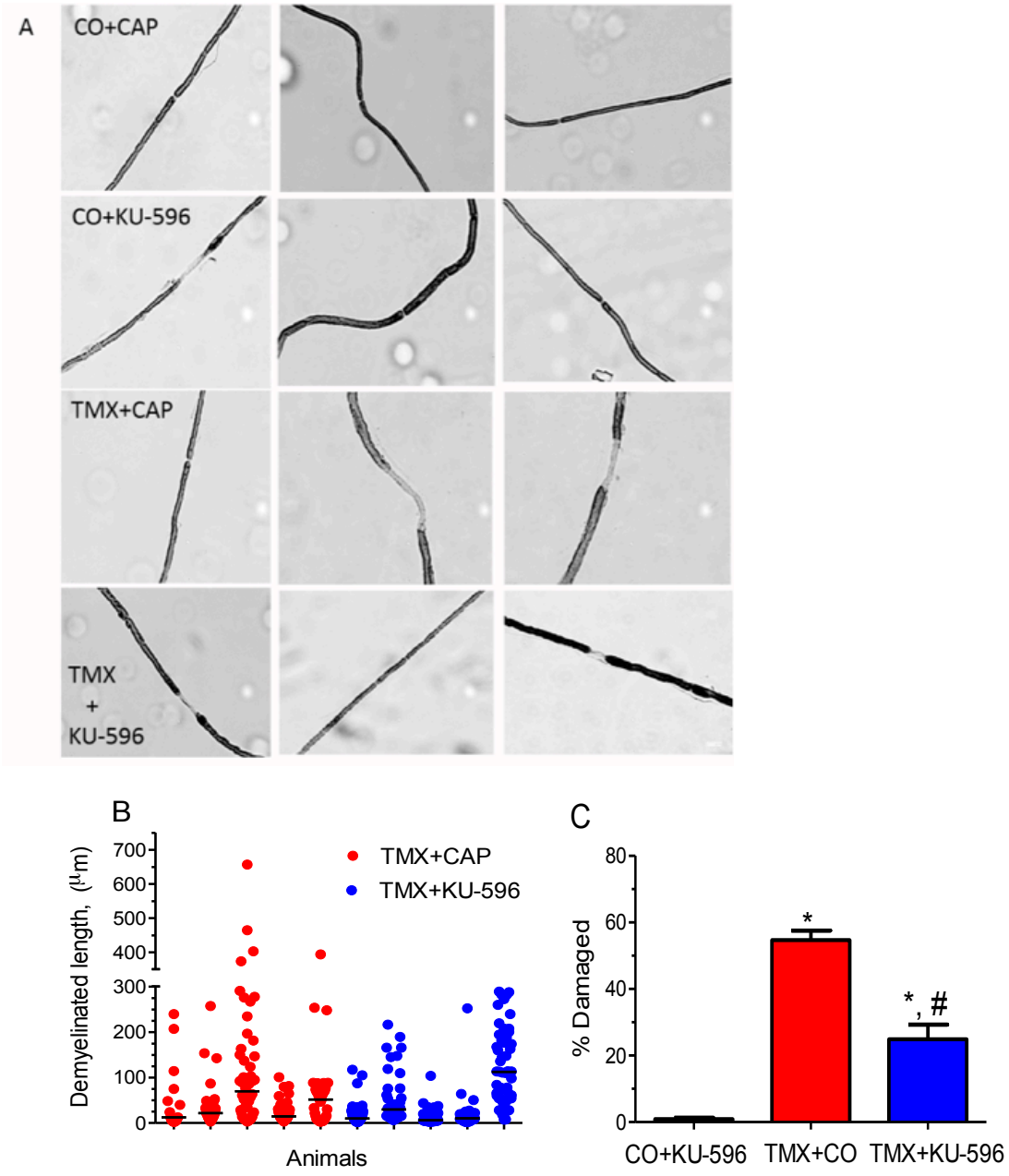

Figure 2.3.2.1: KU-596 improves myelin integrity.
A) Representative pictures of the effect of TMX and KU-596 treatment on myelination in teased sciatic nerves of MPZ-RAF mice (scale bar= 10μm). B) Quantification of the demyelinated length of sciatic nerves in TMX and TMX+KU-596 treated MPZ-Raf mice. Columns represent individual animals and dots represent length of demyelinated regions in individual teased nerves. Bar indicates median. C) Quantification of percentage of damaged nerves in each group. Nerves with demyelinated distances that were at least 10% greater than the average distance between two internodes in the CO+CAP treated MPZ-RAF mice were classified as damaged. *, $p<0.05$ compared with CO+CAP. #, $p<0.05$ compared with TMX+CAP.

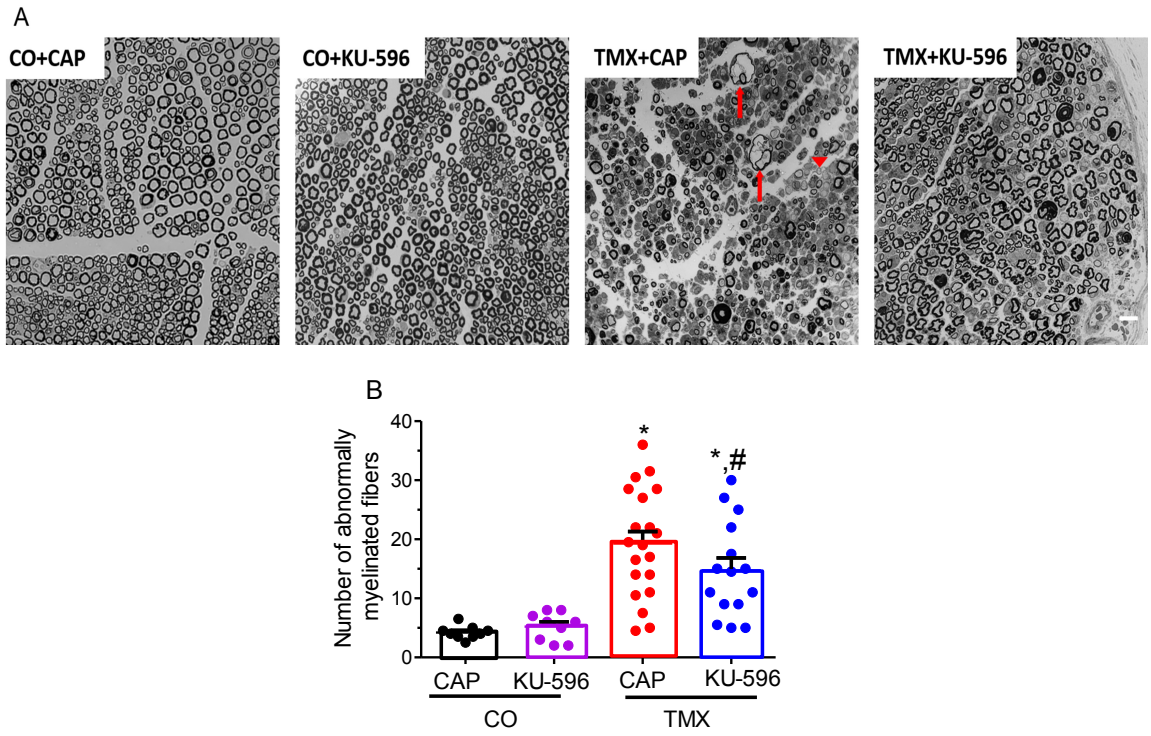

Figure 2.3.2.2: KU-596 decreased abnormally myelinated fibers.
A) Cross section of sciatic nerves of MPZ-RAF mice. Examples of myelin splitting (arrows) and demyelinated fibers (arrowheads) are indicated. Scale bar, 10µm. B) Quantification of abnormally myelinated nerves in each group. Abnormal myelination was defined as the presence of myelin splitting, myelin debris, onion bulbs, myelin ovoids and regeneration clusters. Each symbol represents the average from one section that was counted twice in separate sessions while blinded to treatment. The number of animals per group was CO+CAP (n=4), CO+KU-596 (n=3), TMX+CO (n=6) and TMX+KU-596 (n=5). Kruskal–Wallis non-parametric test, *, $p<0.05$ compared with CO+CAP, #, $p<0.05$ compared with TMX+CAP.

2.3.3. KU-596 improves motor function in MPZ-Raf mice

Since demyelination mainly affects large caliber motor nerves, we sought to test the effects of TMX and KU-596 on motor function by examining the ability of the mice to stay on a ramping rotorod. Animals were randomly assigned to each of the 4 treatment groups and given 5 training trials on the rotorod. MPZ-RAF mice were treated using an alternate day dosing schedule with day 0 serving as the baseline rotorod performance prior to any treatment. Animals were given 20 mg/kg KU-596 on alternate days beginning at day 0, while TMX was administered every other day beginning at day 1.

As expected (Napoli et al 2012a), TMX+CAP treated mice developed an impaired motor coordination and showed a sharp decrease in the latency to fall beginning at day 10 (after 4 TMX doses) (Figure 2.3.3.1A and B). Compared to mice treated with TMX+CAP mice, animals that received TMX+KU-596 showed a significantly delayed onset of the motor deficit and a preservation of motor function. Indeed, TMX+CAP mice showed an abnormal posture and rear limb positioning with the most severe mice exhibiting paraparesis (Figure 2.3.3.1C, top). In contrast, TMX+KU-596 treated mice had a relatively normal posture (Figure 2.3.3.1C, bottom), the limbs were able to support the body weight and the mice more effectively used all four limbs when ambulating, as discussed below.

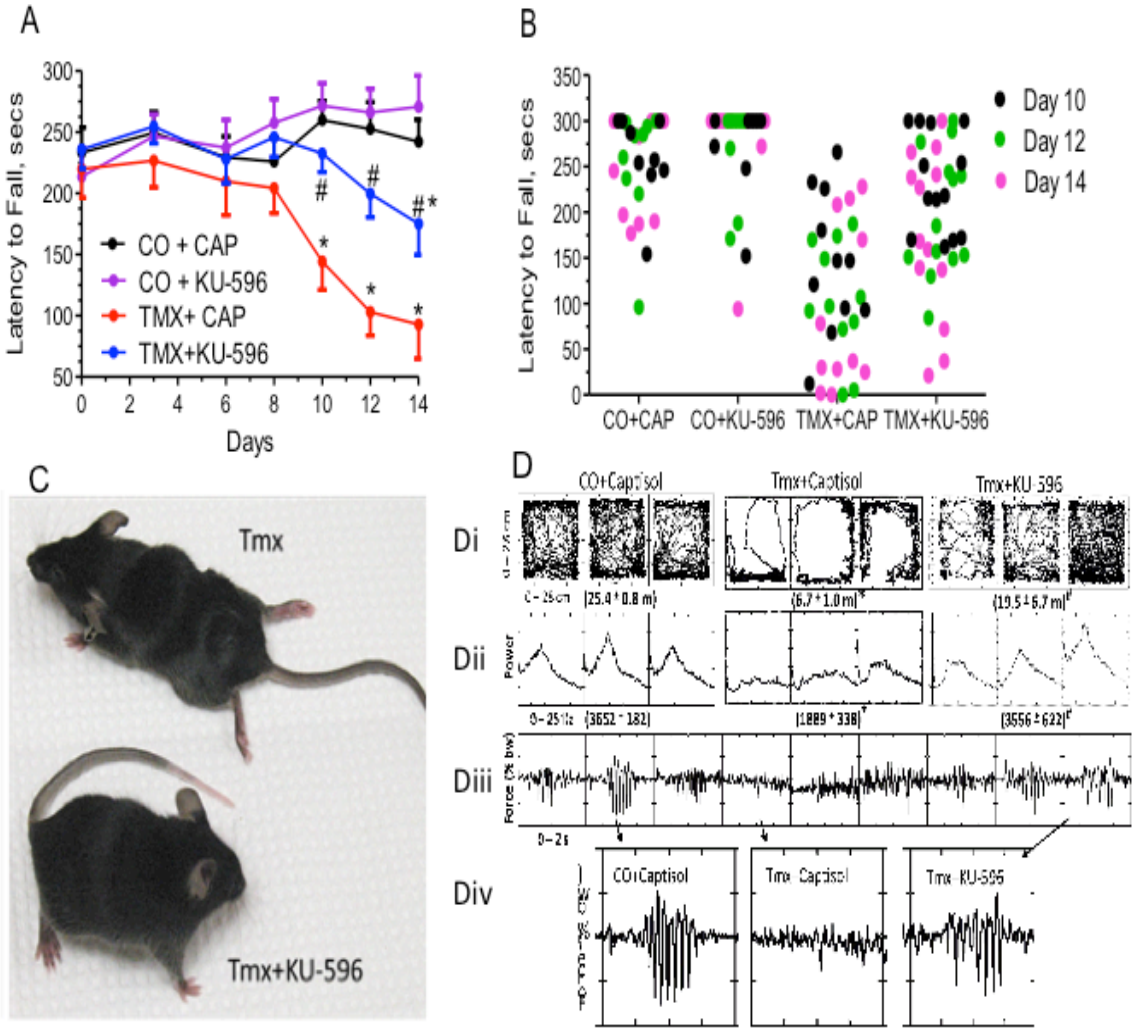

Figure 2.3.3.1: KU-596 improves motor function of TMX treated MPZ-RAF mice.
A) Latency to fall on the rotorod was assessed in 5 trials and the median was recorded. KU-596 increased time on the rotorod indicating improved motor function (n = 8-13). *, $p<0.05$ compared with CO+CAP. #, $p<0.05$ compared with TMX+CAP. B) Latency to fall of individual mice from each group on Days 10, 12, and 14, respectively. C) Representative pictures of MPZ-Raf mice treated with TMX+CAP (top) or TMX+KU-596 (bottom) at the end of the study. D) Mice were placed in the FPA for 10 min and the distance traveled (Di) and paw placement forces (Diii) were recorded. Numerical data for distance traveled in meters are shown in the lower margin of Di for the three groups. The second row of panels (Dii) represents the corresponding Fourier transforms of the force-time waveforms shown in Diii. Together Dii and Diii establish the rhythmic character and power output of individual bursts of locomotion. The fourth row of panels (Div) show enlarged images of force-time waveforms for the indicated animal in each group to more clearly illustrate treatment-related differences in ambulation power and rhythmicity. *, $p < 0.05$ versus CO+CAP; # $p< 0.05$ vs TMX+CAP.

Since the rotorod test is a rather gross indication of motor coordination, we employed a force plate actometer (FPA) to quantify locomotor activity with high temporal (10 ms) and spatial (2 mm) resolution (Fowler et al 2009, McKerchar et al 2006). No training of the animal is required since the FPA measures multiple movement parameters as the mouse freely explores the FPA chamber during a 10 min session. Animals were treated with TMX and KU-596 as discussed above and motor function in the FPA was assessed on day 14. Figure 2.3.3.1Di shows representative patterns of movement and overall distance traveled by the mice in the FPA chamber. Compared to control mice, TMX treated mice tended to restrict their movement around the perimeter of the chamber and showed a significant decrease in the total distance traveled from 25.4 meters to 6.7 meters. This is likely due to the extensive paraparesis (Figure 2.3.3.1C) and not a behavioral deficit induced by TMX; WT mice treated with TMX showed normal exploratory behavior (data not shown). In contrast, the overall distance traveled by mice receiving TMX+ KU-596 was significantly increased compared to the TMX + CAP group, and approximated the exploratory behavior of the control mice, though it remained slightly decreased.

The FPA also measures ambulation rhythmicity (stride) and force of paw placement during the strides. The panels in Figure 2.3.3.1Diii show representative force-time waveforms of paw placement forces during a straight run in the FPA. The symmetry of the force-time peaks represents the rhythmicity of ambulation during the series of strides while the amplitude of the wave measures the force of paw placement (power output). To quantify power output, it is normalized to body weight (%bw) so that variations in amplitude are independent of this variable (Fowler et al 2009). TMX

treatment clearly abolished the peak symmetry (rhythmicity of the stride) and peak amplitude (force of the paw hitting the force plate). The panels in Figure 2.3.3.1Div are a magnified view of the force data from one animal per group to highlight the differences in movement. These deficits result from the loss of limb coordination (Figure 2.3.3.1C) and inability of the limbs to sustain the body weight. Changes in force can be quantified following Fourier transformation of the waveforms which produces a power spectra (Figure 2.3.3.1Dii). The peak around 8-9 Hz in control mice represents normal ambulation rhythmicity and integration of the area under the curve (AUC) provides an indication of the force. TMX clearly abolished rhythmicity and significantly decreased the AUC in the power spectra. However, mice treated with KU-596 showed a significant improvement in ambulation rhythmicity and force. Together, these data indicate that decreased c-jun expression and the improved myelination following KU-596 treatment correlated with the development of a less severe motor neuropathy.

2.3.4. KU-596 improves a pre-existing motor deficit in MPZ-Raf mice

To test the ability of KU-596 to reverse a pre-existing motor deficit, rotorod performance was assessed every other day for 9 days in a group of 42 MPZ-Raf mice. After each session, the mice were administered TMX every other day for a total of 5 doses over the 9 days (Figure 2.3.4.1A). By day 11, the latency to fall was approximately $\leq$ 75% of the baseline on day 1. After assessing the rotorod latency on day 11, the mice were randomly assigned to one of four groups which received daily doses of 0 (n=12), 0.1, 1 or 10 mg/kg of KU-596 (n=10 each) from days 11 to day 18. This log range was chosen since 0.1 mg/kg shows minimal efficacy in improving diabetic peripheral neuropathy. Performance on the rotorod was assessed every other day from days 13 - 19

(Figure 2.3.4.1B). The latency to fall in mice receiving 0.1 mg/kg of KU-596 remained significantly impaired compared to the control mice and was indistinguishable from the mice treated with TMX + CAP. Mice receiving 1 or 10 mg/kg KU-596 did show some improvement in the latency to fall since they were not significantly different from the CO control group at days 13, 15 and 19. However, the magnitude of this improvement was not sufficient to be statistically different relative to the TMX + CAP group at any of the time points. Analysis of the latency to fall responses of individual animals indicated a rather wide variability among those treated with either TMX + CAP or TMX + KU-596 (data not shown). Therefore, to minimize the effect of animals that were either poor or good responders, the median fall latency in each group at each time was used to determine if the drug was having a significant effect over the duration of treatment. The median fall latencies for each treatment at days 13 – 19 were combined (4 time points per group) and analyzed by one-way ANOVA and Scheffe's post-hoc test (Figure 2.3.4.1C). This analysis suggests that daily dosing with 1 and 10 mg/kg KU-596 from days 11-18 significantly increased the fall latency over this treatment period.

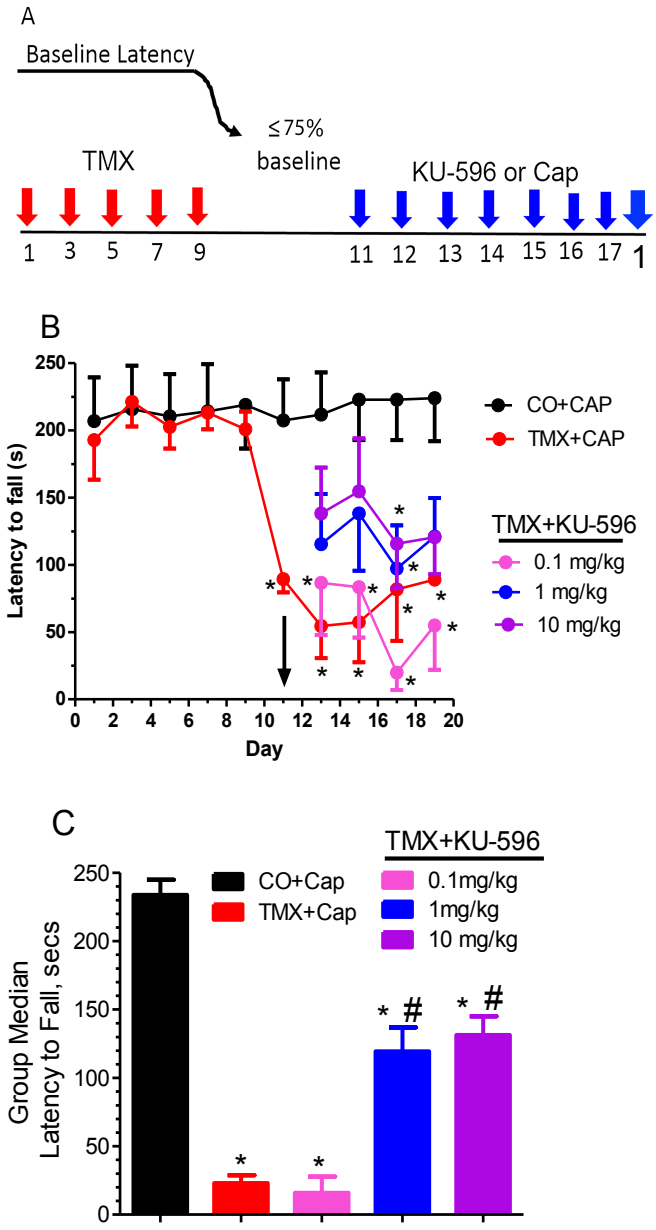

Figure 2.3.4.1: KU-596 improves a pre-existing motor deficit.

A) TMX was given every other day until the latency to fall dropped to about 75% of baseline by day 11. After the rotorod session on day 11, animals were randomly assigned to be treated daily with 0 – 10 mg/kg KU-596 and the dosing was initiated. B) Latency to fall of MPZ-RAF mice on the rotorod. Each mouse received 5 trials and the median of latency to fall was recorded. The arrow points to the start of daily KU-596 or vehicle treatment. TMX produced a statistically significant decrease in response latency that was not improved by 0.1 mg KU-596. *, $p<0.05$ compared with CO+CAP. Though the response latency in mice treated with 1 or 10 mg/kg KU-596 was not significantly different from the control group, it was significantly improved from animals that only received Captisol. C) The median of each treatment at days 13-19 were grouped and analyzed to minimize variability associated with good versus poor responders. One way ANOVA and Scheffe's post-hoc test indicated that 1 and 10 mg/kg KU-596 improved motor function over the duration of treatment.

2.3.5. Hsp70 is required for drug efficacy

Our previous work indicated that the ability of KU-596 to improve sensory deficits associated with the development of DPN is Hsp70-dependent (Li et al 2012b, Ma et al 2014, Ma et al 2015, Urban et al 2010). However, demyelination is not a hallmark of the sensory neuropathy that develops in diabetic rodents. Therefore, to determine if the ability of KU-596 to improve the demyelinating motor neuropathy in MPZ-Raf mice is also Hsp70-dependent, MPZ-Raf × Hsp70 KO mice were generated (Figure 2.3.5.1A). Importantly, deletion of Hsp70 had no effect in altering the expression of the constitutive isoform, Hsc70, in sciatic nerve.

Deletion of Hsp70 did not affect basal motor coordination since untreated MPZ-Raf × Hsp70 KO mice (Figure 2.3.5.1B) performed as well as the MPZ-Raf mice (Figure 2.3.3.1A and B) on the rotorod. As described for Figure 2.3.1.1A, MPZ-Raf x Hsp70 KO mice were also given 20 mg/kg KU-596 on alternate days beginning at day 0, while TMX was administered every other day beginning at day 1. Treating the MPZ-Raf × Hsp70 KO mice with TMX induced a progressive decrease in the latency to fall from the rotorod indicating that Hsp70 is not necessary to develop the motor neuropathy. However, in contrast to the MPZ-Raf mice, 20 mg/kg of KU-596 was unable to improve rotorod performance (Figure 2.3.5.1B). Consistent with this result, KU-596 also did not improve the distance traveled in the FPA (Figure 2.3.5.1Ci and D) nor ambulation rhythmicity (Figure 2.3.5.1Cii). Lastly, although TMX increased c-jun levels in sciatic nerve (Figure 2.3.5.1E), KU-596 was unable to decrease c-jun as occurred in the MPZ-Raf mice. These data indicate that KU-596 requires Hsp70 to improve the motor neuropathy and link Hsp70 to the decrease in c-jun.

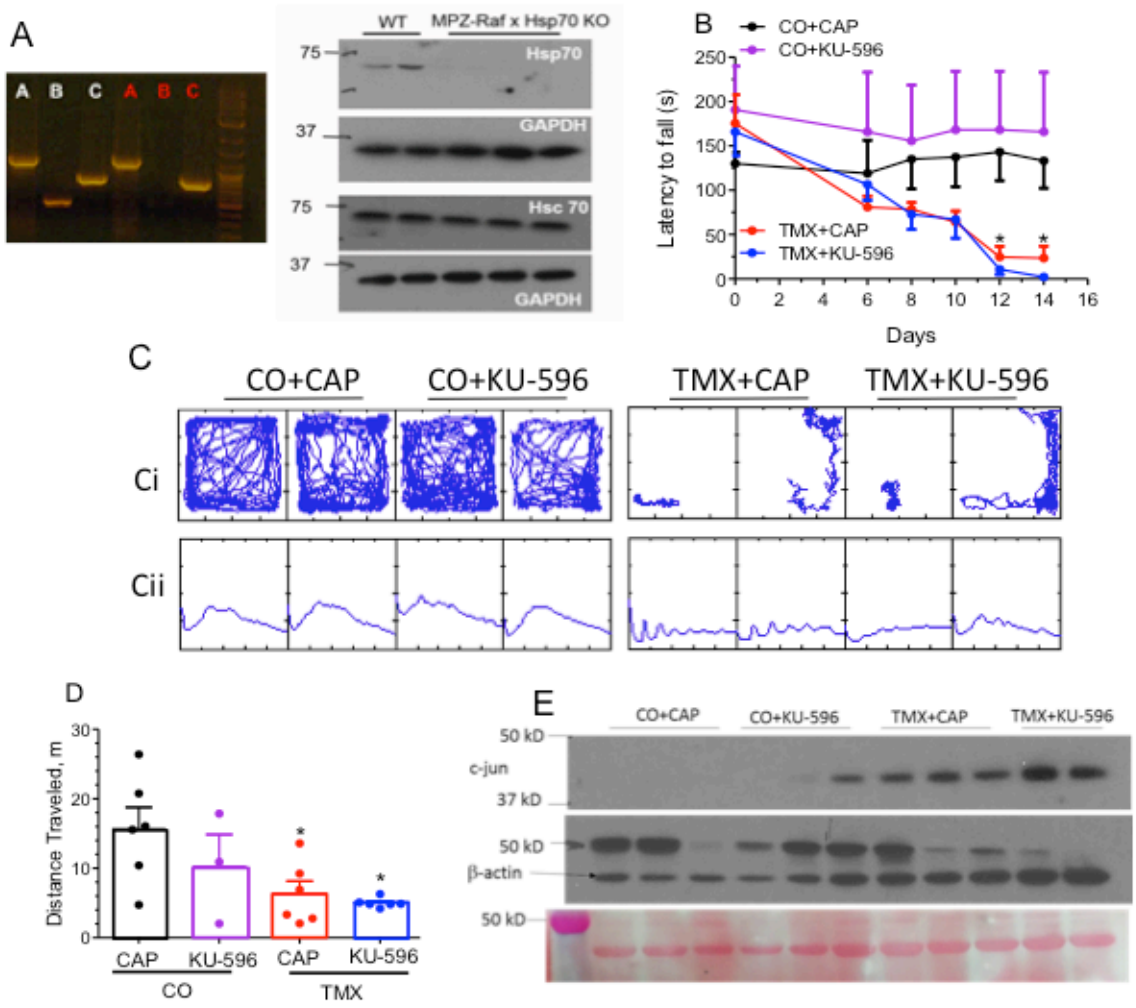

Figure 2.3.5.1: KU-596 improves the motor deficit in an Hsp70 dependent manner.

A) The left panel shows genotype analysis of the MPZ-Raf x Hsp70 KO mice. A- Raf transgene; B, Hsp70 WT; C, Hsp70 KO. The animal in white font was heterozygous for the Hsp70 KO while the animal in red font was homozygous. The right panel shows immunoblot analysis of sciatic nerve from 2 C57Bl/6 mice and four MPZ-Raf x Hsp70 KO mice. The mice lacked Hsp70 expression and this had no effect on altering the expression of Hsc 70. B) Mice were given 20 mg/kg KU-596 on alternate days beginning at day 0, while TMX was administered every other day beginning at day 1. Mice were trained for 5 days on the accelerating rotorod and tested every other day. Each mouse received 5 trials and the median latency to fall was recorded. KU-596 treatment showed no effect on the latency to fall compared with the TMX+CAP group. C) Mice were treated with TMX and KU-596 as described above and on day 15, and the total distance traveled (Ci) was quantified (D). (E) Sciatic nerves were analyzed for c-jun expression by immunoblot and equal loading was verified by immunoblotting for β-actin and via staining with Ponceau red.

2.4. Discussion

c-Jun belongs to the AP-1 transcription factor family and was first discovered as an oncogene (Yamanishi et al 1991). Although elevated c-jun is not the cause of all neuropathies, it may be an important culprit. Parkinson *et al.* were the first to demonstrate that c-jun is a negative regulator of myelination and is required for SC dedifferentiation (Parkinson et al 2008). Our data suggests that decreasing c-jun expression with KU-596 therapy correlates with a decrease in demyelination and improved motor function in MPZ-Raf mice, a robust model of a rapid onset demyelinating neuropathy. Moreover, drug efficacy seems to require Hsp70 as improved motor function could not be recapitulated in MPZ-Raf x Hsp70 KO mice.

Hsp70 is mechanistically known to inhibit the JNK pathway and protect neurons from apoptosis (Bienemann et al 2008, Lee et al 2005). However, the phosphorylation of c-jun by JNK is not necessary for c-jun to promote demyelination(Parkinson et al 2008). Our published work using an earlier generation C-terminal Hsp90 inhibitor, KU-32, indicated that an increase in the proteasomal clearance of c-jun and phospho-c-jun was linked to protecting against demyelination in SC-sensory neuron co-cultures (Li et al 2012b). Thus, we anticipate that the decrease of c-jun expression is more likely due to increased clearance rather than decreased production, but this remains to be demonstrated *in vivo*. One possible mechanism for enhancing c-jun clearance via Hsp70 is through the carboxy terminus of heat shock cognate protein 70 (Hsc70) interacting protein (CHIP). CHIP is an Hsp70 interacting E3 ubiquitin ligase that mediates the proteasomal clearance of Hsp70 substrates by binding to a C-terminal EEVD sequence of the chaperone (Dickey et al 2007b). Since Hsp70 can co-immunoprecipitate c-jun, an Hsp70-CHIP complex may

be involved its clearance. However, no reports have linked CHIP as a critical mediator for c-jun degradation. On the other hand, the F-box protein, Fbw7, is known to enhance the clearance of c-jun by promoting its ubiquitination by the SCF ubiquitin E3 ligase complex (Hoeck et al 2010, Wang et al 2011). Phosphorylation of c-jun at T^{239} and S^{243} is required for its recognition by Fbw7 (Wei et al 2005) and TMX-treated mice showed an increase in c-jun phosphorylation at these residues (data not shown). Fbw7 is readily detected in sciatic nerve extracts and can also co-immunoprecipitate with Hsp70 from cell extracts (data not shown). Little is known about how c-jun is cleared in SC and these observations suggest that Fbw7 may regulate c-jun function. The role of Fbw7 in regulating c-jun clearance via KU-596 and Hsp70 is currently being examined using mice with a SC-specific conditional deletion of Fbw7.

Although KU-596 therapy could not decrease c-jun levels in the absence of Hsp70, it remains unclear if a decrease in c-jun is critical to mediating the improvement in nerve function or is a consequence of other mechanisms by which Hsp70 may ameliorate the neuropathy, i.e., enhancing mitochondrial bioenergetics or decreasing inflammation (Ma et al 2015). Moreover, emerging data suggests that c-jun serves a complicated role in SC function. In response to injury or metabolic insults, robust induction of c-jun in myelinated adult SCs is recognized as essential for promoting dedifferentiation of the myelinated phenotype (Parkinson et al 2008). For instance, an increase in SC c-jun expression correlates with the extensive demyelination that occurs in a mouse model of human CMT1X (Klein et al 2014). Though high levels of c-jun expression are sufficient to drive SC dedifferentiation, c-jun levels decline after loss of the myelin membrane. Recent data supports that a low level of c-jun expression in

injured SCs may be important to produce trophic factors, such as glial derived neurotrophic factor, that can aid the survival of the desheathed sensory neurons (Arthur-Farraj et al 2012, Fontana et al 2012b). For example, the C3 mouse model of CMT1A shows a decrease in the number of myelinated sensory axons compared to wild type mice (Hantke et al 2014). However, SC-specific deletion of c-jun in the C3 mouse exacerbated the loss of myelinated sensory axons, suggesting a supportive role of c-jun in axonal survival (Hantke et al 2014). While pharmacologic modulation of c-jun levels is distinctly different from its genetic deletion, it is translationally important to determine if the drug may interfere with, complement or supplant any trophic actions of c-jun in supporting desheathed axons in relevant disease models that have a SC-specific deletion of c-jun.

A second caveat of our work is that the rapid onset demyelinating neuropathy shown by the MPZ-Raf mice does not mimic a human disease. Importantly, c-jun is elevated in several inherited neuropathies, such as CMT1A, CMT1B, and CMT1X (Hutton et al 2011, Klein et al 2014). The ability of KU-596 to improve motor function in this rapid and robust model of a demyelinating neuropathy suggest it may have clinical potential in these slower onset diseases since muscle weakness and limited mobility are major complaints from afflicted patients (Johnson et al 2014, Kelly et al 2015). Since induction of Hsp70 by N-terminal Hsp90 inhibitors can clear protein aggregates in models of CMT1A (Chittoor et al 2013, Rangaraju et al 2008a), KU-596 may be beneficial in treating this inherited neuropathy since it has a broader therapeutic window that promotes Hsp70 induction without increasing client protein degradation, which would be neurotoxic. The application of KU-596 in treating CMT1X would be intriguing

as well. Since CMT1X is a mixed axonal and demyelinating neuropathy, decreasing c-jun expression may help improve aspects of the demyelinating neuropathy while providing some support for the axonal neuropathy via its documented ability to improve at least sensory neuron mitochondrial bioenergetics. Furthermore, a SC-dependent secondary inflammation that stimulates macrophage-mediated demyelination contributes to the progressive neuropathy in CMT1X (Groh et al 2010, Groh et al 2015). C-C motif chemokine (CCL2) is derived from SCs, and attracts macrophages to infiltrate the endoneurium and directly contribute to myelin degeneration in CMT1X (Martini & Willison 2015). Since c-jun can transcriptionally increase CCL2 (Wolter et al 2008), decreasing its levels may abrogate CCL2 production and decrease macrophage-mediated myelin degeneration in CMT1X. Consistent with this premise, transcriptomic analysis found that KU-596 therapy broadly decreased the expression of inflammatory genes and was predicted to decrease CCL2 activation in diabetic dorsal root ganglia (Ma et al 2015). The potential utility of KU-596 and Hsp70 in improving physiologic read outs of nerve function in mouse models of CMT1X is currently being assessed.

In summary, we show that novologue therapy can attenuate the severe morphologic and physiologic indices of a demyelinating neuropathy that rapidly occurs in the MPZ-Raf mice. Since human demyelinating neuropathies typically show a more gradual development, this bodes well for the drug's translational potential. Combined with our extensive published data on the efficacy of novologues in attenuating a metabolic neuropathy (Ma et al 2014, Ma et al 2015, Urban et al 2010, Urban et al 2012), these data provide strong proof-of-principle that the upregulation of endogenous cytoprotective pathways can attenuate neuropathies of distinct etiologies.

Chapter 3. Modulating Molecular Chaperones Improves Demyelinating Neuropathy in a Mouse Model of Charcot-Marie-Tooth 1X

Abstract

X-linked Charcot-Marie-Tooth (CMT1X) disease is the second most common form of CMT and is caused by mutations of the gap junction beta-1 gene (*GJB1*) which encodes the protein connexin 32 (Cx32). The loss of function of Cx32 accounts for the symptoms of CMT1X due to the development of a mixed axonal and demyelinating neuropathy. Cx32 deficient mice (Cx32def) are an accepted model of human CMT1X and are useful for evaluating novel pharmacologic approaches to treat CMT1X, which are desperately needed by patients. "Novologues" are orally bioavailable, non-toxic small molecules that improve metabolic and clinical indices of diabetic peripheral neuropathy by modulating the expression of the molecular chaperone heat shock protein 70 (Hsp70). We have also identified that novologue therapy has promising efficacy in improving neuromuscular function in the Cx32def animal model of CMT1X. Recent evidence suggests that c-jun could be a potential target for treating CMT1X since elevated levels of c-jun can promote demyelination. Young Cx32def mice exhibit an early axonopathy and treating 3-month-old Cx32def mice for 1 month with the novologue, KU-596, dose dependently decreased c-jun expression in Schwann cells of the femoral nerves and improved motor nerve conduction velocity (MNCV) and compound muscle action potential (CMAP). Older Cx32def mice develop a demyelinating neuropathy and treating 6-month-old Cx32def mice for 3 months with KU-596 improved grip strength and MNCV. The therapeutic effects of KU-596 depend on Hsp70 since grip strength and MNCV were not improved by 3 months of drug therapy in Cx32def x Hsp70 knockout

mice. Collectively, our data indicate that modulating Hsp70 could be beneficial in treating CMT1X possibly due to effects on decreasing the expression of c-jun. Since novologues are entering Phase 2 trials, this therapy shows promise as a rapidly translatable treatment for CMT1X.

3.1. Introduction

X-linked Charcot-Marie-Tooth disease (CMT1X) is caused by mutations in the gap junction beta 1 (*GJB1*) gene (Gal, Mucke et al. 1985). Over 400 mutations of the *GJB1* gene have been reported to be associated with CMT1X (Kleopa et al 2012, Panosyan et al 2017). CMT1X is the second most common type of CMT, accounting for nearly 20% of CMT1 cases (Braathen 2012). Because CMT1X is an X-linked dominant disorder, males have an earlier onset, usually within the first two decades of life, and are more severely affected than female patients. CMT1X patients present classic neuromuscular symptoms including foot drop, steppage gait, and pes cavus. Symptoms first appear in the distal foot and leg muscles and gradually progress to the upper limbs (Shy, Siskind et al. 2007).

The *GJB1* gene encodes the gap junction protein connexin 32 (Cx32) that is found at the Schmidt-Lantermann incisures and within non-compact myelin (Scherer et al 1995). Cx32 contains cytoplasmic amino and carboxy termini, four transmembrane domains, and one intra- and two extra-cellular loops. Hexamers of Cx32 form a hemichannel and in the peripheral nervous system (PNS), gap junction channels are formed by hemichannels that contain only Cx32 (Kleopa & Sargiannidou 2015). The Cx32 gap junction channels allow molecules less than 1 kDa to pass through the SC cytoplasm with a thousand-fold shorter distance than the circumferential pathway (Balice-Gordon et al 1998, Scherer et al 1995). The loss of function of Cx32 solely accounts for the peripheral symptoms in CMT1X and Cx32 deficient (Cx32def) mice mimic many features of the peripheral neuropathy that develop in humans. Thus,

Cx32def mice provide an excellent animal model for assessing mechanisms of disease development and exploring the efficacy of potential therapeutics.

Though the mechanism by which a loss-of-function of Cx32 leads to the neuropathic phenotype is unknown, Cx32def mice clearly exhibit a two-stage neuropathy. In contrast to the initial discovery, where no neurological changes were observed at 3 months of age (Nelles et al 1996), Vavlitou *et al* found that axonal damage started to occur at 2 months of age, prior to demyelination (Vavlitou et al 2010). This first stage of axonopathy is associated with an increase in the transcription factor c-jun, a decrease in phosphorylated neurofilament, and a decrease in axon diameter (Klein et al 2014). The second stage is a macrophage-mediated demyelinating neuropathy that evolves around 6 months of age. It is hypothesized that the mutant SCs send an unidentified signal to fibroblasts, which then secrete colony stimulating factor-1 (CSF-1) that activates the macrophage-mediated neurodegeneration (Groh et al 2016, Groh et al 2015, Martini & Willison 2016). Mutant SCs also secrete C-C motif chemokine (CCL2) that guides macrophages to mutant SCs (Kohl et al 2010). This stage of the neuropathy is associated with a robust increase in c-jun expression (Klein et al 2014), which can induce the transcription of CCL2 (Wolter et al 2008). Since c-jun drives SC dedifferentiation (Jessen & Mirsky 2016) and promotes macrophage-mediated damage, attenuating the expression of c-jun may serve as a valid therapeutic strategy. To this end, we propose using an innovative small molecule chaperone modulator to pharmacologically manage CMT1X.

Molecular chaperones such as Hsp70 and Hsp90 play important roles in protein folding, assembly, regulation and degradation. They also act as the first-line of defense

against stress (Feder & Hofmann 1999). Recent evidence suggests that modulating Hsp70 yields promising neuroprotective effects in neurodegenerative diseases associated with protein aggregation, such as Alzheimer's disease (AD) and Parkinson's disease (PD)(Dickey et al 2006, Dickey et al 2007a, Luo et al 2007a, Putcha et al 2010). However, the use of small molecules directly targeting Hsp70 has been shown to be challenging (Assimon et al 2013). Alternatively, Hsp70 expression could be regulated indirectly through the modulation of Hsp90 to induce an HSR. The binding of Hsp90 inhibitors to Hsp90 disrupts the Hsp90-HSF1 complex and releases HSF1. Following phosphorylation and trimerization, the released HSF1 binds to the HSE and induces the transcription of Hsps, especially Hsp70 (Neef et al 2011).

N-terminal Hsp90 inhibitors have been shown to reduce toxic aggregates in neurodegenerative diseases, such as AD and PD (Luo et al 2007a, Putcha et al 2010). However, many N-terminal inhibitors have limited application since they induce degradation of normal client proteins in addition to the induction of HSR. We developed a series of novobiocin-based small molecule C-terminal Hsp90 inhibitors, termed novologues, which induce the HSR at a much lower concentration than the concentration needed to induce client protein degradation. The second-generation novologue, KU-32, has been shown to protect neurons from amyloid-β induced toxicity (Ansar et al 2007). Moreover, in mouse models of diabetic peripheral neuropathy (DPN), weekly treatment of KU-32 improved mitochondrial bioenergetics and reversed sensory deficits (Ma et al 2014). Importantly, KU-32 was also found to attenuate demyelination by regulating c-jun expression. Using myelinated SC-dorsal root ganglia co-cultures, c-jun induction and demyelination can be rapidly induced by

the addition of neuregulin 1 Type 1. Treating the myelinated co-cultures with KU-32 prior to inducing demyelination with neuregulin 1 decreased c-jun expression, and blocked the extensive demyelination. Mechanistically, this neuroprotection required Hsp70 since the drug could not prevent neuregulin-induced demyelination in co-cultures prepared from Hsp70 KO mice (Li et al 2012a).

Although KU-32 is a potent neuroprotective C-terminal Hsp90 inhibitor, further structure activity studies identified KU-596 as a next generation novologue with a more facile synthesis that protected sensory neurons with an improved ED_{50} (Kusuma et al 2012a). Like KU-32, KU-596 improved mitochondrial bioenergetics and sensory deficits in a mouse model of DPN in an Hsp70-dependent manner (Ma et al 2015). As discussed in Chapter 2, oral administration of KU-596 reduced c-jun expression, the extent of demyelination and improved motor function in a transgenic model of a demyelinating neuropathy. To more fully evaluate the potential of KU-596 to improve a neuropathy that models a human disease, we used Cx32def mice to explore whether KU-596 may be beneficial in the context of CMT1X. Our data suggests that modulating molecular chaperones could provide a new therapeutic strategy towards the treatment of CMT1X.

3.2. Materials and Methods

3.2.1. Materials

KU-596, N-(2-(5-(((3R,4S,5R)-3,4-dihydroxy-5-methoxy-6,6-dimethyltetrahydro-2H-pyran-2-yl)oxy)-3'-fluoro-[1,1'-bi- phenyl]-2-yl)ethyl)-acetamide was synthesized as previously described (Kusuma et al 2012a). Compound purity routinely exceeded 95%.

Captisol (CAP) was purchased from Cydex Pharmaceuticals Inc. (Lenexa, KS) and was used to solubilize KU-596 for oral administration and served as the drug vehicle.

c-Jun antibody was purchased from Cell Signaling Technology (#9165, Danvers, MA). The specificity of the antibody was demonstrated using nerves isolated from animals in which c-jun was conditionally deleted in Schwann cells (data not shown). Goat anti-mouse-HRP and goat anti-rabbit-HRP were purchased from Santa Cruz Biotechnology (Santa Cruz, CA). β-actin antibody was purchased from MP Biomedical (Santa Ana, CA). Goat anti-rabbit Alexa Fluor-647, Diamond prolong antifade mounting solution with 4', 6-diamidino-2-phenylindole (DAPI) and 10% normal goat serum (NGS) in phosphate buffered saline (PBS) was purchased from Life technologies (Calrsbad, CA). Tissue-Tek Optimum cutting temperature (OCT) was purchased from Electron Microscopy Sciences (Hatfield, PA).

3.2.2. Animals

Thanks to Dr. Rudolf Martini for his generous gift of Cx32 deficient (Cx32 def) mice (Nelles et al 1996). Cx32 def x Hsp70 KO mice were generated by crossing Cx32 def mice with Hsp70.1/Hsp70.3 knockout (Hsp70 KO) mice (Mutant Mouse Resource and Research Center (Davis, CA)). C57Bl/6 mice were used as wild type (WT) controls. Genotypes were confirmed using the primers listed in Table 3.2.1.1. All animals were maintained on a 12h light/dark cycle and given ad libitum access to water and chow (NIH diet 7005).

Table 3.2.1.1: Primers for genotyping

Gene	Primer	Band size
Cx32 WT	5’-GAGCATAAAAGTGAAGACGG -3’	881bp

Cx32 def	5’-CCATAAGTCAGGTGTAAAGGAGC-3’ 5’-ATCATGCGAAACGATCCTCATCC-3’ 5’-CCATAAGTCAGGTGTAAAGGAGC-3’	414bp
Hsp70 WT	5’-GTACACTTTAAACTCCCTCC-3’ 5’-CTGCTTCTCTTGTCTTCG-3’	450bp
Hsp70 KO	5’-ATGGGATCGGCCATTGAACAAG-3’ 5’-ACTCGTCAAGAAGGCGATAGAAGG-3’	850bp

3.2.3. Immunoblot Analysis

Sciatic nerves were collected and homogenized in lysis buffer (50mM Tris-HCl, pH 7.4, 150mM NaCl, 1mM EDTA, 1% NP-40, 1% deoxycholate, 0.1% SDS, 0.5 mM sodium orthovandate, 40mM NaF, 10mM β-glycerophosphate and 1X Complete Protease Inhibitors). After centrifuging at 10,000 x g for 10 min at 4°C, protein concentration of lysates was determined using DC (detergent compatible) protein assay (Bio-Rad Laboratories, Inc.). 20 μg of protein were separated by SDS-PAGE and transferred to a nitrocellulose membrane. Membrane was blocked with 5% non-fat milk in phosphate buffered saline (PBS) containing 0.1% Tween-20 (PBST) and incubated with primary antibody overnight at 4°C. On the next day, the membrane was washed and followed by incubation with HRP-conjugated secondary antibody. After 2h, the membrane was washed and the immunoreactivity was detected using enhanced chemiluminescence detection kit (GE Healthcare Life Sciences). The films were scanned and Image J is used to analyze the density of the blot.

3.2.4. Immunofluorescence Analysis

Motor branch of femoral nerves were collected and immersion fixed in Zamboni's fixative overnight at 4°C. After washing three times with PBS, nerves were cryoprotected with 30% sucrose until the tissue sinked in the solution. Nerves were embedded in OCT and cut at 10 μm using a cryostat. Sections were first re-hydrated with PBS three times for 5 min each cycle followed by permeabilization with 0.1%Triton X-100 in PBS for 20 min. After blocking with 0.3% Triton X-100 in 10% normal goat serum (NGS, Life technologies, Calrsbad, CA) for 1h, tissues were placed at 4°C and incubated with primary antibodies diluted in 10% NGS in PBS overnight. Sections were washed with PBS and incubated with conjugated goat anti-rabbit-Alexa Fluor-647 for 2h in dark. Slides were mounted with Diamond prolong antifade with DAPI and imaged on an Olympus/3I Spinning Disk Confocal/TRIF Inverted Microscope. 3-5 random sections were captured using SlideBook 6.4 (Intelligent Imaging Innovations Inc.) for each animal. Images were quantified using CellProfiler software. The percentage of c-jun positive nucleus was calculated by dividing the number of positive nucleus by the number of total nucleus (3-5 sections per animal).

3.2.5. Behavioral Tests

For the grip strength test, mice were placed parallel on the grid. After the hindpaws attached to the grid, the mouse was horizontally and steadily pulled back until their grip was released. The average of eight readings was used. High-resolution force plate actometer (FPA) (Bioanalytical Systems Inc.) was used to assess the paw placement force of the mice. Mice were placed on the FPA for a 10 min session every week. The FPA measures the force of paw placement during strides and present it as a force-time

waveform normalized to bodyweight (%bw) (Fowler et al 2009, McKerchar et al 2006). The amplitude of the wave represents the force of paw placement. Max power was calculated after Fourier transformation of the force-time waveform data using a Hanning data window from Matlab's Signal Processing Toolbox.

3.2.6. Electrophysiological measurements

At the end of the study, mice were anesthetized with mixed solution of ketamine and xylazine. MNCV, SNCV (McGuire et al 2009) and CMAP (Ruiz et al 2005, Simon et al 2010) were measured as previously described.

3.2.7. Luciferase activity assay

50B11 cells were transfected with a dual reporter plasmid that expressed secreted alkaline phosphatase (SEAP) under a CMV promoter and *Gaussia* luciferase driven by a 1.5 kb region of the CCL2 promoter that contains two c-jun recognition elements. Following transfection, the cells were treated with DMSO or 1μM KU-596 and were serum deprived overnight to render them quiescent. The following day, the cells were stimulated for 2h by the addition of 10% serum. The medium was collected and cell lysates were collected for western blot. Luciferase and SEAP activity were measured using a secrete-pair dual luminescence assay kit (GeneCopeia). Luminescence was measured by a plate reader at 480 nm. Data were represented as relative luminescence unit (RLU), which is the ratio of luciferase to SEAP. Control cells remained in complete medium (DMEM, 10% FBS, 1% penicillin and streptomycin) the whole time and were either transfected with CCL2 plasmid or left untransfected. After overnight treatment with either vehicle or 1μM KU-596, cells and media were collected for luciferase assay and immunoblot analysis.

3.2.8. Statistical Tests

All data points shown are presented as means ± standard errors of the mean (SEM). Datasets were first tested for normality using the Shapiro-Wilk test. Groups with equal variances are subjected to one-way analysis of variance (ANOVA) and Tukey's post-hoc test for statistical analysis. Student's t-test was used when comparing two groups. Results are considered significant when $p<0.05$. Krusal-Wallis and Dunn's test were used for non-parametric data sets. All statistical analyses were performed using R (v3.4.1) software.

3.3. Results

3.3.1. KU-596 treatment decreased c-jun expression in young Cx32 def mice

We utilized Cx32def mice to model human CMT1X. We started to test our hypothesis in 3-month-old Cx32def mice. At this stage, axonopathy has already occurred and an increased level of c-jun has been reported, but demyelination does not start to occur until after 4 months of age (Klein et al 2014, Vavlitou et al 2010). To test whether KU-596 could decrease c-jun expression, we performed a dose-response experiment by treating Cx32def mice with 0.3mg/kg, 1mg/kg, or 3mg/kg of KU-596 daily for one month and examined the expression level of c-jun in sciatic nerve extracts. After a month of treatment, KU-596 dose-dependently decreased c-jun expression in the sciatic nerve of Cx32def mice (Figure 3.3.1.1A). We obtained a similar trend when SC c-jun expression was examined in the motor branch of femoral nerves using immunostaining (Figure 3.3.1.1B), but it is likely that more animals are needed to reach statistical significance.

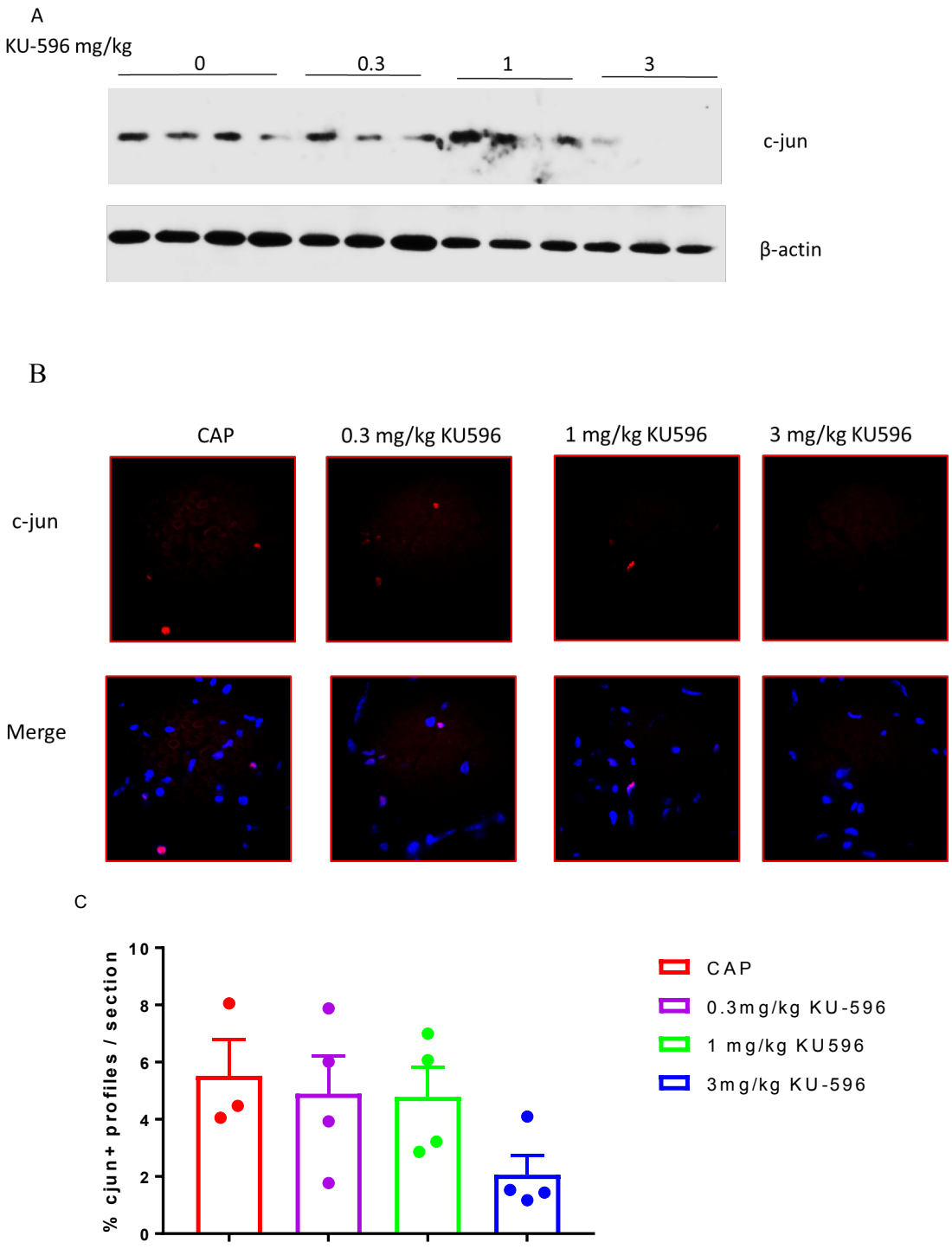

Figure 3.3.1.1: KU-596 decreases c-jun expression in young Cx32def mice.
A) After treatment with CAP/KU-596 for one month, sciatic nerves were collected and prepared for immunoblot. KU-596 dose dependently decreased c-jun expression. B) c-Jun expression in the femoral nerve motor branch. KU-596 dose dependently decreased c-jun expression. C) Quantification of $cjun^{+}$ profiles/section. (CAP, n=3, other groups, n=4)

3.3.2. KU-596 treatment increased the motor function in young Cx32def mice

Recent evidence revealed that axonopathy occurs earlier than the onset of demyelination in Cx32def mice (Vavlitou, Sargiannidou et al. 2010). Accordingly, another indication of axonal loss is that patients exhibit a reduced compound muscle action potential (CMAP) (Birouk et al 1998, Dubourg et al 2001). After one month of therapy, mice were anesthetized and nerve electrophysiology was assessed. Motor nerve conduction velocity (MNCV) reflects the integrity of the myelin while CMAP reflects axonal innervation of neuromuscular junction. KU-596 treatment improved both MNCV and CMAP (Figure 3.3.2.1), indicating that KU-596 is capable of improving the early axonopathy.

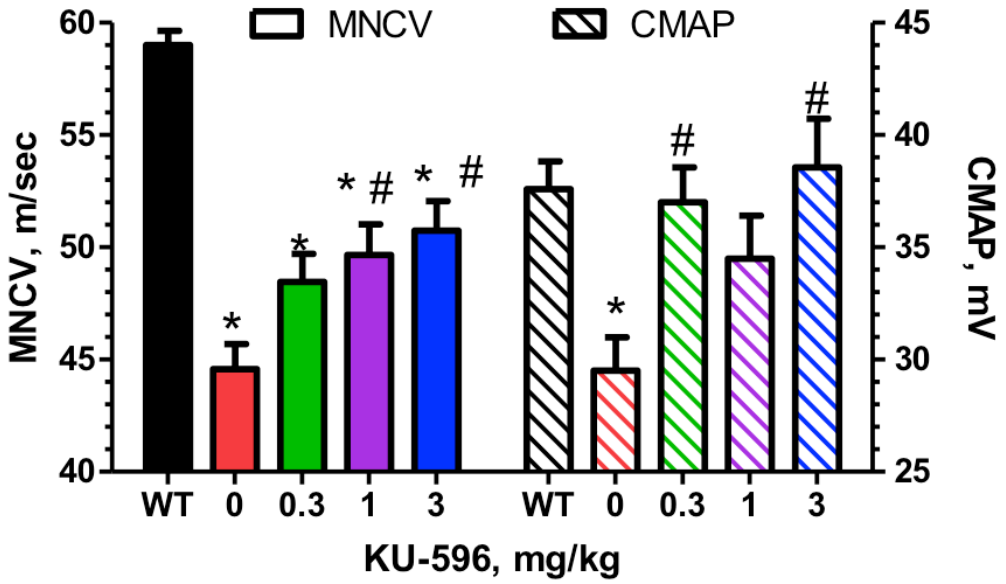

Figure 3.3.2.1: KU-596 improves motor function in young Cx32def mice.
After treatment with CAP/KU-596 for one month, mice were subjected to electrophysiological assessments. KU-596 dose dependently increased both motor nerve conduction (MNCV) and compound muscle action potential (CMAP). *, $p<0.05$ vs. WT. #, $p<0.05$ vs. CAP. (WT, n=7, CAP, n=11, 0.3mg/kg KU-596, n=9, 1mg/kg KU-596, n=9, 3mg/kg KU-596, n=8).

3.3.3. KU-596 treatment decreased c-jun expression in old Cx32def mice.

The second stage of the CMT1X neuropathy is characterized by a profound elevation of c-jun, which takes place at around 6 months of age (Klein et al 2014). c-Jun drives SC demyelination (Parkinson et al 2008) and possibly regulates the expression of CCL2 (Wolter et al 2008) to exacerbate demyelination. To test whether KU-596 could attenuate c-jun expression and exhibit neuroprotection, we treated Cx32def mice daily for 3 months with 3mg/kg KU-596. Consistent with previous literature (Klein et al 2014), Cx32def mice showed an increased level of c-jun in the motor branch of the femoral nerve compared to WT mice. 3-months of daily treatment with KU-596 decreased the level of c-jun as the percentage of c-jun^{+} profiles was reduced to half of the CAP treated mice (Figure 3.3.3.1).

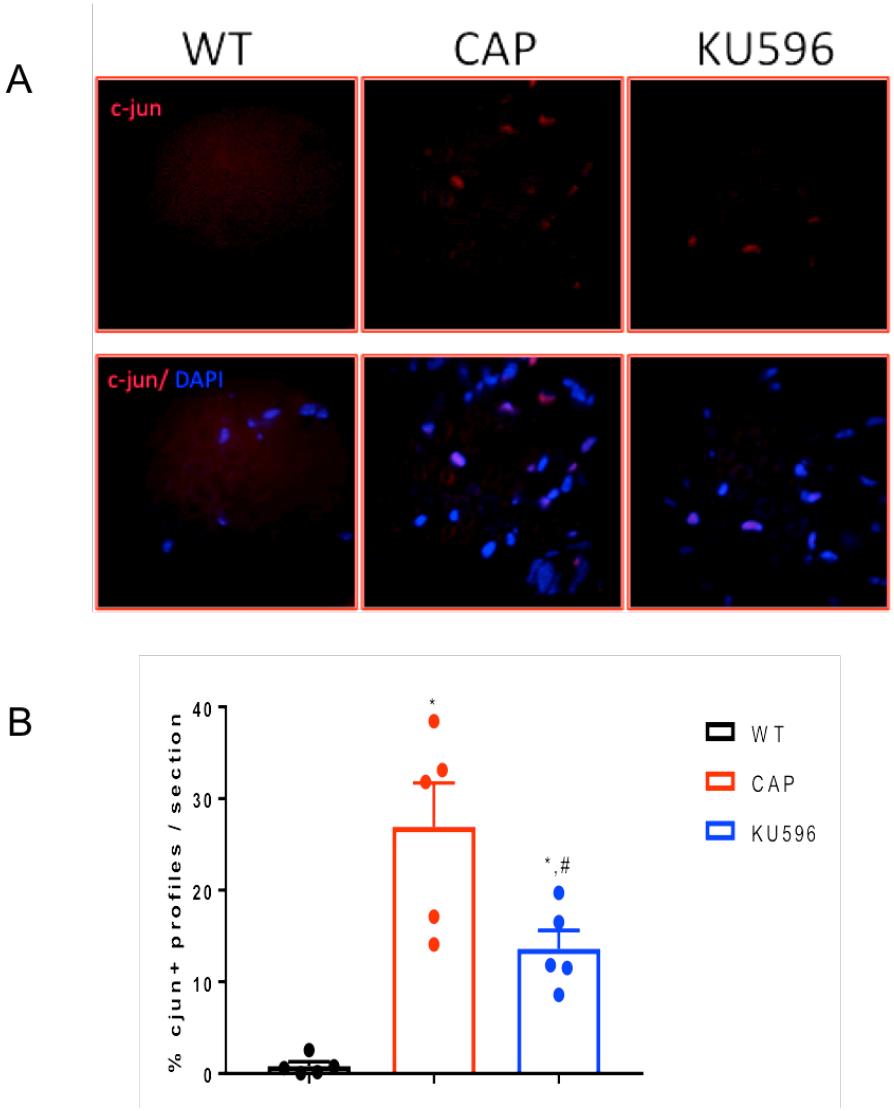

Figure 3.3.3.1: KU-596 decreases c-jun expression in old Cx32def mice.
A) After 3 months of treatment, femoral nerve motor branches of young Cx32def mice were fixed and stained with antibody against c-jun (red). B) Quantification of the percentage of c-jun^{+} nucleus per section. *, $p<0.05$ vs. WT. #, $p<0.05$ vs. CAP.

3.3.4. KU-596 treatment increased the motor function in old Cx32def mice.

As increased levels of c-jun correlate with the decline of motor function, we tested whether KU-596 treatment improved measures of nerve physiology. First, we employed the grip strength test to measure the muscle strength of the mice. In our 3-month dosing paradigm, we monitored the grip strength of the mice weekly. Compared with WT, Cx32def mice exhibit a progressive decline in muscle strength, as seen in previous literature (Groh et al 2010). This decrease in muscle strength is linked to the reduced CMAP seen in patients (Birouk et al 1998, Molin & Punga 2016). 3 weeks after treatment, the two groups began to differ. KU-596 treated animals improved their muscle strength, whereas CAP treated animals showed a progressive decline over time, as expected (Figure 3.3.4.1A).

As a second measure, mice were placed on a Force Plate Actometer (FPA) to monitor changes in their locomotor activity. The FPA contains four force sensors each supporting a corner of the floor. When a mouse runs on the floor, the FPA automatically records the reactive forces and calculates the movement of a given mouse (Fowler et al 2001). Mice were placed on the FPA for a 10 min session each week. The distance traveled within the 10min session was not different across groups. Figure 3.3.4.1C shows the maximum power (max power) of a mouse (normalized to % body weight) when running on the floor. KU-596 treatment improved the max power, indicating an improvement in force. In line with findings in the young mice, KU-596 treatment improved the MNCV and CMAP as well (Figure 3.3.4.1B and D). These data suggest that KU-596 treatment could improve the nerve function and muscle strength of Cx32def

mice, which could be translated to humans as muscle weakness, a major complaint from CMT1X patients.

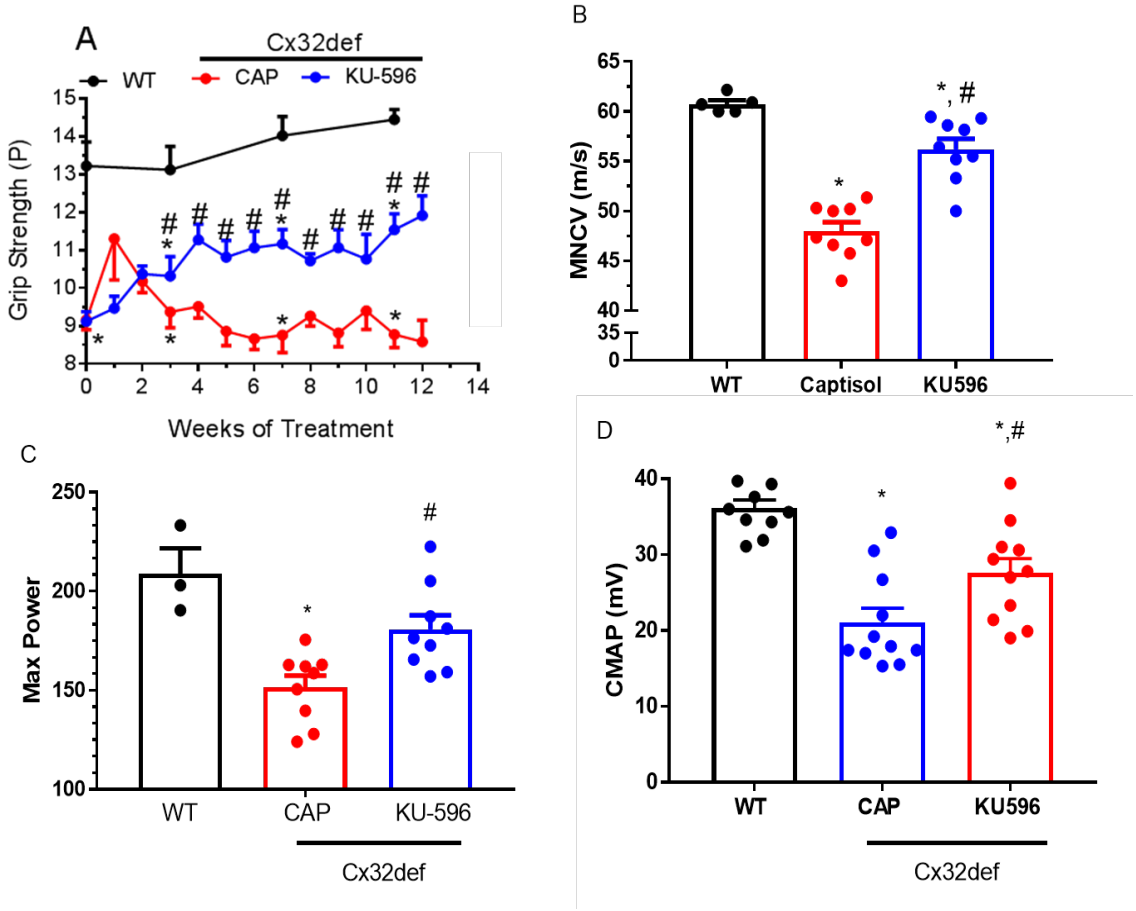

Figure 3.3.4.1: KU-596 improves motor function of old Cx32def mice.
KU-596 improves grip strength (A), MNCV (B), max power (C) and CMAP (D) in 9 month-old Cx32def mice. Max power is measured as percent of body weight during a 10min session on force plate actometer. *, $p<0.05$ vs. WT. #, $p<0.05$ vs. CAP.

3.3.5. KU-596 requires Hsp70 for efficacy.

Our previous work has shown that the ability of KU-596 to protect against diabetic neuropathy is Hsp70-dependent (Ma et al 2015, Zhang et al 2018). We sought to explore whether Hsp70 is also required in preserving the nerve function in this model of CMT1X. We generated Cx32def x Hsp70 KO mice by crossing the Cx32def mice with Hsp70.1/70.3 knockout mice (Figure 3.3.5.1A). We included both young and old Cx32def x Hsp70 KO mice and followed the same experimental design as we did with the Cx32def mice that expressed Hsp70. Deletion of Hsp70 did not affect development of the neuropathy since MNCV, CMAP and grip strength were decreased to levels similar to that observed in the Cx323def mice. Thus, Hsp70 is not necessary for developing the neuromuscular deficits. However, in contrast to the Cx32def mice, KU-596 treatment showed no efficacy in improving the neuropathic phenotype in the Cx32def x Hsp70 KO mice. For example, c-jun levels were unchanged in the motor nerve femoral branches of young mice receiving 1 month of KU-596 treatment or old mice receiving 3 months of KU-596 treatment. In addition, KU-596 treatment failed to preserve motor function as mice receiving KU-596 treatment performed the same as CAP treated animals in the grip strength test and showed no improvements in MNCV and CMAP (Figure 3.3.5.1C, D, G-I). Taken together, these data indicate that Hsp70 is required for drug efficacy, consistent with our previous findings in animal models of metabolic neuropathy (Li et al 2012a, Ma et al 2014, Zhang et al 2018).

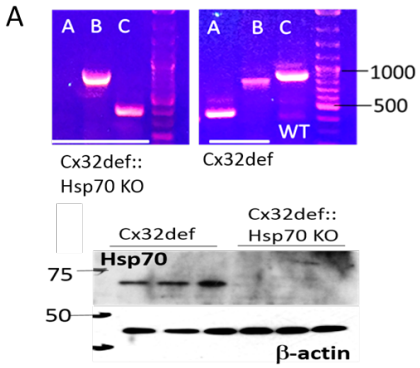
A
A B C
A B C
1000
500
WT
Cx32def::
Hsp70 KO
Cx32def
Cx32def
Cx32def::
Hsp70 KO
Hsp70
75
50
β-actin

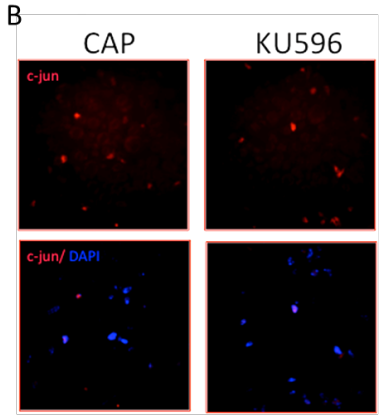
B
CAP
KU596
c-jun
c-jun/ DAPI

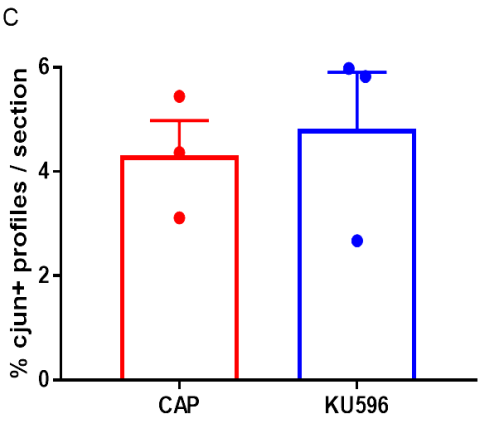
C
% cjun+ profiles / section
6
4
2
0
CAP
KU596

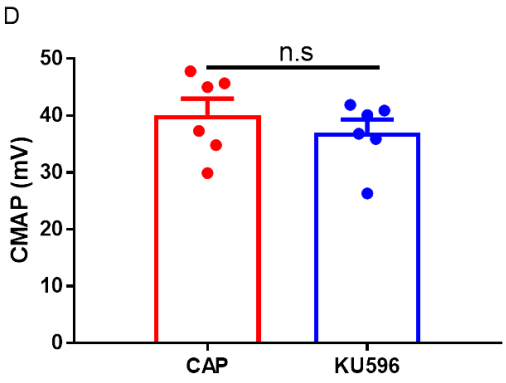
D
n.s
CMAP (mV)
50
40
30
20
10
0
CAP
KU596

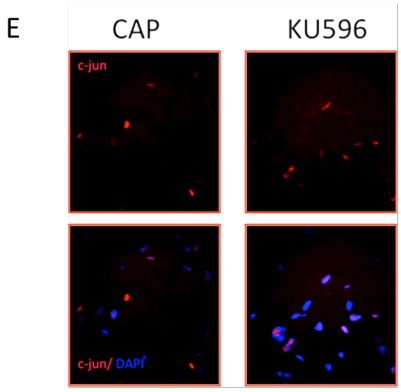
E
CAP
KU596
c-jun
c-jun/ DAPI

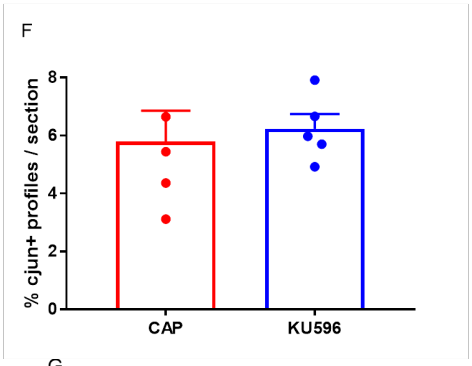
F
% cjun+ profiles / section
8
6
4
2
0
CAP
KU596

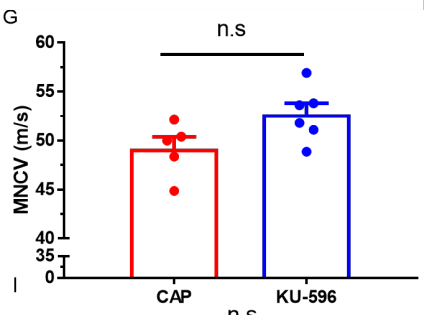
G
n.s
MNCV (m/s)
60
55
50
45
40
35
0
CAP
KU-596

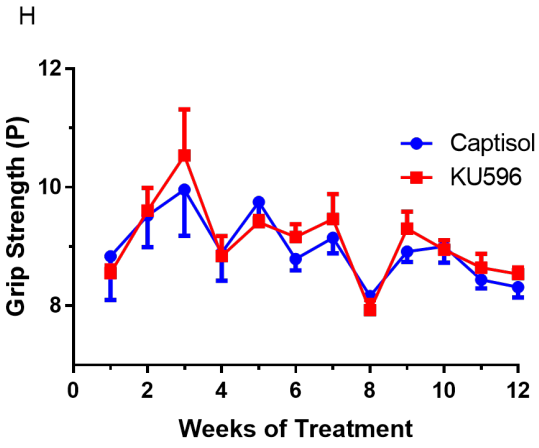
H
Grip Strength (P)
12
10
8
0
2
4
6
8
10
12
Weeks of Treatment
Captisol
KU596

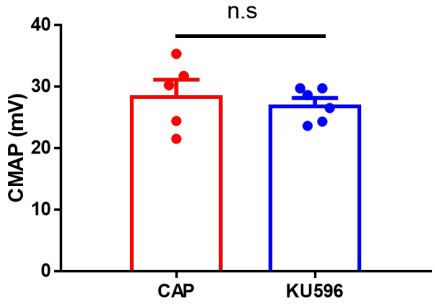
I
n.s
CMAP (mV)
40
30
20
10
0
CAP
KU596

Figure 3.3.5.1: KU-596 improves the motor deficit in an Hsp70 dependent manner.
A) Genotype analysis of the Cx32def x Hsp70 KO mice (top). A, Hsp70 WT; B, Hsp70 KO; C, Cx32. Immunoblot analysis of sciatic nerve from three Cx32def and Cx32def x Hsp70 KO mice (bottom). B) Motor branches of femoral nerves of 4-month-old Cx32def x Hsp70KO mice were harvested after one-month of treatment. Cross sections were stained with antibody against c-jun (red). C) Quantification of the percentage of c-jun+ nuclei per section. D) KU-596 does not improve CMAP in the absence of Hsp70. E-F) Immunostaining of c-jun in cross sections of femoral nerve motor branch of 9-month-old Cx32def x Hsp70KO mice. Quantification is shown in F. G-I) KU-596 treatments did not improve the motor function of Cx32def x Hsp70KO mice. MNCV (G), CMAP (I) and muscle strength (H) were not changed following KU-596 treatment.

3.3.6. KU-596 may improve the neuropathy by decreasing macrophage recruitment

Since CCL2 can be induced by c-jun and downregulation of CCL2 has been shown to be beneficial in Cx32def mice (Groh et al 2010), it is possible that the effects of KU-596 may act through the c-jun-CCL2-macrophage axis. To test this hypothesis, we transfected 50B11 cells with a plasmid, which contains a CCL2 promoter driving expression of a *Gaussia* luciferase reporter.

To determine if the drug had an effect on basal c-jun expression, the cells were treated for 14 hrs with 1 μM KU-596 while maintaining the cells in complete medium containing 10% serum. Under these conditions, KU-596 had no effect on altering c-jun expression or luciferase activity, suggesting that the drug was not decreasing basal c-jun expression (Figure 3.3.6.1B). To determine if the drug might alter an increase in c-jun, transfected cells received vehicle or 1 μM KU-596 and were deprived of serum for 12h to induce quiescence. The cells were then re-stimulated with serum for 2h to induce c-jun. As expected, cells stimulated with 10% serum showed an increase in c-jun levels and luciferase activity. However, KU-596 treatment decreased the serum-induced increase in c-jun expression (Figure 3.3.6.1A) and luciferase activity. These data suggest that KU-596 is blocking the serum-induced increase in c-jun levels but is not affecting basal levels present in the absence of serum deprivation.

The above studies also supported that c-jun can activate the CCL2 promoter. To determine if KU-596 decreased CCL2 levels *in vivo*, extracts of sciatic nerve from mice treated for 3 months with KU-596 were used in a CCL2 ELISA. Due to the use of tissues

for other experiments, only three mice could be assessed. While CCL2 levels were increased in untreated Cx32def mice compared to WT animals, only two of three KU-596 treated animals showed a robust decline in CCL2, which negated statistical significance (data not shown). CCL2 levels will be reassessed in an upcoming cohort of animals.

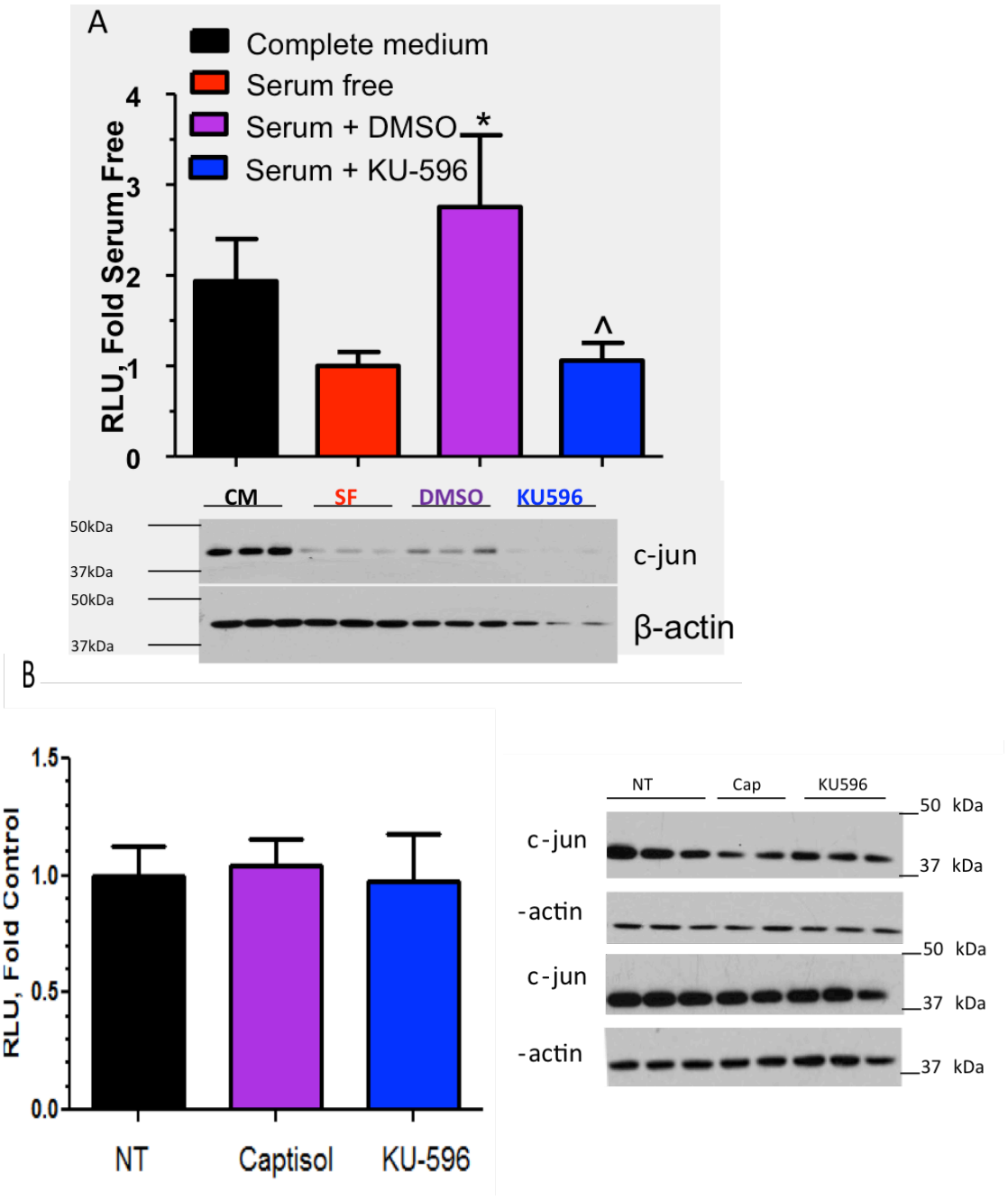

Figure 3.3.6.1: KU-596 decreases CCL2 luciferase activity.
A) Luciferase activity of CCL2 in 50B11 cells. Cells were deprived of serum for 12h or remained in the complete medium as control and treated with the addition of 1μM KU-596. After 2h serum stimulation, media were collected for luciferase assay and cells lysates were used for western blot analysis. Serum induced c-jun expression and corresponding luciferase activity whereas KU-596 treatment decreased both. *, $p < 0.05$ versus SF; # $p< 0.05$ vs DMSO. B) Luciferase activity of CCL2 in 50B11 cells without serum deprivation. Cells were treated with either Captisol or 1μM KU-596 overnight. Media were collected for luciferase activity assay and cell lysates western blot analysis. c-Jun expression and luciferase activity remained regardless of treatment.

3.4. Discussion

CMT1X is the second most prevalent form of CMT disease (Braathen 2012). Though not lethal, it severely affects the quality of life of CMT1X patients (Johnson et al 2014). So far, treatment options are limited to surgeries, braces and pain management. Intrathecal gene delivery of Cx32 markedly improved the motor neuropathy in Cx32def mice (Kagiava et al 2016), yet there are many hurdles to translate such an approach to humans. Here we demonstrated that KU-596, a small molecule Hsp90 inhibitor that is easily translatable to human patients, improved nerve function of Cx32def mice.

The pathology of Cx32def mice presents in two stages, wherein a non-demyelinating axonopathy occurs prior to a demyelinating axonopathy. A molecule of interest in both stages is the leucine zipper transcription factor c-jun. c-Jun is an AP-1 transcription factor that plays important roles in demyelination. c-Jun inhibits myelin gene expression under normal conditions and is required for SC dedifferentiation (Parkinson et al 2008). During the first stage of the CMT1X axonopathy, c-jun expression is elevated likely due to the response to axonal injury. At this stage, c-jun switches on a repair program that downregulates myelin genes, increases the expression of trophic factors, initiates myelin clearance by activating SC autophagy and macrophage recruitment, and more importantly forms the Bungner's band that guide axon regeneration (Jessen & Mirsky 2016). Glial cell-derived neurotrophic factor (GDNF) is found at elevated levels in c-jun positive SCs at this stage (Klein et al 2014), which is induced by c-jun as part of the repair program due to the presence of c-jun response elements in the GDNF gene promoter region (Arthur-Farraj et al 2012). If the c-jun

activated repair program is successful, the axons should be able to regenerate within a certain timeframe. However, an increase in GDNF is insufficient to halt disease progression and sustained high levels of c-jun lead to the gradual onset of SC demyelination. In addition, macrophages directly contribute to myelin degeneration in CMT1X (Martini & Willison 2016); their role is not secondary to myelin breakdown as seen in Wallerian degeneration (Martini et al 2013). It is possible that sustained high levels of c-jun lead to SC demyelination and add to the second wave of inflammatory assault, since CCL2 is driven by c-jun (Wolter et al 2008), which attracts macrophages and leads to the exacerbated demyelination (Figure 3.4.1).

We showed that the decrease of c-jun by KU-596 correlated with an improvement in nerve function in both young and old Cx32def mice in an Hsp70 dependent manner. However, the mechanism of decreased c-jun expression remains unknown. Mechanistically, Hsp70 inhibits the JNK pathway to protect neurons from apoptosis (Bienemann et al 2008, Lee et al 2005). However, phosphorylation of c-jun by JNK is neither necessary to drive demyelination (Parkinson et al 2008) nor to drive axon regeneration (Ruff et al 2012). In addition, we have previously shown that the decrease of c-jun in SC-neuronal co-cultures by KU-32 is due to an increased degradation but not a decreased production of c-jun (Li et al 2012a). In a transgenic mouse model where c-jun is selectively induced in SCs, pMAPK/MAPK level was not affected by KU-596 (Zhang et al 2018). Thus, we anticipate that the decrease of c-jun is likely due to an enhanced clearance rather than compromised production. In this regard, a protein of interest would be the F-box WD repeat domain-containing protein 7 (Fbw7). Fbw7 is an E3 ligase that mediates the degradation of c-jun after phosphorylation by GSK-3β at Thr^{239} and

Ser^{243}(Wei et al 2005). In addition, Hsp70 could coimmunoprecipitate with Fbw7 (unpublished data). These data suggest that KU-596 may decrease c-jun expression through Hsp70-Fbw7 mediated degradation. Further studies using mice that have a SC-specific conditional deletion of Fbw7 crossed into the Cx32def background will help determine the role of Fbw7 in decreasing c-jun by KU-596.

As c-jun not only drives SC dedifferentiation (Parkinson et al 2008) but also supports axon regeneration (Fontana et al 2012a, Ruff et al 2012), it is of vital importance to examine the physiological outcome of decreasing c-jun in Cx32def mice. We showed that decreased c-jun by KU-596 correlated with improved nerve function which could be linked to a decreased inflammatory response. KU-596 has been shown to downregulate the inflammatory transcriptome in a mouse model of DPN (Ma et al 2015). Another Hsp90 inhibitor, 17-AAG, improved neuron survival in a model of traumatic brain injury through down-regulating pro-inflammatory cytokines, such as TNF-α, IL-1β and IL-6 (Gu et al 2016). In the Cx32def mice, mutant SCs send out a signal that induces endoneurial fibroblasts to secrete CSF-1, which activates the macrophage-mediated neurodegeneration. In the meantime, mutant SCs secrete CCL2 to recruit macrophages (Martini & Willison 2016). Since CCL2 could be induced by c-jun (Wolter et al 2008), we performed a luciferase assay to see if KU-596 could regulate CCL2 through c-jun using a luciferase reporter fused with CCL2 promoter. Serum induced the expression of c-jun and CCL2 in 50B11 cells whereas KU-596 treatment decreased the expression of c-jun and CCL2 luciferase activity, indicating that KU-596 may regulate CCL2 expression through c-jun. This suggests that the improved nerve function could be due to decreased macrophage recruitment and activation through c-jun mediated downregulation of CCL2

by KU-596. Thus KU-596 may reduce axon damage through downregulating the c-jun-CCL2-macrophage axis, leading to a decrease in axon damage and a further reduced expression of c-jun. This relationship will be more stringently addressed using Cx32def mice that have a SC-specific conditional deletion of c-jun.

In the C3 mouse model of CMT1A, conditional deletion of SC-c-jun exacerbated the phenotypes of CMT1A and led to loss of myelin-competent neurons (Hantke et al 2014). These data suggest that targeting c-jun may have unwanted side effects on neuronal survival. In contrast to genetic deletion, we showed that the decrease of c-jun by KU-596 correlates with an improvement in nerve function. The difference in the two experiments could be due to the level of c-jun. Instead of complete deletion, KU-596 reduced the c-jun level to a lower state, which helps nerve regeneration without inducing demyelination (**Figure 3.4.1**). This is supported by recent work from Fazal et al., 2017 where they examined graded c-jun expression on myelination (Fazal et al 2017). In mice that heterozygously overexpressed c-jun, developmental myelination was delayed but nerves were able to regenerate and functionally recover after injury. On the other hand, in mice that homozygously overexpressed c-jun, developmental myelination is inhibited. These data suggest that the expression level of c-jun is key to its function where moderate levels increase support for axon regeneration and high expression induces demyelination. Thus, KU-596 may reduce c-jun to moderate elevation level compared with normal condition to reduce axonopathy. Further studies using c-jun conditional knockout mice crossed with Cx32def mice will help determine whether c-jun is necessary for the effects of KU-596 as well as the role of c-jun in the disease progression.

Another possible aspect that KU-596 could act on to attenuate axonopathy would be its documented ability to improve sensory neuron bioenergetics (Ma et al 2015), as ATP supply is critical for axonal regeneration (Han et al 2016, Zhou et al 2016). Innervation of the neuromuscular junction (MNJs) would be another factor that adds to the improvement. Cx32def mice have been shown to have an elevated level of denervated NMJs compared with WT at 12 months of age (Klein et al 2015). Injections of recombinant human Hsp70 arrested denervation and preserved large myelinated axons in a mouse model of amyotrophic lateral sclerosis (Gifondorwa et al 2012). Thus, it is possible that KU-596 improves the innervation of NMJs and the muscle grip strength through Hsp70.

In summary, we provide evidence that KU-596 decreases c-jun expression and improves nerve function in both young and old Cx32def mice in an Hsp70 dependent manner. In Cx32def mice, an unknown assault leads to axon damage resulting in elevated c-jun expression. c-Jun upregulation leads to SC dedifferentiation as part of the repair program, which is insufficient to stop the disease progression. Sustained high levels of c-jun lead to demyelination in the second stage. In the meantime, mutant SCs send an unknown signal to endoneurial fibroblasts which then secrete CSF-1 and activate macrophage-mediated degeneration. In addition, c-jun induces the transcription of CCL2, which leads to a second wave of demyelination. KU-596 may act on antagonizing c-jun-CCL2-macrophage pathway and downregulating c-jun expression to a level that reduces axonopathy through an Hsp70 dependent manner, thus resulting in decreased c-jun level and improved nerve function. Improvement in innervation of NMJs and mitochondrial bioenergetics through Hsp70 mediated mechanisms may also add to the overall

improvement in function (Figure 3.4.1). Although further experiments are needed to pin down the mechanism, our data support the possibility of adding KU-596 as a therapeutic approach to the currently empty list of pharmacological management of CMT1X.

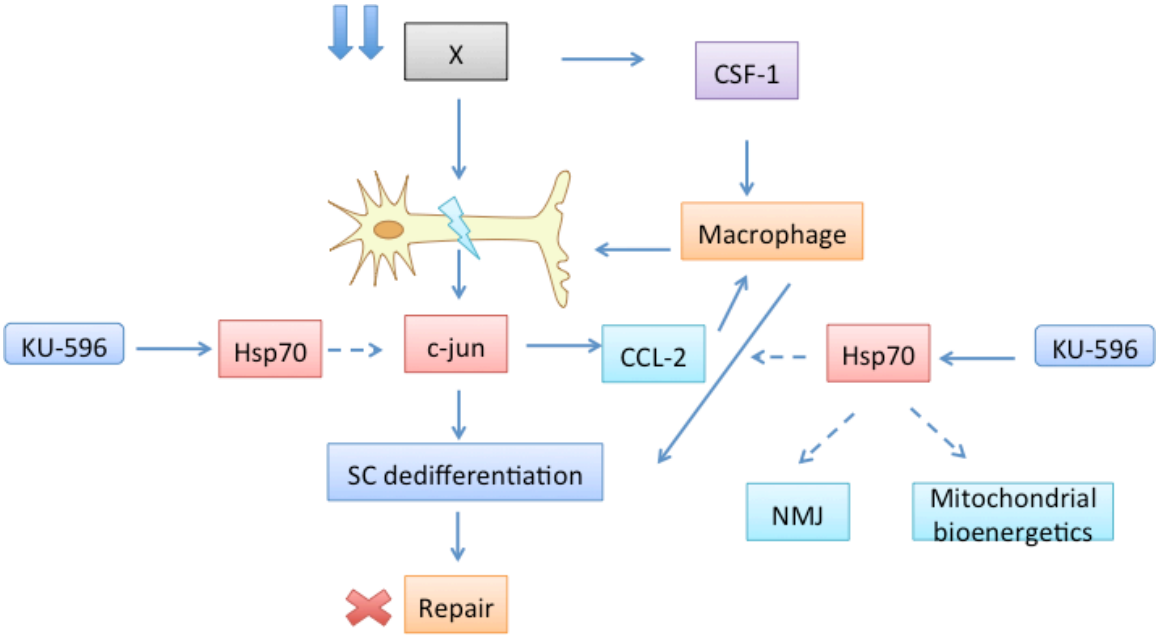

Figure 3.4.1: Proposed mechanism of action of KU-596.
In Cx32def mice, an unknown assault leads to axon damage resulting in elevated c-jun expression. c-Jun upregulation leads to SC dedifferentiation as part of the repair program. The repair program is either unsuccessful or could not meet the rate of axon damage. Constant insult induced sustained high level of c-jun which may lead to the demyelination in the second stage. On the other hand, mutant SCs send an unknown signal to endoneurial fibroblasts which then secretes CSF-1 and activate macrophage-mediated degeneration. c-jun induces the transcription of CCL2 which may leads to a second wave of demyelination. KU-596 may act on antagonizing macrophage pathway and directly/indirectly downregulating c-jun expression to a level that could be well-tolerated through an Hsp70 dependent manner, thus resulting in decreased c-jun level and improved nerve function. Improvement in innervation of NMJs and mitochondrial bioenergetics may also add to the overall improvement in nerve function. Dashed arrows indicates potential mechanism.

Chapter 4. Outlooks

Therapeutic strategies of demyelinating disorders currently remain limited. Understanding the molecular mechanism behind disease progression greatly facilitates finding the right targets for management. Recent studies revealed that c-jun is at the center of the SC demyelinating process. Upregulated c-jun expression leads to the inhibition of myelinating genes (Parkinson et al 2008) and such upregulation after nerve injury leads to SC demyelination and later support of axon regeneration (Fontana et al 2012a, Ruff et al 2012). Results from our previously published work have shown that the Hsp90 inhibitor, KU-32, could attenuate the upregulation of c-jun induced by neuregulin in a SC-DRG co-culture model (Li et al 2012a). The effect is likely due to an increased degradation rather than compromised production, since the effects of KU-32 on downregulating c-jun were abolished when the proteasome was inhibited. Moreover, the protective effects of this compound rely on the presence of Hsp70 since cultures prepared from Hsp70KO mice failed to show improvement in the extent of myelination. The current work focused on investigating the *in vivo* effects of a next generation Hsp90 inhibitor, KU-596, in the context of demyelinating neuropathies. Firstly, the results from the MPZ-RAF mice provided a proof of concept that attenuating the expression of c-jun by KU-596 could improve the motor function of these transgenic mice. Consistent with previous findings, KU-596 required Hsp70 for its efficacy. MPZ-RAF × Hsp70 KO mice treated with KU-596 did not show changes in c-jun expression level nor did they show any improvement in motor function compared with mice receiving the drug vehicle. Although this transgenic model proved useful to provide insight on the neuroprotective ability of KU-596, the model itself has some drawbacks. For example, the onset of the

neuropathy is very fast and it does not recapitulate the breadth of complex vascular, axonal, and SC interactions that contribute to the onset of neuromuscular deficits that contribute to many human neuropathies. Taken a step further, this strategy has been employed in a mouse model of an inherited neuropathy, CMT1X. The neuropathology of CMT1X has two stages, an initial axonopathy followed by a later stage of frank demyelination. KU-596 showed promising effects in downregulating c-jun expression and preserving nerve function in both young mice receiving 1 month of treatment and old mice receiving 3 months of treatment. In line with previous findings, the effects of KU-596 appeared to be dependent on Hsp70 (Ma et al 2015, Zhang et al 2018). This study indicated that modulating molecular chaperones could be beneficial in the context of CMT1X, however the underlying mechanism remains to be uncovered.

The mechanism of how c-jun is cleared is unknown. It is possible that KU-596 functions post-transcriptionally to regulate c-jun expression. c-Jun is first phosphorylated by GSK-3β at Thr^{239} and Ser^{243} and then transported to the proteasome for degradation by the E3 ligase Fbw7 (Welcker et al 2004). As Fbw7 can coimmunoprecipitate with Hsp70 (data not shown), it is possible that KU-596 decreases c-jun expression through an Hsp70-Fbw7 interaction. To investigate the role of Fbw7 on the degradation of c-jun, our lab has generated mice with SC-specific deletion of Fbw7. Fbw7 has been found to inhibit myelin gene expression in oligodendrocytes through inhibiting the mTOR pathway (Kearns et al 2015). As deletion of Fbw7 is associated with the hypomyelination phenotype, the first question we would like to answer is whether this strain would present an exacerbated phenotype when crossed with the Cx32 def mice. The second question we would like to answer is whether the deletion of this protein influences the level of c-jun

as the disease progress. If Fbw7 is important for c-jun clearance, then the onset of the neuropathy may be faster and the neuromuscular phenotype exacerbated. The third question we would like to answer is whether this protein is critical for KU-596 to function. We might anticipate that the drug would lose efficacy if Fbw7 is critical for clearing c-jun.

Another aspect we would like to focus on is the necessity of c-jun for the effects of KU-596. The findings in this dissertation provide a correlation between decreased c-jun function and improved nerve function. However, no causal relationship could be derived based on this study design. It is possible that the altered expression level of c-jun is secondary to other changes following KU-596 treatment. Inflammation plays a key role in the progression of CMT1X, as Cx32def mice deficient in T- and B- lymphocytes showed a mitigated phenotype (Kobsar et al 2003) and heterozygous deletion of CCL2 alleviated the symptoms of CMT1X (Groh et al 2010). Several lines of data suggest that induction of Hsp70 could reduce inflammation and provide neuroprotection. Induction of Hsp70 by the Hsp90 inhibitor, 17-AAG, has been shown to promote optic neuron survival after injury (Kwong et al 2015). The effect of 17-AAG could likely be due to an anti-inflammatory action since the protection of 17-AAG on motor neurons after traumatic brain injury is associated with a decrease in TNF-α, IL-1β and IL-6 (Gu et al 2016). Hsp70 has also been shown to suppress NF-κB signaling and the production of inflammatory cytokines (Chen et al 2006). In experimental stroke, overexpressing Hsp70 inhibited microglia activation (Yenari et al 2005). Moreover, KU-596 decreased the inflammatory transcriptome upregulated by DPN (Ma et al 2015). It is possible that

through down-regulating inflammation, KU-596 protected neurons of Cx32def mice while c-jun level was decreased as a result of attenuated axonal damage.

To more rigorously investigate the role of c-jun in drug efficacy, we have generated another mouse model with a SC-specific deletion of c-jun crossed into the Cx32def background. This model would not only give us an idea as how the effects of KU-596 and c-jun levels are related, but also how the c-jun protein itself contributes to the disease. However, there are concerns about the phenotype of c-jun$^{f/f}$ mice. Recent evidence has suggested that genetic deletion of c-jun in a mouse model of CMT1A exacerbated the phenotype and led to loss of sensory neurons (Hantke et al 2014), indicating c-jun may have a protective role in addition to inducing demyelination. It seems that c-jun$^{f/f}$ × Cx32def mice may have an exacerbated phenotype compared with Cx32def mice and the symptoms may occur at an earlier stage. If these mice fail to show improvement after KU-596 therapy, then the protective effects of KU-596 are c-jun dependent. If these mice are able to response to KU-596 therapy, the protective effects of KU-596 may be c-jun independent; the reduced c-jun expression seen in the Cx32def mice is secondary to other protective mechanisms.

Mitochondrial function could be another interesting area to explore. Recent evidence suggests a role of mitochondria in axon degeneration. The opening of mitochondrial permeability transition pore leads to axonal degeneration induced by mechanical or toxic stimuli (Barrientos et al 2011). Mitochondrial depolarization could induce axon degeneration independent of apoptosis (Gerdts et al 2013). Depolarized mitochondria are associated with the release of reactive oxygen species (ROS) and reduced energy supply (O'Donnell et al 2013). KU-596 has been demonstrated to

improve sensory neuron bioenergetics and reduce ROS production in models of diabetic peripheral neuropathy (Ma et al 2014, Ma et al 2015). Therefore, it is possible that KU-596 improved mitochondrial function that contributes to aspects of the neuromuscular improvement. Further studies looking at the mitochondrial function in young and old mice would help elucidate the role of mitochondrial dysfunction in the progression of the disease and whether KU-596 would exhibit protective effects.

Innervation of the neuromuscular junction (NMJs) would be another exciting area to look at, as CMT1X is a neuromuscular disease to start with. Cx32def mice have been shown to have an elevated level of denervated NMJs compared to WT mice at 12 months of age (Klein et al 2015). Injections of recombinant human Hsp70 arrested denervation and preserved large myelinated axons in a mouse model of amyotrophic lateral sclerosis (Gifondorwa et al 2012). Thus, it is possible that KU-596 could act on NMJs and improved the muscle grip strength through Hsp70.

In summary, this dissertation provides further evidence that modulating molecular chaperones could be beneficial in managing demyelinating neuropathies. Although further studies are needed, it is possible that KU5-96 could improve nerve function of Cx32def mice through multiple mechanisms, including decreasing c-jun expression and inflammatory pathways. Since KU-596 is entering Phase 2 clinical trials, novologue therapy could be a promising translatable approach towards human demyelinating neuropathy, such as CMT1X.

Appendix



Title: Targeting Heat Shock Protein 70 to Ameliorate c-Jun Expression and Improve Demyelinating Neuropathy

Author: Xinyue Zhang, Chengyuan Li, Stephen C. Fowler, et al
Publication: ACS Chemical Neuroscience
Publisher: American Chemical Society
Date: Feb 1, 2018

Reference

Abdul HM, Calabrese V, Calvani M, Butterfield DA. 2006. Acetyl-L-carnitine-induced up-regulation of heat shock proteins protects cortical neurons against amyloid-beta peptide 1-42-mediated oxidative stress and neurotoxicity: implications for Alzheimer's disease. *Journal of neuroscience research* 84: 398-408

Abrams CK, Freidin M. 2015. GJB1-associated X-linked Charcot-Marie-Tooth disease, a disorder affecting the central and peripheral nervous systems. *Cell and tissue research* 360: 659-73

Abrams CK, Goman M, Wong S, Scherer SS, Kleopa KA, et al. 2017. Loss of Coupling Distinguishes GJB1 Mutations Associated with CNS Manifestations of CMT1X from Those Without CNS Manifestations. *Sci Rep* 7: 40166

Abresch RT, Carter GT, Jensen MP, Kilmer DD. 2002. Assessment of pain and health-related quality of life in slowly progressive neuromuscular disease. *Am J Hosp Palliat Care* 19: 39-48

Abresch RT, Jensen MP, Carter GT. 2001. Health-related quality of life in peripheral neuropathy. *Phys Med Rehabil Clin N Am* 12: 461-72

Ansar S, Burlison JA, Hadden MK, Yu XM, Desino KE, et al. 2007. A non-toxic Hsp90 inhibitor protects neurons from Abeta-induced toxicity. *Bioorg Med Chem Lett* 17: 1984-90

Anselmi F, Hernandez VH, Crispino G, Seydel A, Ortolano S, et al. 2008. ATP release through connexin hemichannels and gap junction transfer of second messengers propagate Ca2+ signals across the inner ear. *Proc Natl Acad Sci U S A* 105: 18770-75

Anyika M, McMullen M, Forsberg LK, Dobrowsky RT, Blagg BS. 2016. Development of Noviomimetics as C-Terminal Hsp90 Inhibitors. *ACS Med Chem Lett* 7: 67-71

Aparicio E, Mathieu P, Pereira Luppi M, Almeira Gubiani MF, Adamo AM. 2013. The Notch signaling pathway: its role in focal CNS demyelination and apotransferrin-induced remyelination. *J Neurochem* 127: 819-36

Aridon P, Geraci F, Turturici G, D'Amelio M, Savettieri G, Sconzo G. 2011. Protective role of heat shock proteins in Parkinson's disease. *Neurodegener Dis* 8: 155-68

Arthur-Farraj PJ, Latouche M, Wilton DK, Quintes S, Chabrol E, et al. 2012. c-Jun reprograms Schwann cells of injured nerves to generate a repair cell essential for regeneration. *Neuron* 75: 633-47

Assimon VA, Gillies AT, Rauch JN, Gestwicki JE. 2013. Hsp70 protein complexes as drug targets. *Curr Pharm Des* 19: 404-17

Asthana A, Bollapalli M, Tangirala R, Bakthisaran R, Mohan Rao C. 2014. Hsp27 suppresses the Cu(2+)-induced amyloidogenicity, redox activity, and cytotoxicity of alpha-synuclein by metal ion stripping. *Free Radic Biol Med* 72: 176-90

Bahr M, Andres F, Timmerman V, Nelis ME, Van Broeckhoven C, Dichgans J. 1999. Central visual, acoustic, and motor pathway involvement in a Charcot-Marie-

Tooth family with an Asn205Ser mutation in the connexin 32 gene. *J Neurol Neurosurg Psychiatry* 66: 202-6
Balakumar P, Arora MK, Ganti SS, Reddy J, Singh M. 2009. Recent advances in pharmacotherapy for diabetic nephropathy: current perspectives and future directions. *Pharmacol Res* 60: 24-32
Balice-Gordon RJ, Bone LJ, Scherer SS. 1998. Functional gap junctions in the schwann cell myelin sheath. *The Journal of cell biology* 142: 1095-104
Ballinger CA, Connell P, Wu Y, Hu Z, Thompson LJ, et al. 1999. Identification of CHIP, a novel tetratricopeptide repeat-containing protein that interacts with heat shock proteins and negatively regulates chaperone functions. *Mol Cell Biol* 19: 4535-45
Barrientos SA, Martinez NW, Yoo S, Jara JS, Zamorano S, et al. 2011. Axonal degeneration is mediated by the mitochondrial permeability transition pore. *J Neurosci* 31: 966-78
Behse F, Buchthal F, Carlsen F. 1977. Nerve biopsy and conduction studies in diabetic neuropathy. *J Neurol Neurosurg Psychiatry* 40: 1072-82
Beiswenger KK, Calcutt NA, Mizisin AP. 2008. Epidermal nerve fiber quantification in the assessment of diabetic neuropathy. *Acta Histochem* 110: 351-62
Bertelsen EB, Chang L, Gestwicki JE, Zuiderweg ER. 2009. Solution conformation of wild-type E. coli Hsp70 (DnaK) chaperone complexed with ADP and substrate. *Proc Natl Acad Sci U S A* 106: 8471-6
Bienemann AS, Lee YB, Howarth J, Uney JB. 2008. Hsp70 suppresses apoptosis in sympathetic neurones by preventing the activation of c-Jun. *J Neurochem* 104: 271-8
Birchmeier C. 2009. ErbB receptors and the development of the nervous system. *Exp Cell Res* 315: 611-8
Birouk N, LeGuern E, Maisonobe T, Rouger H, Gouider R, et al. 1998. X-linked Charcot-Marie-Tooth disease with connexin 32 mutations: clinical and electrophysiologic study. *Neurology* 50: 1074-82
Bobkova NV, Garbuz DG, Nesterova I, Medvinskaya N, Samokhin A, et al. 2014. Therapeutic effect of exogenous hsp70 in mouse models of Alzheimer's disease. *Journal of Alzheimer's disease : JAD* 38: 425-35
Boerboom A, Dion V, Chariot A, Franzen R. 2017. Molecular Mechanisms Involved in Schwann Cell Plasticity. *Front Mol Neurosci* 10: 38
Braathen GJ. 2012. Genetic epidemiology of Charcot-Marie-Tooth disease. *Acta Neurol Scand Suppl*: iv-22
Brennan KM, Bai Y, Shy ME. 2015. Demyelinating CMT-what's known, what's new and what's in store? *Neurosci Lett* 596: 14-26
Buchner J. 1999. Hsp90 & Co. - a holding for folding. *Trends Biochem Sci* 24: 136-41
Bukau B, Horwich AL. 1998. The Hsp70 and Hsp60 chaperone machines. *Cell* 92: 351-66
Bukau B, Weissman J, Horwich A. 2006. Molecular chaperones and protein quality control. *Cell* 125: 443-51
Burns J, Ramchandren S, Ryan MM, Shy M, Ouvrier RA. 2010. Determinants of reduced health-related quality of life in pediatric inherited neuropathies. *Neurology* 75: 726-31

Calabrese V, Scapagnini G, Colombrita C, Ravagna A, Pennisi G, et al. 2003. Redox regulation of heat shock protein expression in aging and neurodegenerative disorders associated with oxidative stress: a nutritional approach. *Amino acids* 25: 437-44

Calcutt NA. 2010. Tolerating Diabetes - An Alternative Therapeutic Approach for Diabetic Neuropathy. *ASN Neuro* 2: 215-17

Calcutt NA, Cooper ME, Kern TS, Schmidt AM. 2009. Therapies for hyperglycaemia-induced diabetic complications: from animal models to clinical trials. *Nat Rev Drug Discov* 8: 417-29

Callaghan BC, Cheng HT, Stables CL, Smith AL, Feldman EL. 2012. Diabetic neuropathy: clinical manifestations and current treatments. *Lancet Neurol* 11: 521-34

Calvert M, Pall H, Hoppitt T, Eaton B, Savill E, Sackley C. 2013. Health-related quality of life and supportive care in patients with rare long-term neurological conditions. *Qual Life Res* 22: 1231-8

Carter GT, Abresch RT, Fowler WM, Jr., Johnson ER, Kilmer DD, McDonald CM. 1995. Profiles of neuromuscular diseases. Hereditary motor and sensory neuropathy, types I and II. *Am J Phys Med Rehabil* 74: S140-9

Chance PF, Alderson MK, Leppig KA, Lensch MW, Matsunami N, et al. 1993. DNA deletion associated with hereditary neuropathy with liability to pressure palsies. *Cell* 72: 143-51

Chen H, Wu Y, Zhang Y, Jin L, Luo L, et al. 2006. Hsp70 inhibits lipopolysaccharide-induced NF-kappaB activation by interacting with TRAF6 and inhibiting its ubiquitination. *FEBS Lett* 580: 3145-52

Chittoor VG, Sooyeon L, Rangaraju S, Nicks JR, Schmidt JT, et al. 2013. Biochemical characterization of protein quality control mechanisms during disease progression in the C22 mouse model of CMT1A. *ASN Neuro* 5: e00128

Chittoor-Vinod VG, Lee S, Judge SM, Notterpek L. 2015. Inducible HSP70 is critical in preventing the aggregation and enhancing the processing of PMP22. *ASN Neuro* 7

Christianson JA, Ryals JM, Johnson MS, Dobrowsky RT, Wright DE. 2007. Neurotrophic modulation of myelinated cutaneous innervation and mechanical sensory loss in diabetic mice. *Neuroscience* 145: 303-13

Ciglia E, Vergin J, Reimann S, Smits SH, Schmitt L, et al. 2014. Resolving hot spots in the C-terminal dimerization domain that determine the stability of the molecular chaperone Hsp90. *PloS one* 9: e96031

Coleman MP, Freeman MR. 2010. Wallerian degeneration, wld(s), and nmnat. *Annu Rev Neurosci* 33: 245-67

Corfas G, Velardez MO, Ko CP, Ratner N, Peles E. 2004. Mechanisms and roles of axon-Schwann cell interactions. *J Neurosci* 24: 9250-60

Cunningham CN, Krukenberg KA, Agard DA. 2008. Intra- and intermonomer interactions are required to synergistically facilitate ATP hydrolysis in Hsp90. *J Biol Chem* 283: 21170-8

DCCT Research Group. 1988. Factors in development of diabetic neuropathy. Baseline analysis of neuropathy in feasibility phase of Diabetes Control and Complications Trial (DCCT). . *Diabetes* 37: 476-81

DCCT Research Group, Nathan DM, Genuth S, Lachin J, Cleary P, et al. 1993. The effect of intensive treatment of diabetes on the development and progression of long-term complications in insulin-dependent diabetes mellitus. *N Engl J Med* 329: 977-86
De Vuyst E, Decrock E, Cabooter L, Dubyak GR, Naus CC, et al. 2006. Intracellular calcium changes trigger connexin 32 hemichannel opening. *EMBO J* 25: 34-44
Decker L, Desmarquet-Trin-Dinh C, Taillebourg E, Ghislain J, Vallat JM, Charnay P. 2006. Peripheral myelin maintenance is a dynamic process requiring constant Krox20 expression. *J Neurosci* 26: 9771-9
Dekker SL, Kampinga HH, Bergink S. 2015. DNAJs: more than substrate delivery to HSPA. *Frontiers in molecular biosciences* 2: 35
Deregowski V, Gazzerro E, Priest L, Rydziel S, Canalis E. 2006. Role of the RAM domain and ankyrin repeats on notch signaling and activity in cells of osteoblastic lineage. *J Bone Miner Res* 21: 1317-26
Dickey CA, Dunmore J, Lu B, Wang JW, Lee WC, et al. 2006. HSP induction mediates selective clearance of tau phosphorylated at proline-directed Ser/Thr sites but not KXGS (MARK) sites. *FASEB J* 20: 753-5
Dickey CA, Kamal A, Lundgren K, Klosak N, Bailey RM, et al. 2007a. The high-affinity HSP90-CHIP complex recognizes and selectively degrades phosphorylated tau client proteins. *J Clin Invest* 117: 648-58
Dickey CA, Patterson C, Dickson D, Petrucelli L. 2007b. Brain CHIP: removing the culprits in neurodegenerative disease. *Trends Mol Med* 13: 32-38
Dickey CA, Patterson C, Dickson D, Petrucelli L. 2007c. Brain CHIP: removing the culprits in neurodegenerative disease. *Trends Mol Med* 13: 32-8
Dobrowsky RT. 2016. Targeting the Diabetic Chaperome to Improve Peripheral Neuropathy. *Current diabetes reports* 16: 71
Dubourg O, Tardieu S, Birouk N, Gouider R, Leger JM, et al. 2001. Clinical, electrophysiological and molecular genetic characteristics of 93 patients with X-linked Charcot-Marie-Tooth disease. *Brain* 124: 1958-67
Dyachuk V, Furlan A, Shahidi MK, Giovenco M, Kaukua N, et al. 2014. Neurodevelopment. Parasympathetic neurons originate from nerve-associated peripheral glial progenitors. *Science* 345: 82-7
Edwards JL, Vincent AM, Cheng HT, Feldman EL. 2008. Diabetic neuropathy: mechanisms to management. *Pharmacol Ther* 120: 1-34
El-Abassi R, England JD, Carter GT. 2014. Charcot-Marie-Tooth disease: an overview of genotypes, phenotypes, and clinical management strategies. *PM R* 6: 342-55
Espinosa-Medina I, Outin E, Picard CA, Chettouh Z, Dymecki S, et al. 2014. Neurodevelopment. Parasympathetic ganglia derive from Schwann cell precursors. *Science* 345: 87-90
Fazal SV, Gomez-Sanchez JA, Wagstaff LJ, Musner N, Otto G, et al. 2017. Graded Elevation of c-Jun in Schwann Cells In Vivo: Gene Dosage Determines Effects on Development, Remyelination, Tumorigenesis, and Hypomyelination. *J Neurosci* 37: 12297-313

Feder ME, Hofmann GE. 1999. Heat-shock proteins, molecular chaperones, and the stress response: evolutionary and ecological physiology. *Annu Rev Physiol* 61: 243-82
Feldman EL, Nave KA, Jensen TS, Bennett DL. 2017. New Horizons in Diabetic Neuropathy: Mechanisms, Bioenergetics, and Pain. *Neuron* 93: 1296-313
Fink AL. 1999. Chaperone-mediated protein folding. *Physiological reviews* 79: 425-49
Fontana X, Hristova M, Da Costa C, Patodia S, Thei L, et al. 2012a. c-Jun in Schwann cells promotes axonal regeneration and motoneuron survival via paracrine signaling. *J Cell Biol* 198: 127-41
Fontana X, Hristova M, Da Costa C, Patodia S, Thei L, et al. 2012b. c-Jun in Schwann cells promotes axonal regeneration and motoneuron survival via paracrine signaling. *The Journal of cell biology* 198: 127-41
Fortun J, Dunn WA, Jr., Joy S, Li J, Notterpek L. 2003. Emerging role for autophagy in the removal of aggresomes in Schwann cells. *J Neurosci* 23: 10672-80
Fortun J, Verrier JD, Go JC, Madorsky I, Dunn WA, Notterpek L. 2007. The formation of peripheral myelin protein 22 aggregates is hindered by the enhancement of autophagy and expression of cytoplasmic chaperones. *Neurobiol Dis* 25: 252-65
Fowler SC, Birkestrand BR, Chen R, Moss SJ, Vorontsova E, et al. 2001. A force-plate actometer for quantitating rodent behaviors: illustrative data on locomotion, rotation, spatial patterning, stereotypies, and tremor. *J Neurosci Methods* 107: 107-24
Fowler SC, Miller BR, Gaither TW, Johnson MA, Rebec GV. 2009. Force-plate quantification of progressive behavioral deficits in the R6/2 mouse model of Huntington's disease. *Behavioural brain research* 202: 130-7
Franck E, Madsen O, van Rheede T, Ricard G, Huynen MA, de Jong WW. 2004. Evolutionary diversity of vertebrate small heat shock proteins. *J Mol Evol* 59: 792-805
Gal A, Mucke J, Theile H, Wieacker PF, Ropers HH, Wienker TF. 1985. X-linked dominant Charcot-Marie-Tooth disease: suggestion of linkage with a cloned DNA sequence from the proximal Xq. *Hum Genet* 70: 38-42
Garg G, Khandelwal A, Blagg BS. 2016. Anticancer Inhibitors of Hsp90 Function: Beyond the Usual Suspects. *Advances in cancer research* 129: 51-88
Geller R, Andino R, Frydman J. 2013. Hsp90 inhibitors exhibit resistance-free antiviral activity against respiratory syncytial virus. *PLoS One* 8: e56762
Geller R, Taguwa S, Frydman J. 2012. Broad action of Hsp90 as a host chaperone required for viral replication. *Biochim Biophys Acta* 1823: 698-706
Gentil BJ, Mushynski WE, Durham HD. 2013. Heterogeneity in the properties of NEFL mutants causing Charcot-Marie-Tooth disease results in differential effects on neurofilament assembly and susceptibility to intervention by the chaperone-inducer, celastrol. *The international journal of biochemistry & cell biology* 45: 1499-508
Gerdts J, Summers DW, Sasaki Y, DiAntonio A, Milbrandt J. 2013. Sarm1-mediated axon degeneration requires both SAM and TIR interactions. *J Neurosci* 33: 13569-80

Ghosh S, Liu Y, Garg G, Anyika M, McPherson NT, et al. 2016. Diverging Novobiocin Anti-Cancer Activity from Neuroprotective Activity through Modification of the Amide Tail. *ACS Med Chem Lett* 7: 813-8
Ghosh S, Shinogle HE, Garg G, Vielhauer GA, Holzbeierlein JM, et al. 2015. Hsp90 C-terminal inhibitors exhibit antimigratory activity by disrupting the Hsp90alpha/Aha1 complex in PC3-MM2 cells. *ACS chemical biology* 10: 577-90
Gifondorwa DJ, Jimenz-Moreno R, Hayes CD, Rouhani H, Robinson MB, et al. 2012. Administration of Recombinant Heat Shock Protein 70 Delays Peripheral Muscle Denervation in the SOD1(G93A) Mouse Model of Amyotrophic Lateral Sclerosis. *Neurol Res Int* 2012: 170426
Goldberg AL. 2003. Protein degradation and protection against misfolded or damaged proteins. *Nature* 426: 895-9
Gordois A, Scuffham P, Shearer A, Oglesby A, Tobian JA. 2003. The health care costs of diabetic peripheral neuropathy in the US. *Diabetes Care* 26: 1790-5
Greene MK, Maskos K, Landry SJ. 1998. Role of the J-domain in the cooperation of Hsp40 with Hsp70. *Proc Natl Acad Sci U S A* 95: 6108-13
Griebeler ML, Morey-Vargas OL, Brito JP, Tsapas A, Wang Z, et al. 2014. Pharmacologic interventions for painful diabetic neuropathy: An umbrella systematic review and comparative effectiveness network meta-analysis. *Annals of internal medicine* 161: 639-49
Grim M, Halata Z, Franz T. 1992. Schwann cells are not required for guidance of motor nerves in the hindlimb in Splotch mutant mouse embryos. *Anat Embryol (Berl)* 186: 311-8
Groh J, Basu R, Stanley ER, Martini R. 2016. Cell-Surface and Secreted Isoforms of CSF-1 Exert Opposing Roles in Macrophage-Mediated Neural Damage in Cx32-Deficient Mice. *The Journal of neuroscience : the official journal of the Society for Neuroscience* 36: 1890-901
Groh J, Heinl K, Kohl B, Wessig C, Greeske J, et al. 2010. Attenuation of MCP-1/CCL2 expression ameliorates neuropathy in a mouse model for Charcot-Marie-Tooth 1X. *Hum Mol Genet* 19: 3530-43
Groh J, Klein I, Hollmann C, Wettmarshausen J, Klein D, Martini R. 2015. CSF-1-activated macrophages are target-directed and essential mediators of Schwann cell dedifferentiation and dysfunction in Cx32-deficient mice. *Glia* 63: 977-86
Gruden G, Bruno G, Chaturvedi N, Burt D, Schalkwijk C, et al. 2008. Serum heat shock protein 27 and diabetes complications in the EURODIAB prospective complications study: a novel circulating marker for diabetic neuropathy. *Diabetes* 57: 1966-70
Gu Y, Chen J, Wang T, Zhou C, Liu Z, Ma L. 2016. Hsp70 inducer, 17-allylamino-demethoxygeldanamycin, provides neuroprotection via anti-inflammatory effects in a rat model of traumatic brain injury. *Exp Ther Med* 12: 3767-72
Guo S, Wharton W, Moseley P, Shi H. 2007. Heat shock protein 70 regulates cellular redox status by modulating glutathione-related enzyme activities. *Cell stress & chaperones* 12: 245-54

Haines JD, Fragoso G, Hossain S, Mushynski WE, Almazan G. 2008. p38 Mitogen-activated protein kinase regulates myelination. *J Mol Neurosci* 35: 23-33
Hall JA, Forsberg LK, Blagg BS. 2014. Alternative approaches to Hsp90 modulation for the treatment of cancer. *Future medicinal chemistry* 6: 1587-605
Hamos JE, Oblas B, Pulaski-Salo D, Welch WJ, Bole DG, Drachman DA. 1991. Expression of heat shock proteins in Alzheimer's disease. *Neurology* 41: 345-50
Han SM, Baig HS, Hammarlund M. 2016. Mitochondria Localize to Injured Axons to Support Regeneration. *Neuron* 92: 1308-23
Hantke J, Carty L, Wagstaff LJ, Turmaine M, Wilton DK, et al. 2014. c-Jun activation in Schwann cells protects against loss of sensory axons in inherited neuropathy. *Brain* 137: 2922-37
Harris SF, Shiau AK, Agard DA. 2004. The crystal structure of the carboxy-terminal dimerization domain of htpG, the Escherichia coli Hsp90, reveals a potential substrate binding site. *Structure* 12: 1087-97
Harrisingh MC, Perez-Nadales E, Parkinson DB, Malcolm DS, Mudge AW, Lloyd AC. 2004. The Ras/Raf/Erk signaling pathway drives schwann cell dedifferentiation. *The EMBO journal* 23: 3061-71
Hartl FU, Hayer-Hartl M. 2002. Molecular chaperones in the cytosol: from nascent chain to folded protein. *Science* 295: 1852-8
Hasegawa T, Yoshida S, Sugeno N, Kobayashi J, Aoki M. 2017. DnaJ/Hsp40 Family and Parkinson's Disease. *Front Neurosci* 11: 743
Hoeck JD, Jandke A, Blake SM, Nye E, Spencer-Dene B, et al. 2010. Fbw7 controls neural stem cell differentiation and progenitor apoptosis via Notch and c-Jun. *Nature neuroscience* 13: 1365-72
Hoffman PN, Cleveland DW, Griffin JW, Landes PW, Cowan NJ, Price DL. 1987. Neurofilament gene expression: a major determinant of axonal caliber. *Proceedings of the National Academy of Sciences of the United States of America* 84: 3472-6
Hoke A. 2012. Animal models of peripheral neuropathies. *Neurotherapeutics : the journal of the American Society for Experimental NeuroTherapeutics* 9: 262-9
Hossain S, de la Cruz-Morcillo MA, Sanchez-Prieto R, Almazan G. 2012. Mitogen-activated protein kinase p38 regulates Krox-20 to direct Schwann cell differentiation and peripheral myelination. *Glia* 60: 1130-44
Hur J, Sullivan KA, Pande M, Hong Y, Sima AAF, et al. 2011. The identification of gene expression profiles associated with progression of human diabetic neuropathy. *Brain : a journal of neurology* 134: 3222-35
Hutton EJ, Carty L, Laurá M, Houlden H, Lunn MPT, et al. 2011. c-Jun expression in human neuropathies: a pilot study. *J Periph Nerv Syst* 16: 295-303
Jaegle M, Meijer D. 1998. Role of Oct-6 in Schwann cell differentiation. *Microsc Res Tech* 41: 372-8
Jessen KR, Mirsky R. 2005. The origin and development of glial cells in peripheral nerves. *Nat Rev Neurosci* 6: 671-82
Jessen KR, Mirsky R. 2008. Negative regulation of myelination: relevance for development, injury, and demyelinating disease. *Glia* 56: 1552-65

Jessen KR, Mirsky R. 2016. The repair Schwann cell and its function in regenerating nerves. *J Physiol* 594: 3521-31
Jiang J, Ballinger CA, Wu Y, Dai Q, Cyr DM, et al. 2001. CHIP is a U-box-dependent E3 ubiquitin ligase: identification of Hsc70 as a target for ubiquitylation. *The Journal of biological chemistry* 276: 42938-44
Jiang J, Maes EG, Taylor AB, Wang L, Hinck AP, et al. 2007. Structural basis of J cochaperone binding and regulation of Hsp70. *Mol Cell* 28: 422-33
Jiang J, Prasad K, Lafer EM, Sousa R. 2005. Structural basis of interdomain communication in the Hsc70 chaperone. *Mol Cell* 20: 513-24
Johnson NE, Heatwole CR, Dilek N, Sowden J, Kirk CA, et al. 2014. Quality-of-life in Charcot-Marie-Tooth disease: the patient's perspective. *Neuromuscul Disord* 24: 1018-23
Joseph NM, Mukouyama YS, Mosher JT, Jaegle M, Crone SA, et al. 2004. Neural crest stem cells undergo multilineage differentiation in developing peripheral nerves to generate endoneurial fibroblasts in addition to Schwann cells. *Development* 131: 5599-612
Jurynczyk M, Selmaj K. 2010. Notch: a new player in MS mechanisms. *J Neuroimmunol* 218: 3-11
Kagiava A, Sargiannidou I, Theophilidis G, Karaiskos C, Richter J, et al. 2016. Intrathecal gene therapy rescues a model of demyelinating peripheral neuropathy. *Proceedings of the National Academy of Sciences of the United States of America* 113: E2421-9
Kampinga HH, Craig EA. 2010. The HSP70 chaperone machinery: J proteins as drivers of functional specificity. *Nat Rev Mol Cell Biol* 11: 579-92
Kappe G, Franck E, Verschuure P, Boelens WC, Leunissen JA, de Jong WW. 2003. The human genome encodes 10 alpha-crystallin-related small heat shock proteins: HspB1-10. *Cell Stress Chaperones* 8: 53-61
Kaucka M, Adameyko I. 2014. Non-canonical functions of the peripheral nerve. *Exp Cell Res* 321: 17-24
Kearns CA, Ravanelli AM, Cooper K, Appel B. 2015. Fbxw7 Limits Myelination by Inhibiting mTOR Signaling. *J Neurosci* 35: 14861-71
Kelly JJ, Simek J, Laird DW. 2015. Mechanisms linking connexin mutations to human diseases. *Cell Tissue Res* 360: 701-21
Kim B, Feldman EL. 2012. Insulin resistance in the nervous system. *Trends Endocrinol Metab* 23: 133-41
Klein D, Groh J, Wettmarshausen J, Martini R. 2014. Nonuniform molecular features of myelinating Schwann cells in models for CMT1: distinct disease patterns are associated with NCAM and c-Jun upregulation. *Glia* 62: 736-50
Klein D, Patzko A, Schreiber D, van Hauwermeiren A, Baier M, et al. 2015. Targeting the colony stimulating factor 1 receptor alleviates two forms of Charcot-Marie-Tooth disease in mice. *Brain* 138: 3193-205
Kleopa KA, Abrams CK, Scherer SS. 2012. How do mutations in GJB1 cause X-linked Charcot-Marie-Tooth disease? *Brain research* 1487: 198-205
Kleopa KA, Sargiannidou I. 2015. Connexins, gap junctions and peripheral neuropathy. *Neurosci Lett* 596: 27-32

Kleopa KA, Yum SW, Scherer SS. 2002. Cellular mechanisms of connexin32 mutations associated with CNS manifestations. *J Neurosci Res* 68: 522-34
Kobsar I, Berghoff M, Samsam M, Wessig C, Maurer M, et al. 2003. Preserved myelin integrity and reduced axonopathy in connexin32-deficient mice lacking the recombination activating gene-1. *Brain* 126: 804-13
Kohl B, Fischer S, Groh J, Wessig C, Martini R. 2010. MCP-1/CCL2 modifies axon properties in a PMP22-overexpressing mouse model for Charcot-Marie-tooth 1A neuropathy. *The American journal of pathology* 176: 1390-9
Kopan R, Ilagan MX. 2009. The canonical Notch signaling pathway: unfolding the activation mechanism. *Cell* 137: 216-33
Kovacs JJ, Murphy PJ, Gaillard S, Zhao X, Wu JT, et al. 2005. HDAC6 regulates Hsp90 acetylation and chaperone-dependent activation of glucocorticoid receptor. *Mol Cell* 18: 601-7
Kriehuber T, Rattei T, Weinmaier T, Bepperling A, Haslbeck M, Buchner J. 2010. Independent evolution of the core domain and its flanking sequences in small heat shock proteins. *FASEB J* 24: 3633-42
Kubu CJ, Orimoto K, Morrison SJ, Weinmaster G, Anderson DJ, Verdi JM. 2002. Developmental changes in Notch1 and numb expression mediated by local cell-cell interactions underlie progressively increasing delta sensitivity in neural crest stem cells. *Dev Biol* 244: 199-214
Kumar P, Ambasta RK, Veereshwarayya V, Rosen KM, Kosik KS, et al. 2007. CHIP and HSPs interact with beta-APP in a proteasome-dependent manner and influence Abeta metabolism. *Human molecular genetics* 16: 848-64
Kusuma BR, Zhang L, Sundstrom T, Peterson LB, Dobrowsky RT, Blagg BS. 2012a. Synthesis and evaluation of novologues as C-terminal Hsp90 inhibitors with cytoprotective activity against sensory neuron glucotoxicity. *J Med Chem* 55: 5797-812
Kusuma BR, Zhang L, Sundstrom T, Peterson LB, Dobrowsky RT, Blagg BSJ. 2012b. Synthesis and Evaluation of Novologues as C-Terminal Hsp90 Inhibitors with Cytoprotective Activity against Sensory Neuron Glucotoxicity. *J. Med. Chem.* 55: 5797-812
Kwong JM, Gu L, Nassiri N, Bekerman V, Kumar-Singh R, et al. 2015. AAV-mediated and pharmacological induction of Hsp70 expression stimulates survival of retinal ganglion cells following axonal injury. *Gene Ther* 22: 138-45
Lackie RE, Maciejewski A, Ostapchenko VG, Marques-Lopes J, Choy WY, et al. 2017. The Hsp70/Hsp90 Chaperone Machinery in Neurodegenerative Diseases. *Front Neurosci* 11: 254
Latour P, Gonnaud PM, Ollagnon E, Chan V, Perelman S, et al. 2006. SIMPLE mutation analysis in dominant demyelinating Charcot-Marie-Tooth disease: three novel mutations. *J Peripher Nerv Syst* 11: 148-55
Lee JS, Lee JJ, Seo JS. 2005. HSP70 deficiency results in activation of c-Jun N-terminal Kinase, extracellular signal-regulated kinase, and caspase-3 in hyperosmolarity-induced apoptosis. *J Biol Chem* 280: 6634-41
Lennertz RC, Medler KA, Bain JL, Wright DE, Stucky CL. 2011. Impaired sensory nerve function and axon morphology in mice with diabetic neuropathy. *J. Neurophys.* 106: 905-14

Lev-Ram V, Ellisman MH. 1995. Axonal activation-induced calcium transients in myelinating Schwann cells, sources, and mechanisms. *J Neurosci* 15: 2628-37
Li C, Ma J, Zhao H, Blagg BS, Dobrowsky RT. 2012a. Induction of heat shock protein 70 (Hsp70) prevents neuregulin-induced demyelination by enhancing the proteasomal clearance of c-Jun. *ASN Neuro* 4: e00102
Li C, Ma J, Zhao H, Blagg BSJ, Dobrowsky RT. 2012b. Induction of Heat Shock Protein 70 (Hsp70) Prevents Neuregulin-induced Demyelination by Enhancing the Proteasomal Clearance of c-Jun. *ASN Neuro* 4: 425-37
Li J, Richter K, Buchner J. 2011. Mixed Hsp90-cochaperone complexes are important for the progression of the reaction cycle. *Nat Struct Mol Biol* 18: 61-6
Li Y, Rao PK, Wen R, Song Y, Muir D, et al. 2004. Notch and Schwann cell transformation. *Oncogene* 23: 1146-52
Lüders J, Demand J, Höhfeld Jr. 2000. The ubiquitin-related BAG-1 provides a link between the molecular chaperones Hsc70:Hsp70 and the proteasome. *J. Biol. Chem* 276: 4613-17
Luo W, Dou F, Rodina A, Chip S, Kim J, et al. 2007a. Roles of heat-shock protein 90 in maintaining and facilitating the neurodegenerative phenotype in tauopathies. *Proc Natl Acad Sci U S A* 104: 9511-6
Luo W, Dou F, Rodina A, Chip S, Kim J, et al. 2007b. Roles of heat-shock protein 90 in maintaining and facilitating the neurodegenerative phenotype in tauopathies. *Proc Natl Acad Sci* 104: 9511-6
Lupski JR, de Oca-Luna RM, Slaugenhaupt S, Pentao L, Guzzetta V, et al. 1991. DNA duplication associated with Charcot-Marie-Tooth disease type 1A. *Cell* 66: 219-32
Lupski JR, Garcia CA. 1992. Molecular genetics and neuropathology of Charcot-Marie-Tooth disease type 1A. *Brain Pathol* 2: 337-49
Ma J, Farmer KL, Pan P, Urban MJ, Zhao H, et al. 2014. Heat shock protein 70 is necessary to improve mitochondrial bioenergetics and reverse diabetic sensory neuropathy following KU-32 therapy. *J Pharmacol Exp Ther* 348: 281-92
Ma J, Pan P, Anyika M, Blagg BS, Dobrowsky RT. 2015. Modulating Molecular Chaperones Improves Mitochondrial Bioenergetics and Decreases the Inflammatory Transcriptome in Diabetic Sensory Neurons. *ACS Chem Neurosci* 6: 1637-48
Magrane J, Smith RC, Walsh K, Querfurth HW. 2004. Heat shock protein 70 participates in the neuroprotective response to intracellularly expressed beta-amyloid in neurons. *The journal of Neuroscience* 24: 1700-06
Marcu MG, Chadli A, Bouhouche I, Catelli M, Neckers LM. 2000. The heat shock protein 90 antagonist novobiocin interacts with a previously unrecognized ATP-binding domain in the carboxyl terminus of the chaperone. *The Journal of biological chemistry* 275: 37181-6
Margolis DJ, Malay DS, Hoffstad OJ, Leonard CE, MaCurdy T, et al. 2011. Incidence of diabetic foot ulcer and lower extremity amputation among Medicare beneficiaries, 2006 to 2008: Data Points #2 In *Data Points Publication Series*. Rockville (MD)

Martinez-Ruiz A, Villanueva L, Gonzalez de Orduna C, Lopez-Ferrer D, Higueras MA, et al. 2005. S-nitrosylation of Hsp90 promotes the inhibition of its ATPase and endothelial nitric oxide synthase regulatory activities. *Proc Natl Acad Sci U S A* 102: 8525-30

Martini R, Klein D, Groh J. 2013. Similarities between inherited demyelinating neuropathies and Wallerian degeneration: an old repair program may cause myelin and axon perturbation under nonlesion conditions. *The American journal of pathology* 183: 655-60

Martini R, Willison H. 2015. Neuroinflammation in the peripheral nerve: Cause, modulator, or bystander in peripheral neuropathies? *Glia*

Martini R, Willison H. 2016. Neuroinflammation in the peripheral nerve: Cause, modulator, or bystander in peripheral neuropathies? *Glia* 64: 475-86

Mayer MP, Le Breton L. 2015. Hsp90: breaking the symmetry. *Mol Cell* 58: 8-20

McGuire JF, Rouen S, Siegfreid E, Wright DE, Dobrowsky RT. 2009. Caveolin-1 and altered neuregulin signaling contribute to the pathophysiological progression of diabetic peripheral neuropathy. *Diabetes* 58: 2677-86

McKerchar TL, Zarcone TJ, Fowler SC. 2006. Use of a force-plate actometer for detecting and quantifying vertical leaping induced by amphetamine in BALB/cJ mice, but not in C57BL/6J, DBA/2J, 129X1/SvJ, C3H/HeJ, and CD-1 mice. *J Neurosci Methods* 153: 48-54

Mechta-Grigoriou F, Gerald D, Yaniv M. 2001. The mammalian Jun proteins: redundancy and specificity. *Oncogene* 20: 2378-89

Mehlen P, Kretz-Remy C, Preville X, Arrigo AP. 1996. Human hsp27, Drosophila hsp27 and human alphaB-crystallin expression-mediated increase in glutathione is essential for the protective activity of these proteins against TNFalpha-induced cell death. *EMBO J* 15: 2695-706

Meyer P, Prodromou C, Hu B, Vaughan C, Roe SM, et al. 2003. Structural and functional analysis of the middle segment of hsp90: implications for ATP hydrolysis and client protein and cochaperone interactions. *Mol Cell* 11: 647-58

Mirsky R, Woodhoo A, Parkinson DB, Arthur-Farraj P, Bhaskaran A, Jessen KnR. 2008. Novel signals controlling embryonic Schwann cell development, myelination and dedifferentiation. *Journal of the Peripheral Nervous System* 13: 122-35

Miyata Y, Nakamoto H, Neckers L. 2013. The therapeutic target Hsp90 and cancer hallmarks. *Current pharmaceutical design* 19: 347-65

Molin CJ, Punga AR. 2016. Compound Motor Action Potential: Electrophysiological Marker for Muscle Training. *J Clin Neurophysiol* 33: 340-5

Mollapour M, Bourboulia D, Beebe K, Woodford MR, Polier S, et al. 2014. Asymmetric Hsp90 N domain SUMOylation recruits Aha1 and ATP-competitive inhibitors. *Molecular cell* 53: 317-29

Mollapour M, Neckers L. 2012. Post-translational modifications of Hsp90 and their contributions to chaperone regulation. *Biochimica et biophysica acta* 1823: 648-55

Morgner N, Schmidt C, Beilsten-Edmands V, Ebong IO, Patel NA, et al. 2015. Hsp70 forms antiparallel dimers stabilized by post-translational modifications to position clients for transfer to Hsp90. *Cell Rep* 11: 759-69

Morris JK, Lin W, Hauser C, Marchuk Y, Getman D, Lee KF. 1999. Rescue of the cardiac defect in ErbB2 mutant mice reveals essential roles of ErbB2 in peripheral nervous system development. *Neuron* 23: 273-83

Muchowski PJ, Wacker JL. 2005. Modulation of neurodegeneration by molecular chaperones. *Nat Rev Neurosci* 6: 11-22

Murphy SM, Laura M, Fawcett K, Pandraud A, Liu YT, et al. 2012a. Charcot-Marie-Tooth disease: frequency of genetic subtypes and guidelines for genetic testing. *J Neurol Neurosurg Psychiatry* 83: 706-10

Murphy SM, Ovens R, Polke J, Siskind CE, Laura M, et al. 2012b. X inactivation in females with X-linked Charcot-Marie-Tooth disease. *Neuromuscul Disord* 22: 617-21

Nagarajan R, Svaren J, Le N, Araki T, Watson M, Milbrandt J. 2001. EGR2 mutations in inherited neuropathies dominant-negatively inhibit myelin gene expression. *Neuron* 30: 355-68

Napoli I, Noon Luke A, Ribeiro S, Kerai Ajay P, Parrinello S, et al. 2012a. A Central Role for the ERK-Signaling Pathway in Controlling Schwann Cell Plasticity and Peripheral Nerve Regeneration In Vivo. *Neuron* 73: 729-42

Napoli I, Noon LA, Ribeiro S, Kerai AP, Parrinello S, et al. 2012b. A central role for the ERK-signaling pathway in controlling Schwann cell plasticity and peripheral nerve regeneration in vivo. *Neuron* 73: 729-42

Neef DW, Jaeger AM, Thiele DJ. 2011. Heat shock transcription factor 1 as a therapeutic target in neurodegenerative diseases. *Nat Rev Drug Discov* 10: 930-44

Nelles E, Butzler C, Jung D, Temme A, Gabriel HD, et al. 1996. Defective propagation of signals generated by sympathetic nerve stimulation in the liver of connexin32-deficient mice. *Proc Natl Acad Sci U S A* 93: 9565-70

Niemann S, Sereda MW, Rossner M, Stewart H, Suter U, et al. 1999. The "CMT rat": peripheral neuropathy and dysmyelination caused by transgenic overexpression of PMP22. *Ann N Y Acad Sci* 883: 254-61

Nitzan E, Pfaltzgraff ER, Labosky PA, Kalcheim C. 2013. Neural crest and Schwann cell progenitor-derived melanocytes are two spatially segregated populations similarly regulated by Foxd3. *Proc Natl Acad Sci U S A* 110: 12709-14

O'Donnell KC, Vargas ME, Sagasti A. 2013. WldS and PGC-1alpha regulate mitochondrial transport and oxidation state after axonal injury. *J Neurosci* 33: 14778-90

Oberg C, Li J, Pauley A, Wolf E, Gurney M, Lendahl U. 2001. The Notch intracellular domain is ubiquitinated and negatively regulated by the mammalian Sel-10 homolog. *J Biol Chem* 276: 35847-53

Ogata T, Yamamoto S, Nakamura K, Tanaka S. 2006. Signaling axis in schwann cell proliferation and differentiation. *Mol Neurobiol* 33: 51-62

Okamoto Y, Pehlivan D, Wiszniewski W, Beck CR, Snipes GJ, et al. 2013. Curcumin facilitates a transitory cellular stress response in Trembler-J mice. *Hum Mol Genet* 22: 4698-705
Ortmann KL, Chattopadhyay M. 2014. Decrease in neuroimmune activation by HSV-mediated gene transfer of TNFalpha soluble receptor alleviates pain in rats with diabetic neuropathy. *Brain, behavior, and immunity* 41: 144-51
Padua L, Pareyson D, Aprile I, Cavallaro T, Quattrone DA, et al. 2010. Natural history of Charcot-Marie-Tooth 2: 2-year follow-up of muscle strength, walking ability and quality of life. *Neurol Sci* 31: 175-8
Panosyan FB, Laura M, Rossor AM, Pisciotta C, Piscosquito G, et al. 2017. Cross-sectional analysis of a large cohort with X-linked Charcot-Marie-Tooth disease (CMTX1). *Neurology* 89: 927-35
Parkinson DB, Bhaskaran A, Arthur-Farraj P, Noon LA, Woodhoo A, et al. 2008. c-Jun is a negative regulator of myelination. *J Cell Biol* 181: 625-37
Parkinson DB, Bhaskaran A, Droggiti A, Dickinson S, D'Antonio M, et al. 2004. Krox-20 inhibits Jun-NH2-terminal kinase/c-Jun to control Schwann cell proliferation and death. *J Cell Biol* 164: 385-94
Parkinson DB, Dickinson S, Bhaskaran A, Kinsella MT, Brophy PJ, et al. 2003. Regulation of the myelin gene periaxin provides evidence for Krox-20-independent myelin-related signalling in Schwann cells. *Mol Cell Neurosci* 23: 13-27
Perea J, Robertson A, Tolmachova T, Muddle J, King RHM, et al. 2001. nduced myelination and demyelination in a conditional mouse model of Charcot-Marie-Tooth disease type 1A. *Hum Mol Genet* 10: 1007-18
Perez N, Sugar J, Charya S, Johnson G, Merril C, et al. 1991. Increased synthesis and accumulation of heat shock 70 proteins in Alzheimer's disease. *Brain research. Molecular brain research* 11: 249-54
Perng MD, Cairns L, IJssel Pvd, Prescott A, Hutcheson AM, Quinlan RA. 2009. Intermediate filament interactions can be altered by HSP27 and alphaB-crystallin. *Journal of Cell Sciences* 112
Peterson LB, Blagg BS. 2009. To fold or not to fold: modulation and consequences of Hsp90 inhibition. *Future medicinal chemistry* 1: 267-83
Petrucelli L, Dickson D, Kehoe K, Taylor J, Snyder H, et al. 2004. CHIP and Hsp70 regulate tau ubiquitination, degradation and aggregation. *Human molecular genetics* 13: 703-14
Pop-Busui R, Ang L, Holmes C, Gallagher K, Feldman EL. 2016. Inflammation as a Therapeutic Target for Diabetic Neuropathies. *Curr Diab Rep* 16: 29
Pratt WB, Gestwicki JE, Osawa Y, Lieberman AP. 2015. Targeting Hsp90/Hsp70-based protein quality control for treatment of adult onset neurodegenerative diseases. *Annual review of pharmacology and toxicology* 55: 353-71
Pratt WB, Morishima Y, Gestwicki JE, Lieberman AP, Osawa Y. 2014. A model in which heat shock protein 90 targets protein-folding clefts: rationale for a new approach to neuroprotective treatment of protein folding diseases. *Experimental biology and medicine* 239: 1405-13

Prodromou C, Roe SM, Piper PW, Pearl LH. 1997. A molecular clamp in the crystal structure of the N-terminal domain of the yeast Hsp90 chaperone. *Nat Struct Biol* 4: 477-82

Putcha P, Danzer KM, Kranich LR, Scott A, Silinski M, et al. 2010. Brain-permeable small-molecule inhibitors of Hsp90 prevent alpha-synuclein oligomer formation and rescue alpha-synuclein-induced toxicity. *J Pharmacol Exp Ther* 332: 849-57

Radons J. 2016. The human HSP70 family of chaperones: where do we stand? *Cell Stress Chaperones* 21: 379-404

Raivich G, Behrens A. 2006. Role of the AP-1 transcription factor c-Jun in developing, adult and injured brain. *Prog Neurobiol* 78: 347-63

Rangaraju S, Madorsky I, Pileggi JG, Kamal A, Notterpek L. 2008a. Pharmacological induction of the heat shock response improves myelination in a neuropathic model. *Neurobiology of disease* 32: 105-15

Rangaraju S, Madorsky I, Pileggi JG, Kamal A, Notterpek L. 2008b. Pharmacological induction of the heat shock response improves myelination in a neuropathic model. *Neurobiol Dis* 32: 105-15

Redmond AC, Burns J, Ouvrier RA. 2008. Factors that influence health-related quality of life in Australian adults with Charcot-Marie-Tooth disease. *Neuromuscul Disord* 18: 619-25

Roy N, Nageshan RK, Ranade S, Tatu U. 2012. Heat shock protein 90 from neglected protozoan parasites. *Biochim Biophys Acta* 1823: 707-11

Rudiger S, Germeroth L, Schneider-Mergener J, Bukau B. 1997. Substrate specificity of the DnaK chaperone determined by screening cellulose-bound peptide libraries. *EMBO J* 16: 1501-7

Ruff CA, Staak N, Patodia S, Kaswich M, Rocha-Ferreira E, et al. 2012. Neuronal c-Jun is required for successful axonal regeneration, but the effects of phosphorylation of its N-terminus are moderate. *J Neurochem* 121: 607-18

Ruiz R, Lin J, Forgie A, Foletti D, Shelton D, et al. 2005. Treatment with trkC agonist antibodies delays disease progression in neuromuscular degeneration (nmd) mice. *Hum Mol Genet* 14: 1825-37

Ryan MC, Shooter EM, Notterpek L. 2002. Aggresome Formation in Neuropathy Models Based on Peripheral Myelin Protein 22 Mutations. *Neurobiology of Disease* 10: 109-18

Saibil H. 2013. Chaperone machines for protein folding, unfolding and disaggregation. *Nat Rev Mol Cell Biol* 14: 630-42

Salzer JL. 2008. Switching myelination on and off. *The Journal of cell biology* 181: 575-7

Samadi AK, Zhang X, Mukerji R, Donnelly AC, Blagg BS, Cohen MS. 2011. A novel C-terminal HSP90 inhibitor KU135 induces apoptosis and cell cycle arrest in melanoma cells. *Cancer letters* 312: 158-67

Saporta AS, Sottile SL, Miller LJ, Feely SM, Siskind CE, Shy ME. 2011. Charcot-Marie-Tooth disease subtypes and genetic testing strategies. *Ann Neurol* 69: 22-33

Scherer SS, Deschenes SM, Xu YT, Grinspan JB, Fischbeck KH, Paul DL. 1995. Connexin32 is a myelin-related protein in the PNS and CNS. *J Neurosci* 15: 8281-94

Scherer SS, Kleopa KA. 2012. X-linked Charcot-Marie-Tooth disease. *Journal of the peripheral nervous system : JPNS* 17 Suppl 3: 9-13
Scherer SS, Wrabetz L. 2008. Molecular mechanisms of inherited demyelinating neuropathies. *Glia* 56: 1578-89
Schopf FH, Biebl MM, Buchner J. 2017. The HSP90 chaperone machinery. *Nat Rev Mol Cell Biol* 18: 345-60
Shen Y, Liu J, Wang X, Cheng X, Wang Y, Wu N. 1997. Essential role of the first intron in the transcription of hsp90beta gene. *FEBS Lett* 413: 92-8
Sherman DL, Brophy PJ. 2005. Mechanisms of axon ensheathment and myelin growth. *Nat Rev Neurosci* 6: 683-90
Shi Y, Mosser DD, Morimoto RI. 1998. Molecularchaperones as HSF1-specific transcriptional repressors. *Genes and development* 12: 654-66
Shin YK, Jang SY, Park JY, Park SY, Lee HJ, et al. 2013. The Neuregulin-Rac-MKK7 pathway regulates antagonistic c-jun/Krox20 expression in Schwann cell dedifferentiation. *Glia* 61: 892-904
Shy ME, Siskind C, Swan ER, Krajewski KM, Doherty T, et al. 2007. CMT1X phenotypes represent loss of GJB1 gene function. *Neurology* 68: 849-55
Simon CM, Jablonka S, Ruiz R, Tabares L, Sendtner M. 2010. Ciliary neurotrophic factor-induced sprouting preserves motor function in a mouse model of mild spinal muscular atrophy. *Hum Mol Genet* 19: 973-86
Siskind CE, Murphy SM, Ovens R, Polke J, Reilly MM, Shy ME. 2011. Phenotype expression in women with CMT1X. *J Peripher Nerv Syst* 16: 102-7
Smith DF, Whitesell L, Katsanis E. 1998. Molecular chaperones: biology and prospects for pharmacological intervention. *Pharmacological reviews* 50: 493-514
Soroka J, Wandinger SK, Mausbacher N, Schreiber T, Richter K, et al. 2012. Conformational switching of the molecular chaperone Hsp90 via regulated phosphorylation. *Mol Cell* 45: 517-28
Taipale M, Krykbaeva I, Koeva M, Kayatekin C, Westover KD, et al. 2012. Quantitative analysis of HSP90-client interactions reveals principles of substrate recognition. *Cell* 150: 987-1001
Taipale M, Tucker G, Peng J, Krykbaeva I, Lin ZY, et al. 2014. A quantitative chaperone interaction network reveals the architecture of cellular protein homeostasis pathways. *Cell* 158: 434-48
Tavaria M, Gabriele T, Kola I, Anderson RL. 1996. A hitchhiker's guide to the human Hsp70 family. *Cell stress & chaperones* 1: 23-8
Taylor RP, Benjamin IJ. 2005. Small heat shock proteins: a new classification scheme in mammals. *J Mol Cell Cardiol* 38: 433-44
Tazir M, Hamadouche T, Nouioua S, Mathis S, Vallat JM. 2014. Hereditary motor and sensory neuropathies or Charcot-Marie-Tooth diseases: an update. *J Neurol Sci* 347: 14-22
Tradewell ML, Durham HD, Mushynski WE, Gentil BJ. 2009. Mitochondrial and axonal abnormalities precede disruption of the neurofilament network in a model of charcot-marie-tooth disease type 2E and are prevented by heat shock proteins in a mutant-specific fashion. *Journal of neuropathology and experimental neurology* 68: 642-52

Ullman-Cullere MH, Foltz CJ. 1999. Body condition scoring: a rapid and accurate method for assessing health status in mice. *Lab Animal Sci* 49: 319-23
Urban MJ, Li C, Yu C, Lu Y, Krise JM, et al. 2010. Inhibiting Heat Shock Protein 90 Reverses Sensory Hypoalgesia in Diabetic Mice. *ASN Neuro* 2: 189-99
Urban MJ, Pan P, Farmer KL, Zhao H, Blagg BS, Dobrowsky RT. 2012. Modulating Molecular Chaperones Improves Sensory Fiber Recovery and Mitochondrial Function in Diabetic Peripheral Neuropathy *Exp. Neurol.* 235: 388-96
Vallat JM, Grid D, Magdelaine C, Sturtz F, Tazir M. 2004. Autosomal recessive forms of Charcot-Marie-Tooth disease. *Curr Neurol Neurosci Rep* 4: 413-9
Vartholomaiou E, Echeverria PC, Picard D. 2016. Unusual Suspects in the Twilight Zone Between the Hsp90 Interactome and Carcinogenesis. *Adv Cancer Res* 129: 1-30
Vavlitou N, Sargiannidou I, Markoullis K, Kyriacou K, Scherer SS, Kleopa KA. 2010. Axonal pathology precedes demyelination in a mouse model of X-linked demyelinating/type I Charcot-Marie Tooth neuropathy. *J Neuropathol Exp Neurol* 69: 945-58
Viader A, Golden JP, Baloh RH, Schmidt RE, Hunter DA, Milbrandt J. 2011. Schwann cell mitochondrial metabolism supports long-term axonal survival and peripheral nerve function. *The Journal of neuroscience : the official journal of the Society for Neuroscience* 31: 10128-40
Vihervaara A, Sistonen L. 2014. HSF1 at a glance. *Journal of cell science* 127: 261-6
Wang J, Ren KY, Wang YH, Kou YH, Zhang PX, et al. 2015. Effect of active Notch signaling system on the early repair of rat sciatic nerve injury. *Artif Cells Nanomed Biotechnol* 43: 383-9
Wang Z, Fukushima H, Gao D, Inuzuka H, Wan L, et al. 2011. The two faces of FBW7 in cancer drug resistance. *BioEssays : news and reviews in molecular, cellular and developmental biology* 33: 851-9
Waza M, Adachi H, Katsuno M, Minamiyama M, Sang C, et al. 2005. 17-AAG, an Hsp90 inhibitor, ameliorates polyglutamine-mediated motor neuron degeneration. *Nat Med* 11: 1088-95
Wegele H, Wandinger SK, Schmid AB, Reinstein J, Buchner J. 2006. Substrate transfer from the chaperone Hsp70 to Hsp90. *J Mol Biol* 356: 802-11
Wei W, Jin J, Schlisio S, Harper JW, Kaelin WG, Jr. 2005. The v-Jun point mutation allows c-Jun to escape GSK3-dependent recognition and destruction by the Fbw7 ubiquitin ligase. *Cancer Cell* 8: 25-33
Welcker M, Orian A, Jin J, Grim JE, Harper JW, et al. 2004. The Fbw7 tumor suppressor regulates glycogen synthase kinase 3 phosphorylation-dependent c-Myc protein degradation. *Proc Natl Acad Sci U S A* 101: 9085-90
White PM, Morrison SJ, Orimoto K, Kubu CJ, Verdi JM, Anderson DJ. 2001. Neural crest stem cells undergo cell-intrinsic developmental changes in sensitivity to instructive differentiation signals. *Neuron* 29: 57-71
Wiggin TD, Kretzler M, Pennathur S, Sullivan KA, Brosius FC, Feldman EL. 2008. Rosiglitazone treatment reduces diabetic neuropathy in streptozotocin-treated DBA/2J mice. *Endocrinology* 149: 4928-37

Wolter S, Doerrie A, Weber A, Schneider H, Hoffmann E, et al. 2008. c-Jun controls histone modifications, NF-kappaB recruitment, and RNA polymerase II function to activate the ccl2 gene. *Molecular and cellular biology* 28: 4407-23

Woodhoo A, Alonso MB, Droggiti A, Turmaine M, D'Antonio M, et al. 2009. Notch controls embryonic Schwann cell differentiation, postnatal myelination and adult plasticity. *Nat Neurosci* 12: 839-47

Xu L, Emery JF, Ouyang YB, Voloboueva LA, Giffard RG. 2010. Astrocyte targeted overexpression of Hsp72 or SOD2 reduces neuronal vulnerability to forebrain ischemia. *Glia* 58: 1042-9

Yamanishi DT, Buckmeier JA, Meyskens FL, Jr. 1991. Expression of c-jun, jun-B, and c-fos proto-oncogenes in human primary melanocytes and metastatic melanomas. *J Invest Dermatol* 97: 349-53

Yang DP, Kim J, Syed N, Tung YJ, Bhaskaran A, et al. 2012. p38 MAPK activation promotes denervated Schwann cell phenotype and functions as a negative regulator of Schwann cell differentiation and myelination. *The Journal of neuroscience : the official journal of the Society for Neuroscience* 32: 7158-68

Yang Y, Turner RS, Gaut JR. 1998. The chaperone BiP/GRP78 binds to amyloid precursor protein and decreases Abeta40 and Abeta42 secretion. *The Journal of biological chemistry* 273: 25552-5

Yenari MA, Liu J, Zheng Z, Vexler ZS, Lee JE, Giffard RG. 2005. Antiapoptotic and anti-inflammatory mechanisms of heat-shock protein protection. *Ann N Y Acad Sci* 1053: 74-83

Yoon H, Thakur V, Isham D, Fayad M, Chattopadhyay M. 2015. Moderate exercise training attenuates inflammatory mediators in DRG of Type 1 diabetic rats. *Exp Neurol* 267: 107-14

Young JC, Hartl FU. 2002. Chaperones and transcriptional regulation by nuclear receptors. *Nature structural biology* 9: 640-2

Zhang L, Zhao H, Blagg BS, Dobrowsky RT. 2012. A C-Terminal Heat Shock Protein 90 Inhibitor Decreases Hyperglycemia-induced Oxidative Stress and Improves Mitochondrial Bioenergetics in Sensory Neurons *J. Proteome Res.* 11: 129-37

Zhang M, Windheim M, Roe SM, Peggie M, Cohen P, et al. 2005. Chaperoned ubiquitylation--crystal structures of the CHIP U box E3 ubiquitin ligase and a CHIP-Ubc13-Uev1a complex. *Mol Cell* 20: 525-38

Zhang SL, Yu J, Cheng XK, Ding L, Heng FY, et al. 1999. Regulation of human hsp90alpha gene expression. *FEBS Lett* 444: 130-5

Zhang X, Li C, Fowler SC, Zhang Z, Blagg BSJ, Dobrowsky RT. 2018. Targeting Heat Shock Protein 70 to Ameliorate c-Jun Expression and Improve Demyelinating Neuropathy. *ACS Chem Neurosci* 9: 381-90

Zhou B, Yu P, Lin MY, Sun T, Chen Y, Sheng ZH. 2016. Facilitation of axon regeneration by enhancing mitochondrial transport and rescuing energy deficits. *J Cell Biol* 214: 103-19

Zochodne DW. 2007. Diabetes mellitus and the peripheral nervous system: manifestations and mechanisms. *Muscle Nerve* 36: 144-66